DISSERTATION

PERMEABILITY REDUCTION IN POROUS MEDIA DUE TO SUSPENDED PARTICLES

Submitted by

Hassan Vagharfard
Civil Engineering Department

In partial fulfillment of the requirements for the
Degree of Doctor of Philosophy
Colorado State University
Fort Collins, Colorado
Fall, 2001

COLORADO STATE UNIVERSITY

July 25, 2001

WE HEREBY RECOMMEND THAT THE DISSERTATION PREPARED UNDER OUR SUPERVISION BY HASSAN VAGHARFARD ENTITLED PERMEABILITY REDUCTION IN POROUS MEDIA DUE TO SUSPENDED PARTICLES BE ACCEPTED AS FULFILLING IN PART REQUIREMENTS FOR THE DEGREE OF DOCTOR OF PHILOSOPHY.

Committee on Graduate Work

Advisor

Department Head

ABSTRACT OF DISSERTATION
PERMEABILITY REDUCTION IN POROUS MEDIA
DUE TO SUSPENDED PARTICLES

Artificial recharge is a promising method for replacing water that is being withdrawn from aquifers. Although there are several water sources available, reclaimed agricultural, municipal and industrial wastewaters appear to be the water of choice for injecting into the underground reservoir. Frequently, the recharge capacity of wells decreases with time due to reductions in hydraulic conductivity of the aquifer material by suspended particles, eventually clogging the aquifer. Clogging is the retention of fine particles in a geological formation. This process causes a reduction in pore space, which reduces the aquifer s capacity to store and transmit water. The purpose of this study was to analyze the reduction of hydraulic conductivity in porous media due to retention of fine particles.

To meet the objective of this study, laboratory experiments were conducted. First relationships between hydraulic conductivity, porosity, and density of the porous media with respect to concentration of the particles in suspension were developed, using a constant head permeameter. Separately, a column test experiment was conducted. The sand column was packed homogeneously and a solution containing carbon fines was injected into the column. The water pressure head along the column and outflow were measured during the experiment. The changes in physical and hydraulic properties of the sand were calculated and compared with saturated soil properties at the start of the column test experiment. The results show that most of the carbon was captured in the first centimeter of the soil (69%) and hydraulic conductivity in this region was reduced up to 99%. About 98% of the total carbon injected into the column was entrapped in the

first three centimeters and no carbon could be detected after six centimeters of the sand column.

A numerical model was developed to solve the flow and transport equations and predict the clogging process seen in the column test experiment. This model used empirical equations developed from the laboratory experiments that relate concentration of the fine particles in suspension to physical and hydraulic properties of the porous media. Results from this study show that clogging of the porous media by fine particles is a nonlinear process but one that can be predicted by numerical modeling.

Hassan Vagharfard
Civil Engineering Department
Colorado State University
Fort Collins Colorado 80523
Fall 2001

ACKNOLEDGEMENTS

The author would like to express his sincere appreciation to his committee members: thanks to my advisor Dr. Neil Grigg for his help and support. I extend my special thanks to my co-advisor Dr. Deanna Durnford for her criticism, motivation, excellent guidance, and her valuable time she provided during this study. I am also grateful to my committee members Dr. Maurice Albertson, and Dr. David Zachmann for their time, support and valuable comments.

I extend my thanks to my friends Dr. Bahram Saghafian, Dr. Hamid Jalali-Farahani, Pyman Arasteh, and Alireza Zekavat for their friendship and support. And last but by far not the least my thanks and appreciation to my wife Leila, my son Mojtaba (Ali), my daughters Somayyeh, and Maryam Vagharfard for their sacrifices, support and understanding during my PhD study.

DEDICATION

To my parents
Ali Vagharfard and Khanoom-Bibi Gerashi

And

To my wife Leila Vagharfard,
my son Mojtaba and my daughters Somayyeh and Maryam

TABLE OF CONTENTS

Page

ABSTRACT 3

LIST OF TABLES 9

LIST OF FIGURES 10

LIST OF VARIABLES 12

CHAPTER ONE 17

INTRODUCTION 17
1.1 Description of the Problem 17
1.2 Objective 19
CHAPTER TWO 21

REVIEW OF SIGNIFICANT RESEARCH 21
2.1 Artificial Recharge 21
2.2 Clogging Mechanism 31
2.3 Capture Mechanism 41
CHAPTER THREE 48

LABORATORY MATERIALS AND METHODS 48
3.1 Laboratory Procedure 49
3.1.1 Properties of Poudre Sand 49
3.1.2 Properties of the Activated Carbon 51
3.2 Batch-test Method 53
3.3 Column-test Method 58
CHAPTER FOUR 68

NUMERICAL MODEL 68
4.1 Numerical Solution for Flow and Transport Equations 71
4.1.1 Formulation of the Equations 73
4.1.2 Solution Methods 77
4.1.3 Solution Procedure 80
CHAPTER FIVE 82

RESULTS AND DISCUSSION 82
5.1 Batch-Test 82
5.2 Column-Test 86
5.3 Computer Simulation 104

5.3.1 Retention Factor (R) 104
5.3.2 Evaluation 111
CHAPTER SIX 115

SUMMARY AND CONCLUSIONS 115
REFERENCES 123

APPENDIX A 128

DERIVATION OF FLOW EQUATION 128
APPENDIX B 140

DERIVATION OF SOLUTE TRANSPORT EQUATION 140
APPENDIX C 150

ONE-DIMENSIONAL COMPUTER PROGRAM LISTING 150
APPENDIX D 166

DATA BANK 166

LIST OF TABLES

Page

Table 2.1: Effect of different forces on clogging process of porous media 33
Table 3.1: Physical and hydraulic properties of Poudre Sand and Carbon 50
Table 4.1: Model input data 70
Table 5.1: Batch-test results 83
Table 5.2: Head values for the first six centimeter of the sample in the column 90
Table 5.3: Column test results for the first centimeter of the sample during the experiment 92
Table 5.4: Column test results for the second centimeter of the sample during the experiment 93
Table 5.5: Column test results for the third centimeter of the sample during the experiment 94
Table 5.6: Concentration profile data for different times during the experiment based on measured Δh and Eq 3.3 95
Table 5.7: Measured carbon distribution and properties of the sample at the end of the experiment 96
Table 5.8: Curve matching between model concentration and column test data to determine R in three centimeters of the column 107
Table 5.9: Parameter used as input data in Simulation Model 111
Table 5.10: Conductivity results from column test and model simulation for the first centimeter of the column 113
Table D1: Manometer levels in column test (cm) 167
Table D2: Computer output data 173

LIST OF FIGURES

Page

Figure 3.1: Particle size distribution of Sieved Poudre Sand 50
Figure 3.2: Schematic of the column test design 59
Figure 3.3: Photograph of the laboratory experimental set-up 63
Figure 3.4: Diagram of the experimental procedure 67
Figure 4.1: Simplified computer flow chart 69
Figure 4.2: Preissmann reference box scheme 79
Figure 5.1: Variation of measured hydraulic conductivity (K) with respect to concentration of the particles in suspension (C) 84
Figure 5.2: Correlation between relative hydraulic conductivity (K_0/K) and concentration of the particles in suspension (C). 84
Figure 5.3: Variation of porosity (n) with respect to concentration of the particles in suspension (C) 85
Figure 5.4: Variation of bulk density (ρ_b) with respect to concentration of the particles in suspension (C) 86
Figure 5.5: Variation of hydraulic heads with respect to distance in the column at t=12 hours 91
Figure 5.6: Variation of hydraulic heads with respect to time in the column 91
Figure 5.7: Carbon distribution in column test at the end of the experiment 96
Figure 5.8: Comparison between column test concentration at different times with measured concentration at the end of the experiment 98
Figure 5.9: Concentration profile in column test based on measured Δh to calculate the mass of carbon under the curve at t=11 hours 99
Figure 5.10: Comparison of calculated and measured conductivities in three centimeters of the sample for t=12 hours 100
Figure 5.11: Percentage reduction of conductivities in measured, and column test for the first centimeter at t=12 hours 101
Figure 5.12: Comparison of calculated porosity in column test with measured porosity at the end of the experiment at t=12 hours 102
Figure 5.13: Comparison of calculated density in column test with measured density at the end of the experiment at t=12 hours 103
Figure 5.14: Matched concentration profile from calibration model output and column test data at t=12 hours 108
Figure 5.15: Estimated values for parameters α and β in retention factor equation for three centimeters of the sample at t=12 hours 109
Figure 5.16: Nonlinear isotherm relationship between χ and C at t=12 hours 110
Figure 5.17: Comparison between model and column concentration for three centimeters of the sample at t=12 hours 112
Figure 5.18: Reduction of hydraulic conductivity with respect to time by column test and model simulation for the first centimeter of the sample 114

Figure 6.1: Estimated values for parameters α and β in retention factor equation for three centimeters of the sample at t=12 hours 120
Figure 6.2: Comparison of hydraulic conductivity from column test and model simulation 121
Figure. A1: Control volume for mass balance calculation in flow through porous media 136
Figure. B1: Control volume for mass balance calculation in transport phenomena 141
Figure B2: Nonlinear isotherm relationship between χ and C at t=12 hours 147

LIST OF VARIABLES

Symbol	Description
A	area of the interest (L^2)
A_s	geometric factor, function of porosity (dimensionless)
c'	volume of the particles / unit volume of the matrix (dimensionless)
C_s	sediment accumulation, volume of deposited or suspended per unit volume of the matrix (dimensionless)
C	mass of fine/mass of fine plus mass of sand (dimensionless)
C	concentration of fine particles in suspension (M/V)
C_i	initial concentration (M/V)
C_0	injection rate of the particles in suspension (M/V/T)
D^*	coefficient of molecular diffusion (L^2/T)
e	void ratio of sediment deposit (dimensionless)
g	gravity force (L/T^2)
H	Hamaker constant- the value is 10E-13 to 10E-14 (ergs)
H_L	head at the end of the column (L)
H0	measured head at zero centimeter from manometer #1 (L)
H1	interpolated head at one centimeter of the sample (L)
H2	measured head at two centimeters of the sample manometer #2 (L)
H3	interpolated head at three centimeters of the sample (L)
H4	interpolated head at four centimeters of the sample (L)

H5	interpolated head at five centimeters of the sample (L)
H6	measured head at six centimeters of the sample manometer #3 (L)
H(x)	value of head at point of interest in sand column (L)
H	length of the gravel pack (L)
Hi	initial head (L)
h	hydraulic head (L)
K′	the clogging rate constant (1/T)
k′	retention probability of the particles / unit of time (1/T)
K	saturated hydraulic conductivity (L/T)
K_0	initial saturated hydraulic conductivity (L/T)
K_c	hydraulic conductivity of carbon (L/T)
k_c	permeability of the clogged material (L/T)
L	length of the flow domain in well/column (L)
m_f	mass of fine particles (M)
m_s	mass of sand (M)
M	constant parameter in equation 5.5 (l/g)
M_{cv}	mass in control volume (M)
$\overline{M}$	mass rate in control volume (M/T)
$\overline{M_x}$	mass rate of solute transported in x-direction (M/T)
N	constant parameter in equation 5.5 (l/g)
n_0	initial porosity (dimensionless)
n_d	deposited porosity, is in the range of 0.4-0.5(dimensionless)

n	porosity (dimensionless)
p	pressure of water (F/L^2).
P_e	Peclet number (dimensionless)
Q	flow rate (L^3/T)
q	Darcy's velocity (L/T)
R	retention factor (dimensionless)
R_0	constant in retention factor equation (dimensionless)
r_v	distance from center of the well to place where clogging occurs (L)
r_0	borehole radius (L)
r_g	radius of the grain or porous medium (L)
r_p	radius of the particle or fines (L)
Sh	Sherwood number or coefficient of adsorption (dimensionless)
S_s	specific storage (1/L)
t	time (T)
t_{max}	maximum time to run the model (T)
v_s	sedimentation velocity (L/T)
V_v	volume of the voids (L^3)
V_b	bulk volume (L^3)
V_s	volume of solid (L^3)
V_{pm}	volume of porous media (L^3)
V_f	volume of fine particles (L^3)

V	seepage velocity (L/T)
V_{rp}	velocity of the retained particles (L/T),
V_0	superficial velocity of the suspension in the bed-flow rate / unit cross-section of the bed (L/T).
$\Delta h_v = h - h_0$	rise of water head in the well caused by clogging (L)
h	water head in the injection well above the static water level (L)
h_0	water head in the well resulting from the clean soil (L)
Δx	increment of L in the model, this should be a correct fraction of length (L)
α_p	compressibility of the aquifer by porous media (LT^2/M)
α_p	compressibility of the aquifer by carbon (LT^2/M)
α	parameter in retention factor equation (dimensionless)
β	parameter in retention factor equation (V_l/M)
β_w	compressibility of water (LT^2/M)
γ	parameter in hydraulic conductivity equation (V_l/M)
μ	parameter in porosity equation (V_l/M)
η	parameter in density equation (V_l/V)
ω	empirical constant (dimensionless)
ε	Accuracy factor (dimensionless)
θ	Crank-Nicholson weighting factor (dimensionless)
Ψ	Preissmann weighting factor (dimensionless)

λ	angle between vertical line and porous media column position
ρ_s	density of the solid (M/L^3)
ρ_l	density of the liquid (M/L^3)
ρ_f	particle density of fine (M/L^3)
ρ_b	bulk density of porous media (M/L^3)
ρ_p	particle density of porous media (M/L^3)
ρ_0	initial bulk density of porous media (M/L^3)
σ	retention, volume of deposited particles / unit volume of matrix (dimensionless)
σ_T	total stress (F/L^2)
σ_e	effective stress, the stress that is actually applied to the grain of aquifer material (F/L^2)
σ_{es}	effective stress caused by sand on aquifer material (F/L^2)
σ_{ec}	effective stress caused by carbon on aquifer material (F/L^2)

CHAPTER ONE

INTRODUCTION

1.1 Description of the Problem

The increasing world's population will cause a concurrent rise in demand for water. Overcrowded populations along with an ever-increasing development in both industry and agriculture will lead to the onset of a serious water shortage worsened by the fact that surface water today is often polluted by external sources and is quite difficult and expensive to purify. The high cost of storing natural precipitation is also a consideration that must be taken into account when dealing with problems pertaining to a worldwide potable water shortage.

A large percentage of precipitation will infiltrate into the world's underground aquifers. Approximately 97 percent of the world's potable water supply that is available for man's use occurs as groundwater. Groundwater supplies are second only to glaciers and ice caps (McWhorter and Sunada, 1977); hence, the importance of groundwater as a total water resource is unparalleled. Unfortunately, the natural replacement of our groundwater occurs over a long time period. Thus, usage of groundwater on a continual basis will inevitably cause a decline in the groundwater level. This is especially true if the rate of use greatly exceeds that of replenishment. There are numerous problems that

can occur as a result of decline in groundwater levels. Associated problems are increased pumping cost, soil subsidence, and salt-water intrusion.

Fortunately, groundwater resources are renewable and artificial recharge is a viable alternative that can be used when a water supply is present. Aquifers forming underground reservoirs are often a valuable asset for the storage of our world's water supplies. These reservoirs can also serve as natural water storage facilities and thus will help to alleviate some of the water shortages.

The future of artificial recharge of groundwater looks extremely good as dams are losing popularity and underground storage is becoming a major alternative for overcoming short-term, seasonal, or long-term differences between water supply and demand. Since the use of an infiltration basin requires the availability of adequate areas of permeable soils, vadose zones, unconfined aquifers, absence of contaminated zones and suspended solids (whose concentration should be low enough to avoid the need for frequent drying and cleaning the basin), the best alternative is well injection. Recently, there has been increasing interest in the use of larger diameter dry wells even for the recharge of unconfined aquifers (Bouwer, 1996).

Although there are several sources of water available for recharge, reclaimed agricultural, municipal, and industrial wastewater appears to be the water of choice. Wastewater must undergo advanced treatment prior to its use in groundwater recharge (Takashi, 1985). Currently thousands of injection wells are in operation throughout the world where treated water is injected into the aquifer through the injection wells. Studies show that some of these wells are losing their intake capacity and are no longer usable

because residual fines in water attach to the aquifer material causing a reduction in permeability and eventually clogging the injection well.

1.2 Objective

The purpose of this study is to analyze hydraulic conductivity reduction of aquifer material in artificial recharge wells due to carbon fines when treated water is injected into the aquifer. This phenomenon causes a reduction in recharge capacity often leading to the complete cessation of the well's use. Reduction of hydraulic conductivity is directly related to the concentration of suspended particles in porous media that varies with respect to space and time. The main purpose of this study is to predict the potential clogging of aquifer material by suspended particles.

Permeability has been shown to decrease with time owing to the following factors, percolating water releasing dissolved air into the pores, swelling of colloidal material, the growth of organisms in the pore space, the chemical effect of the flowing liquid upon the material, and finally the mechanical blocking by movement of the suspended particles in porous media. The only factor considered in this study is the mechanical blocking by suspended particles in porous media.

Many researchers have studied relationships between hydraulic conductivity and soil grain diameter proposing various theories and formulas, but comprehensive studies are needed to develop relationships between hydraulic conductivity, porosity, and density as functions of the influent concentration of particles in suspension and evaluate the potential clogging of the aquifer by suspended particles.

To meet the objectives of this study, the following process were undertaken:

1- Develop a relationship between hydraulic conductivity and concentration of the particles in suspension, K=K(C), using a constant head permeameter (batch test).

2- Derive flow and transport equations with hydraulic conductivity, porosity, density, and a retention factor as functions of concentration.

3- Develop a one-dimensional finite difference model to solve the flow and transport equations, using hydraulic conductivity, porosity, density and retention factor relationships mentioned above, and

4- Evaluate the results by comparing the computer model output with a data from laboratory column test.

In order to compare the calculated concentration of the particles in suspension with the measured concentration and compare the results with the model concentration, a column test was set up. This column consists of a plexiglass cylinder to enable visualization of particle movement through the column. Different sections of the column were analyzed for suspended particles and hydraulic conductivity at the end of the experiment. The mathematical formulation of the problem includes both partial differential flow and transport equations.

The groundwater flow equation is solved for head distribution and the solute transport equation is simultaneously solved for concentration of the particles. By relating these equations with hydraulic conductivity, porosity, density and retention factor equations, the rate of clogging is predictable. The computer model is a basic tool to help professionals to investigate the preliminary study of the clogging process of the aquifer caused by particles in suspension.

CHAPTER TWO

REVIEW OF SIGNIFICANT RESEARCH

The literature review consists of three sections: artificial recharge, clogging mechanisms, and capture mechanisms.

2.1 Artificial Recharge

Artificial recharge has received much attention recently from water resource researchers. Scientists have realized that reusing water, which is currently available, could ease the water shortage problem in the world, but this water needs to be treated before injection into underground reservoirs through recharge wells. In many cases, injection of treated water results in a loss of intake capacity of the well after a period of time because of suspended particles in water. The purpose of this dissertation is to analyze the problem of decreased intake capacity of injection wells due to suspended particles, which is the most common cause of clogging.

In recent years, the use of injection wells for artificial recharge has grown, although artificial recharge by the spreading method of surface water is the most common. However, it is easy to see why injection wells are popular. Injection wells have the advantage of by passing areas of low permeability and needing only a small area, which is critical in cities and renders them useful in other specific locations. In spite of the advantages, there are some limitations, and the most serious one is clogging.

Different factors contribute to clogging, but suspended solids seem to be the most common cause (Hutchinson and Randall, 1994).

If the composition of suspended matter is fairly constant and filtration by soil is highly efficient, it will usually generate a considerable increase in resistance per mass of deposited material causing the head loss. In water with low concentrations of suspended solids (e.g. drinking water), no relation exists between the concentrations and clogging of an injection well (Olsthoorn et al, 1982). Fortunately clogging is no longer an unsolvable problem, but it is one of the most important technical aspects of injection well application. Therefore, recharge wells may be considered a technical means to inject water into underground strata. Olsthoorn et al. (1982) suggested the following equation for finding clogging process of the aquifer matrix in artificial recharge wells:

$$\Delta h_v = \frac{Q}{2\pi k_v H} \ln\left(\frac{r_v}{r_0}\right) \qquad (2.1)$$

where:

$\Delta h_v = h - h_0$ rise of water head in the well caused by clogging (L),

h = change in water pressure head in the injection well above the static water level (L),

h_0 = change in water pressure head in well resulting from the clean soil (L),

H = length of the gravel pack (L),

k_v = clogged permeability (L/T),

r_v = distance from center of the well to place where clogging occurs (L),

r_0 = borehole radius (L).

The equation is valid as long as the Boltzmann variable $u=\frac{Sr^2}{4Tt}$ is ≤ 0.01. If the injection rate (Q) is held constant, T and S are constant and the water level rise varies with log of t/r^2. So after u drops below 0.01, the rate of water level rise in the injection and observation wells will vary with the log of time (Hutchinson and Randall, 1994). The method is based on Theis equation, and subject to all the standard assumptions in that equation, including aquifer homogeneity and uniform injection rate.

The clogging rate is measured by the water level difference (WLD) method. The water level in the injection well is always higher than in the observation well, but the rate of increase should be the same in both if no clogging is occurring. Experience shows that the rate of water level increase in the injection well is always greater than in the observation well, which shows that clogging is in progress.

Suspended particles tend to concentrate at the borehole wall and penetrate a few centimeters into the surrounding formation (Olsthoorn et al, 1982). The gravel pack surrounding the well screen corresponds to that of the first coarse layer of a multi-bed filter which traps the particles without appreciable increase in resistance. The gravel pack thereby relieves the formation wall where clogging is concentrated and provides a substantial reduction in the clogging rate. Sometimes the clogging rate does not lessen despite reduction in concentration of fines in water, because the pore spaces are already occupied by suspended particles and no more particles can infiltrate through the matrix.

Kovacs and Ujfaludi (1983) stated that the phenomenon of moving fine particles into the aquifer is called suffusion and mainly happens during aquifer recharge. Their experiment shows that soil suffusion occurs with an increase in flow velocity. At low

velocity, the fine particles maintain their original position and the flow can be described by Darcy's law that is valid as long as the Reynolds number does not exceed values between 1 and 10 (when flow velocity changes from laminar to turbulent). When the flow velocity increases to a critical velocity, the fine particles start to move, plugging the pores of the aquifer. If the flow velocity is raised again, the development of micro channels occurs and the fine particles will move into the aquifer causing the wall of the aquifer to become tighter, compact, and more stable. This allows clogging to occur and often the well becomes damaged and no longer usable.

Zappi et al. (1989) studied the contamination removal from groundwater by using activated carbon adsorption and then recharging the treated water into the aquifer through injection wells. This process was shown to decrease the well capacity after a period of time. The study was directed toward assessing the potential for clogging of the recharge well due to carbon fines and/or microbial fouling. They concluded that suspended solids and microorganisms are two probable factors causing the reduction in permeability.

Warner et al. (1992) used four trenches to study clogging in artificial recharge wells. The results indicated that two main factors were involved in clogging: suspended particles and microbial growth in the trenches. Observations made at the interface between the gravel and sand indicated that carbon fines moved only about 1.5 cm into the sand after passing through gravel pack and geotextile fabric, which was installed between gravel and sand (Namvargolian, 1992). Furthermore, some of the carbon was used as a food source by microorganism, adding to the problem. This work is predominantly applied to recharge trenches used for unconfined aquifers, but there are numerous wells in operation worldwide that are recharging both confined and unconfined aquifers.

An important difference between groundwater recharge by wells and that via ponds/trenches is that the entry velocity into the wells is approximately twice that of pools or trenches so the wells become clogged quicker. As a result, the risk of clogging is much greater with recharge wells because of the entry velocity, which are used on large scales in other sectors, particularly in oil recovery, deep well waste injection, and in water distribution industry.

The study by Dillon et al. (1994) emphasized injecting water into the aquifer by recharge well for storage and reuse. Injection of storm water and treated wastewater into the aquifer for reuse has become a very attractive means of enhancing water resources in urban areas. The area where aquifers are confined or semi-confined by overlying clay where recharge pond and channels are ineffective, injection wells are more appropriate and economical, but well injection is not sustainable due to clogging process over time. This study covers over 50 cases of artificial recharge wells worldwide that are injecting treated wastewater into the aquifers. In some cases, aquifers with little or no previous beneficial use have been transformed into valuable water resources in just a few years of operation (Dillon et al, 1994).

Clogging in or near a well is often a limiting factor in recharging an aquifer by injection well. Suspended particles, even low concentrations (<10 mg/l) can cause clogging of the pores as recharge progresses, particularly in fine media. The study shows that groundwater recharge via injection wells have been a successful technique for augmenting water resources around the world for many years (Dillon et al, 1994).

Hutchinson and Randall (1994) studied the correlation between well clogging rates, clogging potential, and aquifer hydraulic conductivity. In their field experiment,

the task was to examine the impact of clogging in injection wells to develop an optimal injection rate, redevelopment schedules, and pretreatment requirements for full-scale artificial recharge operations. They used membrane filter index (MFI), the test is done by passing water through a membrane filter at a constant pressure (30 psi) and recording the time that it takes for water to flow through the filter. Recording the total elapsed time after every 200 ml has passed through the filter until the flow rate has declined significantly. The membranes used are Millipore brand type HA (hydrophilic) that have 0.45 μm pores and 47 mm diameters. Water with high MFI has high clogging rate and water with low MFI has lower clogging rate.

Schippers, et al (1995) investigated clogging of recharge wells by suspended particles and microorganisms when water is injected into the aquifer. In practice, it is difficult to predict the clogging rate of these recharge wells. The modified fouling index (MFI) measured with membrane filters (0.45 μm pores) and the assimiable organic carbon content AOC (which is determined microbiologically by plating out and incubating a water sample for growth of bacteria) are valuable parameters with regard to the clogging potential of the water to be infiltrated. As they have mentioned, for reliable prediction of the clogging rate of recharge wells, these parameters prove to be inadequate.

The MFI and AOC methods show the clogging process in the filters, which the simulated clogging process occurs in an accelerated way. This work is mainly based on the ideas of Olsthoorn (1982) who suggested it is plausible that a correlation exists between the level of the modified fouling index (MFI) and the rate of increasing pressure drop in the recharge well as a result of particle deposition. In general, researchers

believed that bacterial growth played only a minor role in clogging when infiltrating water with low turbidity into the recharge well. There is no direct correlation has been found between the AOC content and the clogging rate (Schippers et al, 1995).

In this situation, the MFI was considered to be the general parameter for the clogging potential of water to be infiltrated. It was suggested by Schippers et al (1995) that lower MFI and AOC mean a lower clogging rate, but in reality, this is not the case (Schurmans and Steinmetz, 1984; Konijnenberg, 1984). The clogging rate cannot be reliably predicted on the basis of the MFI and the AOC content (Schippers et al, 1995).

The most important causes of clogging for which there is not yet an effective solution are:

1- the presence of particles in water to be infiltrated

2- the presence of assimiable organic material causing growth of bacteria in the soil.

Bouwer (1996) stated that the future of the artificial recharge of groundwater looks extremely good as dams are losing popularity and underground storage is becoming a major alternative for overcoming short-term, seasonal, or long-term differences between water supply and demand. Since the use of an infiltration basin requires the availability of adequate areas of permeable soils, vadose zones, unconfined aquifers, absence of contaminated zones and suspended solids (whose concentration should be low enough to avoid the need for frequent drying and cleaning the basin) the best alternative is well injection. Recently, there has been increasing interest in the use of larger diameter dry wells even for the recharge of unconfined aquifers.

In summary, the main problem with injection wells is clogging by suspended particles. Experience has shown that MFI and AOC are useful parameters to compare the relative clogging potential of the water, but they can not be used to predict clogging and declines in injection rates in actual recharge wells. Thus, full-scale studies on injection wells are still necessary to determine feasibility, design and operational criteria for actual recharge wells (Bouwer, 1996).

Practical aspects such as varying the flow of the water supply pipes to the recharge project, and the associated possibility of fluctuating suspended solids in the water for well injection can also play a major role in well clogging. The formation of biofilms in the pipelines during periods of low flow and the erosion of the biofilm during high flow cause the fluctuation of suspended solids (Bouwer, 1996).

The study by Frycklund (1998) concluded that a gradual decrease in infiltration rates has been seen over a period of a decade in infiltration pounds in Sweden. This indicated that long-term clogging is taking place below infiltration ponds. One of the reasons for clogging is the polluted surface water that is used for artificial recharge. In order to sustain drinking water production, the undesired compounds need to be removed in the initial stage of infiltration (i.e. in the filters). To attain knowledge about how to reach these goals, further research into the mechanisms involved in the retention and transport of various compounds through porous media is crucial. Clogging or plugging during recharge usually results in an increased head build up in an injection well, thereby changing the hydraulic characteristics of the well and severely restricting further injection of the wastewater is required (Rinck-Pfeiffer et al, 1998).

Frycklund (1998) pointed out that the literature dealing with the transport and retention of particles and colloids in porous media is quite voluminous. Handbooks (e.g. Hiemenz and Rajagopalan 1997) and work by McDowell-Boyer (1992), Harvey et al (1993), and Ryan and Elimelech (1996) are available. Despite the apparently thorough research carried out, the results are often difficult to generalize and make practical use (Harvey et al, 1993). In addition, the present modeling tools often have little practical value for predicting clogging development in natural systems (Hiemenz and Rajagopalan, 1997).

The study by Perez-Paricio and Carrera (1998) was focused on the water and soil investigation to obtain the basic parameters to identify the aquifer characteristics and to assess some clogging related properties. They believed that natural heterogeneity and main hydraulic conductivity couldn't be derived through laboratory analysis. Therefore, various field tests are being carried out. Tap water with chlorine was injected into the aquifer-storage and recovery (ASR) well, and two major issues were investigated, clogging and redox reaction.

The concentration of suspended particles is obviously low. Conventional techniques, such as membrane filtration (concentration of suspended solids) and turbidity measurement cannot provide detailed information for high quality water (Perez-Paricio, 1998). Instead, special optical method has been applied to obtain precise determination of the particle size distribution and mean value. Few tests were done in order to achieve the clogging potential:

1- Tracer test- these tests are essential to obtain travel time, assess interaction between aquifer material and non-conservative tracers, and monitor breakthrough curves for redox compound.

2- Long-term recharge test- the purpose of this test is to measure clogging-induced reductions of intrinsic permeability around ASR well, basically by retention of suspended particles.

3- Analysis of clogging material- just after stopping recharges an immediate pumping test was done to redevelop ASR well and to examine the composition of the clogging layer.

Perez-Paricio and Carrera (1998) concluded that when dealing with complex inter-related phenomena, as is the case in clogging, detailed characteristics of the artificial recharge well site is essential. Analysis of water and aquifer material provides evidence of the major issues, but is only through field tests that a reliable representation of the system can be drawn. The development of more elaborated mathematical models is essential to improve the performance of operating facilities, but it is also necessary from a conceptual point of view.

The concentration of suspended particles in recharge water might be low but large amounts of water are recharged during one recharge season causing an increase in the accumulation of suspended particles. Approximately 1000 kilograms of suspended solids will accumulate in and on the porous media in the vicinity of wells for every million cubic meters of water recharged. The retained and accumulated solid material causes

both a considerable declines in permeability and intake capacity of the well (Rebhun and Schwarz, 1968).

2.2 Clogging Mechanism

The term clogging of a porous media connotes the phenomenon of retaining fine solid particles in the porous media while liquid containing fines flows through the geological formation. Clogging is characterized by a reduction in a pore space of the aquifer, which can reduce the aquifer's capacity to store and transmit water. More than 70% of the injection wells reported some degree of clogging (Pavelic and Dillon, 1997).

In the final stage, the pores are completely filled with fine particles preventing further motion of such particles. The study of clogging and declogging is very important in order to know how the particles are retained in the aquifer. Larger particles appear to be fixed in porous media, whereas small particles appear to be detained temporarily. Clogging is one of the most troublesome phenomena concerning artificial recharge and different approaches exist in dealing with clogging (Perez-Paricio Carrera, 1998)

In the absence of chemical reactions in the well, when clogging by air or gas bubbles and bacteria can be excluded, suspended substances are the most common cause of clogging (Olsthoorn et al, 1982). The flow of suspensions through porous media is a natural occurrence since it often appears when water seeps into geological masses, the residual concentration of suspended particles depends upon the composition of untreated water.

The process that involves deposition of particles on an aquifer is called transport and attachment. In the transport step, particles are transported from the bulk of the liquid

to the substrate. Retention forces such as convection, gravitational and surface forces normally control the particles in transport. In the attachment step the particles are retained on porous media by direct interception and sedimentation (Herzig et al., 1970).

The flow of suspension through porous media is a very complex phenomenon due to the diversity of the mechanisms involved. Liquid-solid separation happens when particles are retained on porous media while flowing through. The particles are brought into contact with the possible retention site that normally stop or carried away by the stream. Deposition of suspended particles on the porous media will change the geometry and surface characteristics of the aquifer grains, and reduce the area available for water to flow, causing intake capacity reduction. Most natural waters contain a mixture of particle sizes that are transported toward the aquifer grain, which is due to the action of several forces.

The speed at which these particles are deposited on the grain depends on the nature and the magnitude of the mentioned forces. In order to solve the problem, the clogging rate must be related to the number of retained particles per unit of time and volume of porous media. These factors must be related to the various components that define the system, such as the carrier fluid consisting of flow rate, viscosity and density, as well as suspension of the particles such as concentration, particle size and shape.

It is well known that sedimentation moving through porous media causing clogging. However, the process by which clogging takes place has not yet been clearly defined (Sakthivadivel and Einstein, 1970).

Herzig et al. (1970) studied the clogging process in deep bed filtration and the mechanism of clogging and declogging in porous media, as well as the forces that are

involved in this phenomenon. The study shows two processes that cause particles to remain on the porous media and finally clog the aquifer are retention forces and capture process as shown in Table 2.1.

Table 2.1: Effect of different forces on clogging process of porous media

Type	Particle Size	Retention Forces	Capture Mechanism
Mechanical	$\geq 30\mu$	Friction,Fluid Pressure	Direct interception, Sedimentation
PC	$\leq 30\mu$	VDWF, EF	Direct interception
Colloidal	$< .1\mu$	VDWF, EF, CB	Direct interception, Diffusion

VDWF=Van Der Waal Forces PC=Physiochemical EF=Electrokinetic Force
CB=Chemical Bonding

The clogging of porous media is described mathematically by mass balance and kinetic equations. The latter describes the rate of clogging and declogging with the assumption that the removal of previously retained particles is negligible, as is usually the case. Although the mass balance equation is independent of the clogging mechanisms, the kinetic equation, which describes the rate of transfer of particles to the porous media, is a function of the elementary processes of this transfer. The kinetic equation of clogging may be written as:

$$\frac{\partial \sigma}{\partial t} = K'c' \qquad (2.2)$$

where:

$K' = k'n$ the clogging rate constant (1/T),

k' = retention probability of the particles / unit of time (1/T),

n = porosity (dimensionless),

σ = retention volume of deposited particles / unit volume of porous media (dimensionless),

c' = volume of the particles / unit volume of the matrix (dimensionless).

Rajagopalan and Tien (1979) studied the clogging process of porous media. In their research, they discovered that when the suspension flows through a granular bed, some particles under the influence of different forces may come into contact with the porous media and become deposited on the grains and onto already deposited particles. Consequently, the geometry, structure and surface characteristics of the grains will be changed. This affects the flow of suspension through the porous media that has a direct effect on the hydraulic conductivity of the aquifer.

The rate of deposition is largely determined by any of the transport mechanisms such as convection, gravity, diffusion, and Van Der Waals attraction (Rajagopalan and Tien, 1979; Kovacs and Ujfaludi, 1983).

$$Sh = .25\, A_S\, N_{LO}^{1/8}\, N_R^{15/8}\, P_e + .85E - 3\, N_G^{1.2}\, N_R^{4}\, P_e + A_S^{1/3}\, P_e^{1/3} \qquad (2.3)$$

where:

A_s = geometric factor (function of porosity),

Sh = Sherwood number or the coefficient of adsorption (dimensionless),

$P_e = \frac{Vd}{D^*}$ Peclet number (dimensionless),

d = diameter of the particles (L),

V = velocity (L/T),

D^* = coefficient of molecular diffusion (L^2/T).

The dimensionless equations are as follow (Ives, 1979):

Interception equation is:

$$N_R = \frac{r_p}{r_c} \tag{2.4}$$

where:

r_p = radius of the particle or fines (L),

r_c = radius of a grain of porous media (L).

Gravity and Buoyancy term is:

$$N_G = \frac{2 r_p^2 (\rho_p - \rho_f) g}{9 \mu V_0} \tag{2.5}$$

Van Der Waals attraction term is:

$$N_{LO} = \frac{H}{9 \mu \pi r_p^2 V_0} \tag{2.6}$$

where:

ρ_p = density of the particles (M/L^3),

ρ_f = density of the fluid (M/L^3),

μ = fluid viscosity (M/LT),

g = gravity force (L/T^2),

V_0 = superficial velocity of the suspension in the bed, which is the flow rate / unit cross-section of the bed (L/T).

H' = Hamaker constant, for most systems H' is about 10E-13 to 10E-14 ergs Visser.J (1972),

The first two terms on the right-hand side of equation 2.3 are for geometric interception and gravitational forces, an important concept for larger particles ($d \geq 1\mu$). The third term is convective diffusion of the particles ($dp \leq 1\mu$).

In the smooth coating of the porous media, the deposition increases the grain size of the porous media and decreases the macroscopic porosity, but the general shape of the porous media remains unchanged. The change in porosity is related to the amount of fines deposited. The deposition rate of fines on the aquifer material can be calculated (Rajagopalan and Tien, 1979 and Ives, 1979):

$$\sigma = (1 - n_d)[n_0 - n] \qquad (2.7)$$

where:

σ = deposition rate, volume of the particles retained per unit volume of the porous media (dimensionless),

n_0 = initial porosity (dimensionless),

n_d = deposited porosity, normally is in the range of .4-. 5 (dimensionless),

n = instantaneous porosity (dimensionless).

Perez-Paricio and Carrera (1998) stated that clogging is one of the most troublesome phenomena concerning artificial recharge. Different approaches exist in dealing with clogging, however, because clogging is affected by several mechanisms, a comprehensive model is not available. Clogging is a ubiquitous and may cause serious difficulty in artificial recharge systems, irrespective of specific conditions such as the water quality, aquifer properties or type of recharge system. This is why many studies have been conducted to improve our knowledge of this problem. But at least two main problems remain unsolved:

1- the basic mechanisms are not properly described from the quantitative point of view, especially with regards to the combined effects of different process.

2- its prediction is very complex task that extends beyond existing capabilities, as recognize by Pyne (1995). However, promising techniques are under continuous experimentation.

The author mentioned even the new and comprehensive model is available, but the limitations still exist. Uncertainties at field scales are numerous, as some microbiological and geochemical parameters and reaction are poorly understood.

Pavilic et al (1998) stated that clogging in an injection wells is a complex problem. Their study covers the effect of physical, chemical and biological on clogging process. The result shows that no chemical or biological had a significant effect on clogging, but there is some clogging by injected sediment, especially where sediment concentration is high. Clogging is characterized by a reduction in the pore space of the

aquifer, which can reduce the aquifer's capacity to store and transmit water. In some circumstances this may limit the viability of the artificial recharge operation. Therefore, any study on artificial recharge must at least consider the potential for clogging. For instance, a recent survey of current and historic artificial recharge practices by injection Aquifer Storage and Recovery (ASR) has shown that 70% of the injection wells report some degree of clogging even the water was with high quality (Pavelic and Dillon, 1997).

The method is used to measure the clogging rate is the water level difference (WLD) between the recharge and observation wells, which was first proposed by Olsthoorn, 1982. The method is based on Theis equation and so subject to standard assumptions, aquifer homogeneity and uniform injection rate. According to the Theis equation, during an injection event, the rate of piezometric head rise between these two wells should be equal if there is no clogging after some quasi-steady-state is reached. Therefore, any deviation from this behavior could be attributed to clogging. Of course, this clogging rate does not provide direct information on the type of clogging, nor its precise position in the aquifer.

In this experiment the sediment was injected into the aquifer. The data shows that virtually all of the injected sediment are retained and eventually settle within the pore space of the aquifer. The data also suggests that these injected sediments do not accumulate around the well, but penetrates further into the aquifer to distance, which airlifting (or perhaps any mechanical method to clean up) is ineffective in their removal. The continual rise in the peizometric head differences must be attributed to clogging of the aquifer between observation wells. The clogging rate depends on suspended solid concentration, temperature, injection rate and duration of injection.

The interest in the use of artificial recharge of pretreated surface water in deep sandy aquifers in the Netherlands for drinking water production has increased. To obtain an economically interesting operating process, clogging of the recharge well should be avoided as much as possible. For assessment of the clogging potential of water used for artificial recharge in deep sandy aquifers a set of tools was developed.

From the MFI and AOC of water the clogging rate of a recharge well cannot be predicted. For this purpose an experimental filtration device was developed, the Parallel Filtration Device (PFD). PFD consists of sand columns supplied with the pretreated surface water before infiltration. To simulate the clogging process in the aquifer, the sand columns are filled with material derived from the aquifer of the borehole or composed of sand material with the same hydraulic characters (grain size distribution) as the aquifer material. The head loss over the sand column is measured during operation at a constant filtration rate (flow rate controlled). The clogging process in the column is described using an appropriate filtration model and from estimated filtration constant the clogging rate in the aquifer is predicted (Schippers et al. 1995).

Slow Sand Filtration (SSF) is the last stage of the pretreatment process of the surface water. The treated water was injected into the underground reservoir by recharge wells in DIZON project in Netherlands. To predict clogging of the recharge wells and to investigate the effect on well clogging of using slow sand filtration (SSF) as the final pretreatment step. A laboratory simulation using Parallel Filtration Device (PFD) with four columns were conducted (Straatman et al, 1998).

The results revealed that the clogging rate in the recharge well could not be predicted by the PFD, the columns showed a significant smaller clogging rate than

observed in the recharge well. The clogging rate in the PFD columns was hardly observed even with a flow rate of 1 or 2 m/h was not as fast as the clogging rate in the recharge well. The permeability of the sand in the PFD columns was somewhat higher than the permeability observed direct surrounding of the recharge well (Hijnen et al. 1998).

Hijnen et al (1998) conducted another laboratory experiment with the more pretreated water. The pretreatment consisted of a full scale coagulation/filtration (COA/FIL) followed by a pilot plan with advanced oxidation (ozone and peroxide: AOP) and a post filtration either filled with anthracite sand filter (ASF) or with granular activated carbon (GAC) with PFD columns. The objective of this study was to verify the influence of the increase of the AOC concentration after oxidation on the clogging potential of the water. The experiment showed that the clogging rate in the PFD columns was higher compared to the clogging rate in the PFD columns supplied with drinking water with a low MFI and a higher AOC concentration. They concluded that:

1- the prediction of the clogging rate of a recharge well with a PFD is difficult.

2- The MFI and the AOC concentration of water are valuable parameters to estimate the clogging potential of water.

3- the clogging potential of water can be assessed more accurately when MFI and AOC are used with combination with the PFD using a standard filter medium.

4- Further research is necessary to select a filter and to elucidate the relationship between the clogging process in these PFD columns and in recharge wells.

2.3 Capture Mechanism

The capture processes (attachment step) enables particles to overcome any repulsive surface forces that may prevail near the substrate in order for contact to occur. The particle becomes deposited if it reaches the stagnation point. The stagnation point is located at the proximity of the grain where particles are held stationery, and the net forces on the particle are zero (Herzig, 1970).

Surface forces and particle velocity influences the attachment rate. In some instances, particles contacting the aquifer material can become permanently attached in the presence of favorable surface forces. Straining and interception due to geometry of the aquifer materials will also affect particle attachment rate. The attachment of the particles on the aquifer material increases the grain size and decreases the porosity, yet the general shape of the grain remains unchanged. A change in porosity of the aquifer material will affect both the pressure gradient and the deposition rate.

Each fluid has its own pressure and saturation that may create different flow velocities for both air and water. The effect of saturation on deposition of the particles has to be considered. The volume of captured particles increases with decreasing degrees of saturation due to the fact that in the case of unsaturated pores, the distance traveled by the particles is shorter than for those with saturated pores (Corapcioglu et al, 1984).

Once the particles are in close vicinity of the porous medium they might be captured because of their small size. This phenomenon is called interception. Interception and straining are not caused by any forces acting on the fines, but are due to the geometry of the particles and pore system (Rajagopalan and Tien, 1979).

If the size ratio (pore size to fine size) is between $7<d_p/d_f<15$, interception will occur and will clog the porous media after a period of time. For other ratios the fine would not enter into the pores and will stay on top of the soil, constructing a mat. Three mechanisms that bring the particles together are, thermal agitation of the suspension, the internal shearing that comprises the flow process, and the settling velocities that depend on the concentration of suspended material (Sakthivadivel and Einstein, 1970).

Yao (1974) suggests that the transport of suspended particles with $d_p>5\mu m$ occur mainly because of interception and sedimentation. Particles with $d_p<1\mu m$ diffusion are solely responsible for transport and particles with diameters of 1 or $2\mu m$ show a minimum transport efficiency. Particle accumulation causes an increase in interstitial velocity and hydrodynamic forces, these forces cause the breakaway of the retained particles that are less strongly attached (Mintz, 1967).

In the case of larger particles ($d \geq 30\mu m$), declogging is rare even when the fluid flow rate is increased by a factor of 3 or 4, and even with impulse or a sudden variation in velocity of the flow (Herzig et al, 1970). In water, the transport of particles larger than approximately 1 micron is accomplished by velocity gradients or fluid motion, and for smaller particles Brownian diffusion is effective.

If the particles have a density different from that of the liquid, they are subject to gravity and their velocity is no longer the same as fluid velocity (Herzig et al, 1970). Occasionally the particle density is exactly the same as the fluid density, but the particles are not able to follow the smallest tortuosities of streamlines (because of their sizes) and thus will collide with the wall of the convergent area of the pores. Sedimentation velocity is very important in transport of fines particles by water, the fall velocities of

dispersed particles are the basis of particle size distribution measurements and are easily measured in terms of the weight of the sediment.

In small clay particles, Brownian motion alone is nearly able to keep them in permanent suspension. The floc of such particles is sufficiently great and heavy enough to make them settle in still water, larger floc has a settling velocity measured in feet per hour. Deposition occurs not only in still water, but also in flowing water up to a flow velocity of 15 cm/sec.

Sakthivadivel and Einstein (1970) stated that sediment moving through a porous media causes clogging of the material. The mechanism of the deposition for small and larger particles is different, colloidal fines depend mainly on the surface properties of the suspended particles and the matrix, while the deposition of sediment particles (silt and sand) sizes will be mainly due to the mechanical behavior of sediment in the matrix. The critical parameter controlling the clogging or non-clogging of the porous media is the ratio of pore diameter of the matrix to the diameter of fine added to the system. When the fine diameter is equal or greater than half of the pore diameter, the fine will deposit on porous media and in time, completely clog the matrix. The study concluded that sediment accumulation in porous media primarily depends on the ratio of the pore size to the fine size, the liquid flow velocity, and the fine supply rate. This study affirmed the calculation of hydraulic conductivity in a vertical column as follow:

$$\frac{K}{K_0} = \frac{[n-(e+1)C_s]^3}{[1-n+(e+1)C_s]^2} \qquad (2.8)$$

where:

K = hydraulic conductivity of clogged matrix (L/T),

K_0 = hydraulic conductivity of clean matrix (L/T),

e = void ratio of sediment deposit (dimensionless),

n = porosity (dimensionless), and

C_s = sediment accumulation, volume of deposited or suspended per unit volume of the matrix (dimensionless).

They stated that equation 2.8 does not apply in the case of horizontal columns, because in downward flow when sediment suspension is going through a vertical column of porous media, the fall velocity of fine acts in the same direction as the average flow velocity when water flowing from top (inlet reservoir) to bottom of the column (outlet reservoir). As a result, sedimentation of the fines inside the matrix is not the primary factor causing clogging.

In horizontal columns when sediment suspension flows through a column of porous material, the fall velocity of fine is in a different direction than the average flow velocity. The pattern of deposition, clogging and sediment movement will be different from that of downward flow in a vertical column.

Ives (1979) developed the following equation to calculate sedimentation velocity:

$$v_s = \frac{d^2}{18\mu}(\rho_s - \rho_l)g \qquad (2.9)$$

where:

v_s = sedimentation velocity (L/T),

μ = dynamic viscosity (M/LT),

ρ_s = density of the solid (M/L^3),

g = gravity (L/T^2),

ρ_l = density of the liquid (M/L^3), and

d = diameter of the particle (L).

Simon's and Senturk (1992) developed another equation, which is basically the same as equation 2.9, they mentioned both equations work fine to calculate fall velocity of the particles as long as the diameter of the particles is less than 0.062 mm and large enough to overcome any Brownian movement.

In the case of small particles (approximately 1μ) calculations using this formula determine that sedimentation is negligible. Sedimentation does not occur if $(\rho_s-\rho_l)$ is small because the particles that are subject to gravity are moving with respect to carrier fluid and their velocity is not the same as fluid velocity due to different densities. For particles larger than ($d > 25\mu$) sedimentation will occur in the aquifer and both the effects of gravity and fluid drag influence the path of the particle. Colloidal particles have a diameter in the range of $1\mu > d > 0.001\mu$. They are large in comparison with a small molecule, but sufficiently small such that interfacial forces are significant in controlling their behavior.

Injecting water into underground reservoirs through recharge wells is viewed as a partial solution to minimize the society's water shortage. Injection wells are also used in

other sectors, for instance on large scales in oil recovery, deep well waste injection, and in water distribution industry. As summarized previously, clogging is one of the unfortunate realities of injection wells where more than 70% have reported some degree of clogging. In some cases clogging has caused wells to become obsolete.

An important difference between groundwater recharge by wells and that via pools, ponds, and trenches is that the entry velocity into the wells is approximately twice as large, which increases the rate of clogging in wells. As a result, the risk of clogging is greater with recharge wells. Clogging is affected by several mechanisms and different approaches have been practiced to eliminate the clogging process. As discussed previously, different theories and formulas have been suggested to minimize the clogging problem.

The rate of clogging has been calculated by a number of methods, including water level differences in recharge and observation wells (WLD) and the other methods of MFI and PFD. These methods mostly rely on similar principles. Researchers have argued that such methods have limitations and thus may not apply to anticipate the clogging process (Sakthivadivel and Einstein 1970, Schurmans and Steinmetz 1984, Konijnenberg 1984, Hutchinson and Randall 1994, Schippers et al 1995, Pyne 1995, Bouwer 1996, Hiemenz and Rajagopalan 1997, Pavelic and Dillon 1997, Frycklund 1998, Straatman et al 1998, Perez-Paricio 1998, Perez-Paricio and Carrera 1998, Straatman et al 1998).

The most important aspect of clogging is the reduction in hydraulic conductivity. Many previous investigators have studied the relationship between hydraulic conductivity and clogging, where most of the proposed conductivity functions were based on fixed diameter of the particle (Laroussi et al 1981; Puckett et al 1985; Shepherd 1989; Uma et

al 1989, and Mishra et al 1989). Unfortunately, only a few studies have explored the relationship between hydraulic conductivity and concentration of the particles in the influent. Because of the importance of concentration of the particles in suspension and the apparent lack of mathematical relationships between concentration of the suspended particles and hydraulic conductivity, this study will attempt to explore the clogging phenomenon in a laboratory setup and establish concentration versus conductivity relationships.

Clogging causes changes in both physical and hydraulic properties of the soil thus altering factors other than hydraulic conductivity (K), for instance retention factor (R), density (ρ), and porosity (n). The eventual outcome of such effects is that the soil becomes heterogeneous, a process that has been hardly discussed in previous studies. To enhance our understanding of the heterogeneity caused by clogging, the research presented herein will additionally explore changes in R, ρ, and n caused by varying concentration of the suspended particles in water. It is noted that the changes in these parameters with respect to space and time will significantly increase the complexity of the relevant flow and transport equations.

A computer model will be presented to solve the flow and transport equations by accounting for parameter modifications caused by heterogeneity. The model will utilize hydraulic conductivity, porosity, density, and retention factor equations (developed experimentally) to anticipate the clogging process of the recharge wells. In summary, the research presented herein is intended to extend the previous research by examining the noted deficiencies both experimentally and numerically. However, finding a comprehensive solution to the clogging problem will certainly require further research.

CHAPTER THREE

LABORATORY MATERIALS AND METHODS

The objective of this study is to analyze hydraulic conductivity reduction in aquifer material near artificial recharge wells due to suspended particles in influent water. A reduction in recharge capacity eventually can lead to the complete cessation of the well's use. Many researchers have studied relationships between hydraulic conductivity and soil grain diameter proposing various theories and formulas, but comprehensive studies are needed to establish the relationship between hydraulic conductivity and concentration of the suspended particles in influent water. Such relationships can be used to evaluate the potential clogging process of the aquifer material by suspended particles.

To meet the objective of this study, the following tasks were undertaken in the laboratory.

The relationship between hydraulic conductivity and concentration of the particles in suspension was developed using a physical model in the laboratory. The calculated concentration values from the column test were compared with measured concentration results after taking the column apart. The proposed equations were evaluated by comparing results from the computer model and column test.

3.1 Laboratory Procedure

3.1.1 Properties of Poudre Sand

Poudre Sand (also referred to as porous media) from Lafarge Company, Ft. Collins, CO is used in all laboratory experiments in this study. The sand was washed, oven dried, and sieved to remove clay and silt particles from the sample, retaining only the particles in the range from 0.075 mm to 2 mm. These are the limits of the sand range (Bedient, 1999). The sand was then washed again five times and soaked in dispersion agent (a solution of sodium hexamethaphosphate and water) with 40 g/l of solution for 12 hours. Following soaking the sand was washed an additional 12 times and passed through a 75-micron sieve to remove particles smaller than 75-micron. The sand was finally sieved for particle size distribution as shown in Figure 3.1. The physical and hydraulic properties of the sand are shown in Table 3.1.

The main reason for the above procedure is to be able to measure concentration of the fine particles at the end of the column test. This is considered an effective method to separate and measure the mass fraction of the suspended particles and porous media in the column test method.

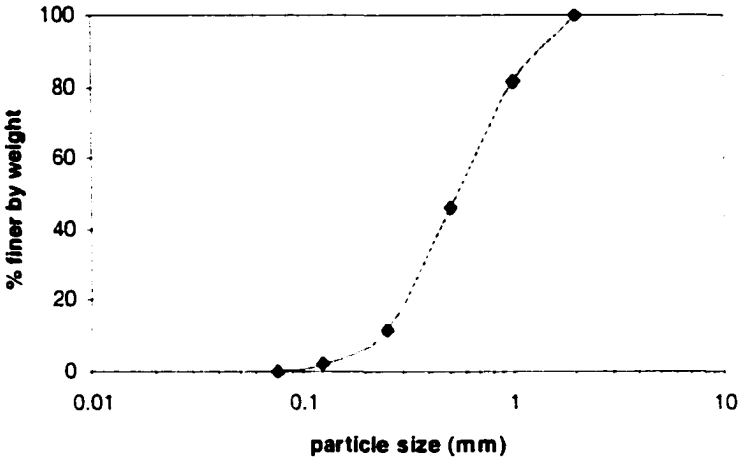

Figure 3.1: Particle size distribution of Sieved Poudre Sand

Table 3.1: Physical and hydraulic properties of Poudre Sand and Carbon

Sample	d_{50} (mm)	ρ_p (g/cm^3)[1]	ρ_b (g/cm^3)[2]	n	K (cm/sec)[3]
Sand	0.55	2.63	1.65	0.369	0.062
Carbon[4]	<0.03	2.17	0.59	0.68	0.0000062

1- ASTM method number D 5030
2- ASTM method number D 2937
3- ASTM method number D 2434
4- Calgon Carbon Company
d_{50} =diameter of the particles at 50%
ρ_p =particle density of the sample
K=hydraulic conductivity of the sample
ρ_b =bulk density of the sample
n=porosity of the sample

3.1.2 Properties of the Activated Carbon

The carbon (also referred to as suspended/fine particles) used in all laboratory experiments is Pulverized Activated Carbon (PAC) type BL (Calgon Carbon Co, Pittsburgh, PA). Properties are shown in Table 3.1. A suspension particle of this carbon was injected into the porous media column. Carbon and carbon compounds have been used in various ways throughout history as early as 1550 B.C. the use of charcoal in medicine is documented. Around 1800, wood char was first used to purify and decolonize cane sugar, a practice that is still in use today. In the mid-1800's, carbon was used in water purification.

Taste and odor of water for human consumption was the prime concern of researchers at the beginning of the 20th century. Research has shown that activated carbon is an important element for purifying industrial water of chlorine and other compounds. The advantages of using granular carbon are safety, availability, and cost effectiveness. Today granular activated carbon is commonly used to purify the world's water supplies (Hassler, 1974).

Carbon is an excellent adsorbent due to its large surface area that ranges from 500-2000 m^2/g. Activated carbon is a form of carbon that is achieved through a carefully controlled oxidation process that develops a porous carbon structure with a large surface area. This large surface area gives the activated carbon a high capacity to adsorb dissolved organic materials from water. The increased surface to volume ratio of carbon produces an extensive network of internal pores that are required for adsorption. High quality activated carbon should contain a high proportion of pores, which will

provide transportation of the adsorbate to the interior, as well as a sufficiently large internal surface.

Adsorption takes place mostly within the porous network. Larger pores ($d_p \geq 5000$ A°) extend through the length of the whole particle and the fine pores are contained within the larger pores. The large pores serve as a pathway to transport adsorbate material from the external surface to the interior of the particle where the finer pores adsorb them readily. Such surfaces are accessible to those small molecules, which can enter the micro pore ($d_p \leq 40$ A°) area. Micropores provide most of the surface area for adsorption. The minimum pore diameter for an adsorbate should be no less than 10 A°.

Carbon treatment is a physio-chemical process that removes a wide variety of contaminants by adsorbing them from liquid and gas streams. This treatment is most commonly used to separate organic contaminants from water or air; it can also be used to remove a limited number of inorganic contaminants GAC (EPA, 1991). Although different methods have been utilized in the treatment of groundwater, the Environmental Protection Agency (EPA) has chosen granular activated carbon (GAC) as a mandated technique for water treatment. It is considered feasible according to the 1986 amendments (EPA, 1991). The purpose of these amendments is to establish GAC as a baseline technology for the removal of synthetic organic chemicals (Clark and Lykins, 1989).

3.2 Batch-test Method

The batch test method is a constant head permeameter test designed to measure the effect of different carbon concentrations added to the sieved Poudre Sand on hydraulic conductivity. Reduction of hydraulic conductivity (K) in a porous media is assumed to be a function of concentration of the suspended particles in water (C) according to the following proposed equations. The hydraulic conductivity equation with respect to total mass fraction of fines in porous media (C) that is used in batch test method is as follow:

$$K = K_0 e^{-\omega C'} \tag{3.1}$$

where:

C = mass fraction, mass of fines per mass of sand plus fines (dimensionless),

K = saturated hydraulic conductivity (L/T),

K_0 = initial saturated hydraulic conductivity (L/T),

ω = empirical constant (dimensionless).

The following conversion equation can be used to calculate the concentration of suspended particles in volume of water from the mass fraction of fine particles in porous media.

$$C' = \frac{Cn}{1000\rho_b} \tag{3.2}$$

where:

C = mass of fine per mass of sand plus fine (dimensionless),

C = concentration of particles in suspension (g/l),

n = porosity of porous media plus fines (dimensionless), and

ρ_b = bulk density of porous media plus fines (M/L^3).

Note that n and ρ_b vary with the mass of retained fines. Now the conversion factor equation (Eq 3.2) is substituted into equation 3.1 with new parameter (γ) to get the final proposed hydraulic conductivity equation with respect to concentration of the particles in suspension (C) that is used in this research is:

$$K = K_0 e^{-\gamma C} \tag{3.3}$$

where:

K = saturated hydraulic conductivity (L/T),

K_0 = initial saturated hydraulic conductivity (L/T),

C = concentration of the particles in suspension (M/V_l),

γ = empirical constant (V_l/M).

To evaluate equation 3.3 and calculate the parameter γ, a strong correlation between hydraulic conductivity and concentration of the suspended particles should be achieved experimentally.

In the batch test method, a constant head permeameter (made of clear plexiglass 5.2 cm in diameter and 18 cm in height) was constructed in the laboratory to measure the saturated hydraulic conductivity of Poudre Sand uniformly mixed with known amounts of carbon particles. To achieve near field conditions, the flow rate (Q) was calculated

and kept constant (Q=25 ml/min) with Reynolds number (Re=0.11) using the average diameter of the sand d_{50} =0.55 mm.

To prepare the permeameter, the sand was weighed and carefully packed to keep the bulk volume of the sand constant (V = 301.61 cm^3). Multiple samples (sand plus carbon) were prepared for the permeability test with a constant amount of sand and varying amounts of carbon. The mass of carbon added to the sand varied from 0 to 10% (in increments of 1%) of the mass of the sand. This yielded a total of 11 permeability tests with samples having varying degrees of carbon mass. The samples were prepared by evenly distributing the carbon fines through the column to get the most uniform mixing of carbon throughout the sand. Since the volume of all samples and the mass of sand remained the same, the increasing amounts of carbon fines added to each sample resulted in an increasing sample density and decreasing porosity.

The sample (sand plus carbon) was first slowly saturated from the bottom using deaired water with an initially low flow rate of 7 ml/min to minimize entrapped air in the sample. A set of preliminary experiments using tap water resulted in significant amounts of entrapped air, undesirably affecting conductivity. For that reason deaired water was used throughout this experiment. The sample was saturated for one hour with Q=7 ml/min before the flow rate was increased slowly to the desired 25 ml/min.

In most cases, steady state flow was achieved in about 10 hours during which data were collected every half an hour. Data consisted of flow rate and hydraulic head gradient between the ends of the sample. Darcy's equation was then utilized to calculate saturated hydraulic conductivity for each sample. The calculated results are used herein to justify the experimental form of equation 3.3.

A plot of hydraulic conductivity versus concentration of the fines (K vs. C) will be discussed and compared to other test results in chapter 5. The other objective of the batch test experiments was to calculate the fitting parameter γ in equation 3.3. This parameter was calculated by taking the log of equation 3.3 plotted on a semi-log paper, γ is the slope of the best fit to the line, which will be discussed in chapter 5.

Soil porosity is affected by concentration of the fine particles in water. When finer particles are retained between larger particles, porosity is reduced.
To calculate the variation of porosity as a function of concentration of the fine particles the following general porosity formulas is used:

$$n = \frac{V_v}{V_b} \qquad (3.4)$$

$V_v = V_b - V_s$ volume of the voids (L^3),

$V_s = V_{pm} + V_f$ volume of solid (L^3),

V_b = bulk volume (L^3),

V_{pm} = volume of porous media (L^3),

V_f = volume of fine particles (L^3).

Replacing volumes in Eq 3.4 with mass and density variables, after some mathematical manipulation, yields:

$$n = 1 - \frac{m_s}{\rho_p V_b} - \frac{m_f}{\rho_f V_b} \qquad (3.5)$$

where:

m_f = mass of fine (M),

m_s = mass of sand (M),

ρ_p = particle density of sand (M/L^3),

ρ_f = particle density of fines (M/L^3).

Equation 3.5 is used to calculate porosity with different percents of fine particles and estimate the parameter μ. The following equation is used in the model to simulate the variation of porosity with concentration of the particles in suspension:

$$n = n_0 - \mu C \qquad (3.6)$$

where:

n = porosity of the sand plus fines (dimensionless),

n_0 = initial porosity of the sand (dimensionless),

C = concentration of the particles in suspension (g/l),

μ = constant parameter (l/g).

Bulk soil density is increased by concentration of the particles when suspended particles are retained in pore spaces. The following equation shows the relationship between density of the porous media and concentration of the particles in suspension:

$$\rho = \rho_0 + \eta C \qquad (3.7)$$

where:

ρ_b = bulk density of the sand with fines (g/cm^3),

ρ_0 = initial bulk density of the sand (g/cm^3),

C = concentration of the particles in suspension (g/l),

η = constant parameter (l/cm^3).

The particle density was measured by the water-displacement method, which is the oven-dried mass divided by the volume displaced by the solid particles. Volume of the solid particles is measured by volume of water displaced in a graduated cylinder when one adds some solid particles to the specific amount of water (Freeze and Cherry, 1979).

3.3 Column-test Method

The column test was used to compare the calculated concentration of the particles in suspension with measured concentration (after taking the column apart). Further more the column test results were used to match the concentration profile (C vs. x) to estimate values for parameters α and β in the retention factor equation (Eq 3.9), which were required by the Simulation Model.

The porous media column consists of a plexiglass cylinder with dimensions of 68 cm in length and 10.16 cm in inner diameter. The first and last 2 cm of the column are used as inflow and outflow reservoirs. The remainder of the cylinder (64 cm) is filled

with the sieved Poudre Sand with known physical properties (Table 3.1). The movement of suspended particles, the pattern of the deposition, and interaction of sediment particles with the matrix during the experiment can be observed through the clear plexiglass.

Figure 3.2 presents a schematic of the column test. Two removable plexiglass plates with multiple 3.25 mm openings are installed on both ends of the column to contain the sand and separate the sand from the reservoirs. All sections are screwed together. Sixteen manometers, 4 cm apart are installed in eight sections of the column with an extra manometer installed at the inlet of the column to measure the head distribution.

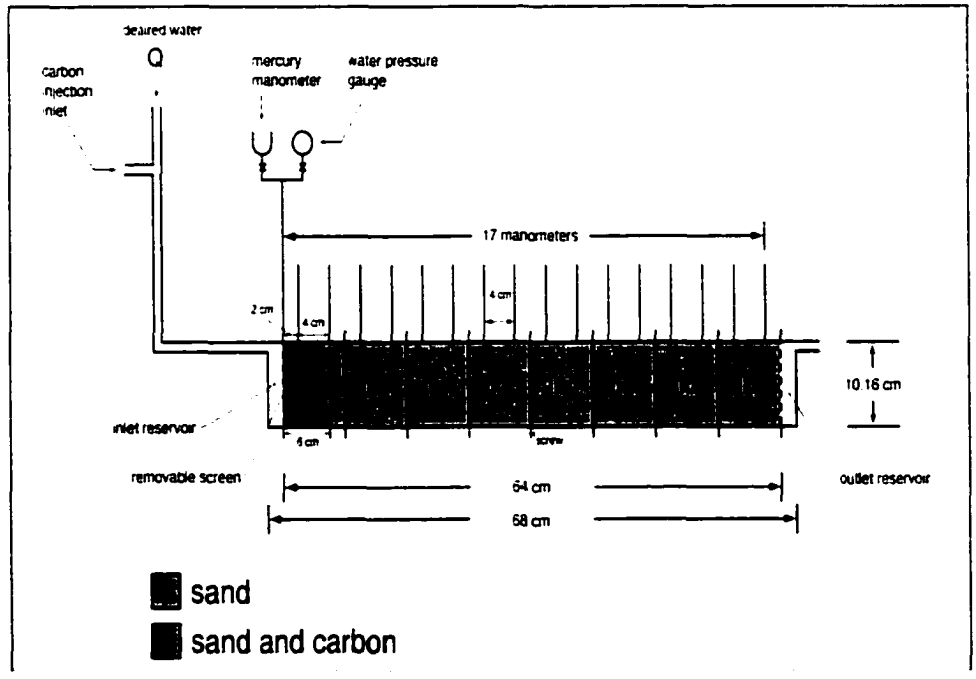

Figure 3.2: Schematic of the column test design

The column was packed by dry rainers. The mass of the sand to be filled in the column was first calculated from the desired density (ρ_b=1.65 g/cm^3) of the sand and volume of the column (V=5.19 l). The total mass of the sand in the column was 8.56 kg.

The rainer used in this study was a piece of pipe about 4 feet in length and 2 inches in inside diameter with a screen mesh installed inside and halfway down the pipe. When pouring the sand from the top into the porous media column through the rainer, the sand would be distributed evenly and become uniformly packed, since faster moving particles are slowed down by the screen mesh. Following packing, deaired water with a low flow rate (7 ml/min) was introduced through the bottom of the column as it remained in a vertical position for two days to saturate the sand completely. The manometers were all closed. A vacuum was applied to the column and slowly saturated from the bottom in order to minimize air entrapment.

The column was then carefully positioned horizontally for the rest of the experiment to better simulate a field situation and minimize the effect of settlement of the fine particles. The driving forces are the water pressure and gravity forces (depends on the position of the column) while the resistance is the friction force. These forces have some effects on the particles depending on the position of the porous media column. When the column is vertical, the gravity and resistance forces (if the water is flowing from bottom up) are in the same direction causing the particles to settle faster at the inlet, but when the column is horizontal (λ=90°), the effect of these forces are minimized since the gravity and resistance forces act perpendicular to each other.

The flow rate was kept constant (Q=100 ml/min) with Reynolds number equal to 0.11. The sedimentation velocity was calculated by using equation 2.9. In this

calculation, the average diameter of the carbon particles was used (d=0.03 mm), because the average diameter of the particles was smaller than 40 micron. This was determined by passing the carbon solution through the filter number 4 (20-25μ) by Whatman Company and observing that some of the fine would pass through the filter. For this reason the average diameter was taken as 30 microns. The Stokes law (Simon and Senturk, 1992) was used to calculate the velocity of the particles in suspension, the value calculated was v_s =0.06 cm/sec.

The seepage velocity (V) for the fluid was calculated from a Darcy velocity (q) equal to 0.02 cm/sec and initial porosity of the Sieved Poudre Sand equal to 0.369, which the velocity of the fluid would become almost equal to 0.06 cm/sec the same as particle velocity. The effect of the forces on the particles would be minimal and sedimentation would not occur, because of the following reasons:

1- The particles velocity and seepage velocity are almost the same ($v_s = V_l$ =0.06cm/sec)

2- The bulk density of the carbon is less than water density, carbon particles would float in water

3- The average particle diameter of the carbon is less than 40 micron

4- Sedimentation does not occur since the density difference between particle and liquid is very small

5- A preliminary experiment was conducted by making the carbon particles in suspension (carbon plus water) in a container and leaving it for several days to settle the particles by gravity. It took more than three days to settle some larger particles but not all, the small particles remained in suspension.

The carbon fine with deaired water was injected into the horizontal column using a 0.64 cm inner diameter tube, at a constant flow rate of 100 ml/min. The experiment ran for 82 hours (from beginning of carbon injection t=0.0 hours to the time column was taken apart t=82 hours). It was anticipated that the pressure head would rise particularly in the first manometer, so both mercury and water pressure gauges were installed at the inlet of the column to be able to shift from one to another if needed. Indeed this expected situation happened during the course of the experiment forcing a change from using the water manometer tube to the mercury gauge and finally to water pressure gauge in order to record the pressure heads in the first manometer.

Two Masterflex pumps (Cole Palmer Company, Chicago, Illinois) were used to inject deaired water with carbon particles in suspension into the column. Pulverized activated carbon type BL with the physical and hydraulic properties given in Table 3.1 was used in this experiment. Preliminary experiments (batch test) were run with different percentages of carbon (1-10%, M/M) mixed with sand to determine the most appropriate percentage of carbon to start the column test (prototype of the real situation in short time). This was done because it takes years for porous media to clog, particularly if the concentration of particles in suspension is low when recharging the aquifer. Based on the batch test experiments, 6% carbon was chosen for this experiment. The amount of carbon to be injected into the porous media column was calculated to be 30 g/day.

The carbon was mixed with deaired water in the barrel with a stirrer to prevent settling, and then it was injected into the column test with a pump at the constant rate of 100 ml/min with concentration of 0.25 g/l for 12 hours. The experiment continued for

the next 70 hours. It is assumed that no carbon concentration is gone into the sand after 12 hours from beginning of the injection, but settled in the screen, tubes and reservoir. This assumption is made based on observation, comparing the physical and hydraulic properties of the sample (K, n, C, and ρ) in column test with batch test and measured data after taking the column apart. A photo of the experimental set up is shown in Figure 3.3.

Figure 3.3: Photograph of the laboratory experimental set-up

During the experiment, following injection of carbon into the porous media column, the hydraulic head was measured and recorded hourly in all seventeen manometers and also the flow rate was measured prior to hydraulic head data collection. The temperature of the influent water was kept at 18 ° C, the same as the antecedent water temperature. Hydraulic conductivity in each section of the column could be calculated directly from the column test at any time during the experiment by knowing the cross section area of the column (A), distance between the manometers (ΔL), head difference from the manometers (Δh) and the flow rate (Q). Thus from Darcy's law K is:

$$K = \frac{Q}{A}\frac{\Delta L}{\Delta h} \qquad (3.8)$$

The hydraulic conductivity of the sand in different sections of the column is a function of the concentration of carbon particles in that section. Since the hydraulic conductivity, initial hydraulic conductivity and value of parameter γ (batch test) are known, the concentration of the particles in suspension was calculated by using (Eq 3.3). The data is tabulated and presented later in Table 5.3.

At the end of the experiment (t=82 hours), the last set of manometer data were recorded prior to disassembling the column. At this point without adjusting the pump to keep the flow rate constant (Q=100ml/min) the heads start falling to the same place the experiment had started and the outflow was measured it was 7.5 ml/min. The comparison between the clean sand outflow (Q=100 ml/min) at the beginning of the column test experiment with plugged sand outflow (Q=7.5 ml/min) at the end of the experiment

before taking the column apart shows a reduction of 92.5% intake capacity of the porous media.

Different sections of the column were separated to measure the concentration of the particles in each section. The carbon could be detected in only the first 6 cm of the sand column. For this reason, the rest of the saturated sand in the column was ignored during analysis. The procedure for measuring concentration in each centimeter of the porous media column is as follow:

1-The sample (sand plus carbon) was collected from each centimeter by scrapping the column that was marked in one centimeter sections prior the sample collection.

2-The sample was soaked for 24 hours. Following soaking, the sample was passed through 75-micron sieve to separate the carbon and water from the sand, this step was repeated several times until there were no more carbon fines with the sand.

3-The carbon and water was filtered through filter paper grade 413 with particles retention of 5 micron (VWR Company, Media, PA) to separate the carbon from the water.

4-The filter plus carbon was dried in an oven at 110° C for 24 hours.

5-The weight of the filter paper was subtracted from the total weight (carbon plus filter) to get the mass of carbon in that centimeter of the column.

6-The sand left on the sieve from step 2 for each centimeter was oven dried separately (110° C) for 24 hours and weighed.

7-The mass fraction of carbon retained with respect to dry mass of sand (C') in that centimeter of the sample was measured.

8-The conversion factor (Eq 3.2) is used to get concentration of the particles in water.

9-The data are tabulated in Table 5.7 and the carbon distribution is shown in Figure 5.7.

As a result of retaining fine particles on porous media, the velocity of the suspended particles would be slower than seepage velocity by a factor R, this phenomenon is called retention and quantified by a retention factor (R). The physical significance of the retention factor is that it measures how much slower the particles migrate than the water. If the retention factor is small, the particles gradually occupy a larger part of the flow domain and if R gets larger, it means more fines are retained on porous media, which has direct effect on the particle movement. The following equation is used to calculate a retention factor:

$$\frac{V}{V_{rp}} = R = 1 + \alpha[\exp(\beta C)] \qquad (3.9)$$

where:

V_{rp} = velocity of the retained particles (L/T),

V = seepage velocity (L/T),

R = retention factor greater than one (dimensionless),

C = concentration of the particles in suspension (g/l),

α = empirical parameter (dimensionless),

β = empirical parameter (l/g).

The values for parameters α and β are calculated by computer simulation that can be used as input data for the model.

Figure 3.4 shows the summarized laboratory tests conducted in this study, which are referred to as Batch-tests and Column-tests.

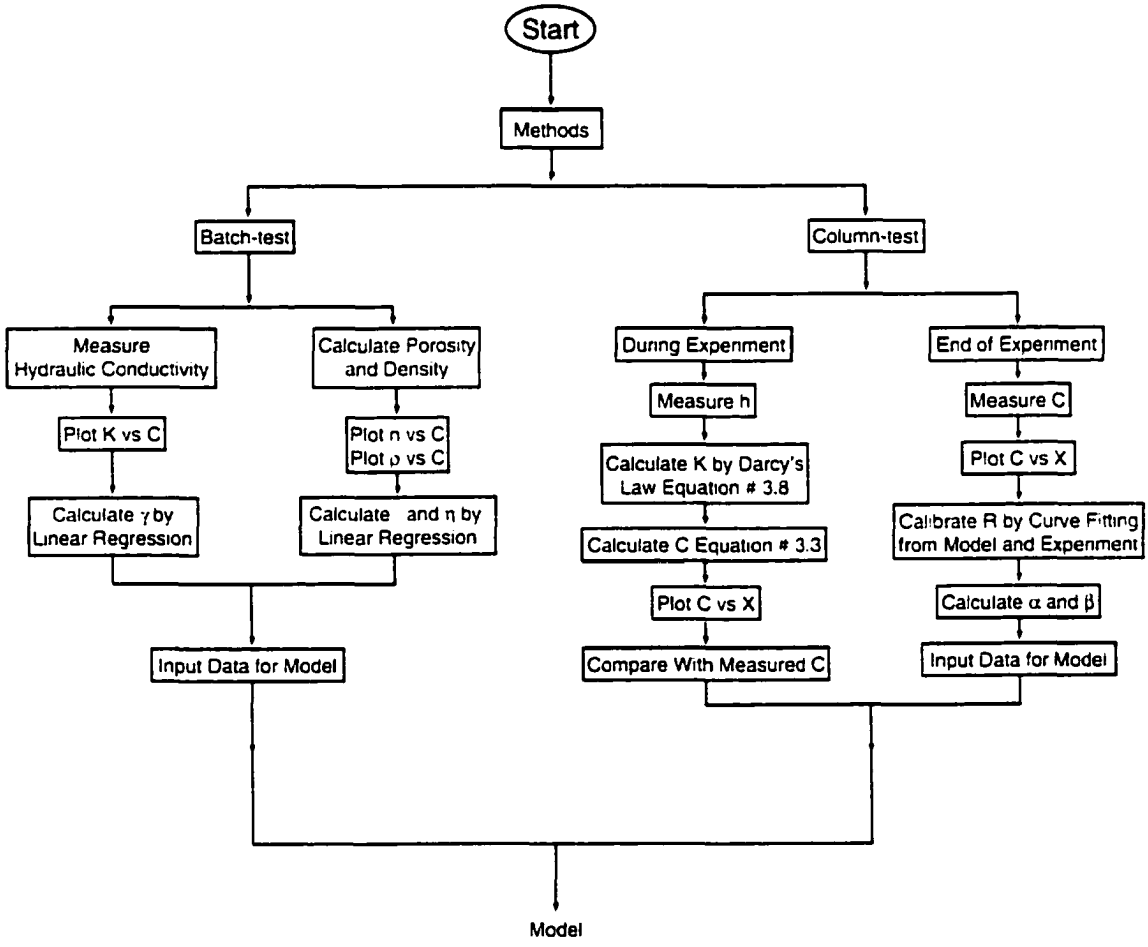

Figure 3.4: Diagram of the experimental procedure

CHAPTER FOUR

NUMERICAL MODEL

To evaluate the results from the experiment, a computer model was developed to solve the appropriate groundwater flow and transport equations. The computer model is in FORTRAN 90, which simulates one-dimensional unsteady transport of fine particles moving by advection in a heterogeneous porous media. The computational domain is a column that is positioned horizontally.

The model derives flow and transport equations with hydraulic conductivity, porosity, density, and retention factor equations. The flow equation (Eq 4.1) is solved for the head distribution to calculate seepage velocity, using seepage velocity to solve the transport equation (Eq 4.2) for concentration of suspended particles in water (C). The new concentration is used to calculate new values for hydraulic conductivity (K), porosity (n), density (ρ), and retention factor (R). The model repeats the same process with new values for K, n, ρ and R at each time step and the results obtained from the numerical solution were compared with experimental data to evaluate the clogging process of the aquifer. A simplified flow chart is shown in Figure 4.1.

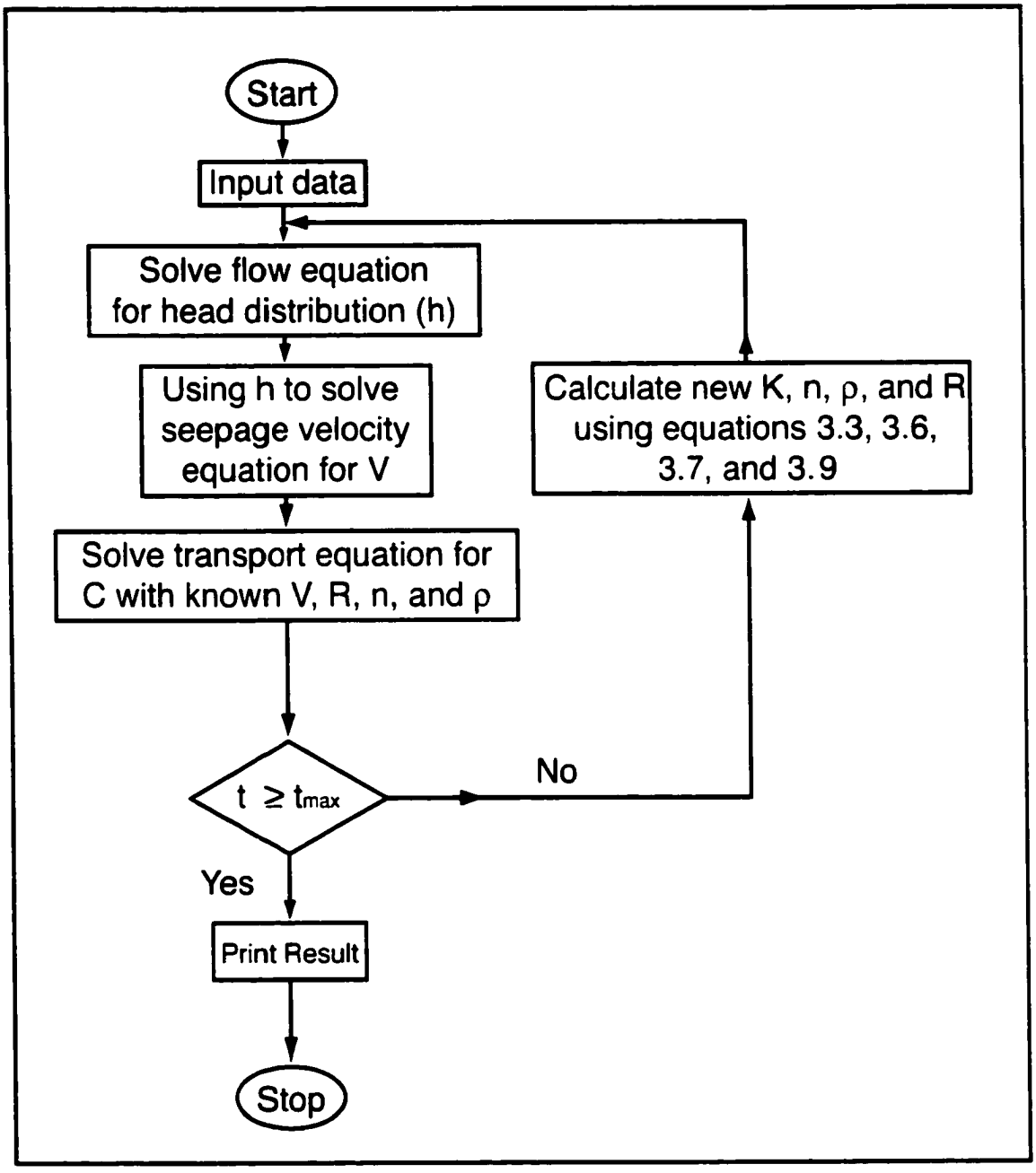

Figure 4.1: Simplified computer flow chart

The input data for numerical simulation is selected based on the physical model and laboratory experiments. The carbon concentration in the column at the beginning of the experiment is assumed to be zero because the porous media is clean. Also assumed no chemical reaction, radioactive decay and no microorganism growth are present in the system. Model input data requirements and variables are summarized in Table 4.1.

Table 4.1: Model input data

Parameters	Description
L	length from beginning of porous media to the point of interest (L)
Δx	increment of L, this should be a correct fraction of length (L)
R_0	constant value in retention factor equation (dimensionless)
K_0	initial hydraulic conductivity (L/T)
n_0	initial porosity of porous media (dimensionless)
ρ_0	initial bulk density of porous media (M/L^3)
μ	parameter in porosity equation (l/g)
γ	parameter in hydraulic conductivity equation (l/g)
α	parameter in retention factor equation (dimensionless)
β	parameter in retention factor equation (l/g)
η	parameter in density equation (l/cm^3)
Ψ	Preissmann factor values between (0.5-1)
θ	Crank-Nicholson factor equal to 0.5
ε	Accuracy factor
S_s	specific storage (1/L)
C_0	injection rate of suspended particles in influent water (g/l/s)
C_i	initial injection concentration to calculate C_0 (g/l)
t_{max}	maximum time to run the model
Hi	initial head (L)
C(x,0)	initial concentration for clean soil (g/l).

4.1 Numerical Solution for Flow and Transport Equations

The governing equations consist of a one-dimensional partial differential flow equation in x-direction that describes the potentiometric head distribution in porous media and a one-dimensional transport equation, which determines concentration in relation to the average linear velocity (seepage velocity). The form of the developed flow equation (Equation A37) is as follow:

$$\frac{\partial}{\partial x}(K\frac{\partial h}{\partial x}) = S_s \frac{\partial h}{\partial t} \tag{4.1}$$

where:

K = hydraulic conductivity (L/T),

h = piezometric head (L),

S_s = specific storage (1/L).

and the transport equation (Equation B26) is developed as:

$$\frac{\partial}{\partial t}(RC) + \frac{\partial}{\partial x}(CV) = 0.0 \tag{4.2}$$

where:

C = concentration of the particles in suspension (g/l),

R = retention factor (dimensionless),

V = seepage velocity (L/T).

Advection is the component of solute movement attributed to transport by the flowing groundwater. The rate of transport is equal to the average linear groundwater velocity:

$$V = \frac{q}{n} = \frac{I}{n}\left(-K\frac{\partial h}{\partial x}\right) \qquad (4.3)$$

where:

q = Darcy's velocity (L/T),

n = porosity (dimensionless).

The following equations are used in the model to calculate hydraulic conductivity, porosity, density, and retention factor as function of concentration of the particles in suspension.

$$K = K_0 e^{-\gamma C} \qquad (4.4)$$

$$n = n_0 - \mu C \qquad (4.5)$$

$$\rho = \rho_0 + \eta C \qquad (4.6)$$

$$\frac{V}{V_{rp}} = R = 1 + \alpha[\exp(\beta C)] \qquad (4.7)$$

where:

V_{rp} = velocity of the retained particles (L/T),

V = seepage velocity (L/T),

ρ_b = bulk density of the porous media (M/L^3),

n = porosity (dimensionless),

β,γ,μ = constant parameters (l/g),

η = constant parameter (V/V),

α = constant parameter (dimensionless),

C = concentration of the particles in suspension (g/l),

K = saturated hydraulic conductivity (L/T),

K_0 = initial saturated hydraulic conductivity (L/T).

4.1.1 Formulation of the Equations

Equation 4.1 is a parabolic partial differential equation (PDE) and equation 4.2 is a hyperbolic PDE. The above equations must be linearized in order to be able to solve them numerically. The average hydraulic conductivity $\overline{K}$ (in each cell) and mean average linear velocity $\overline{V}$ are substituted into the equations instead of K and V.

$$S_s \frac{\partial h}{\partial t} = \overline{K} \frac{\partial^2 h}{\partial x^2} \tag{4.8}$$

$$\frac{\partial C}{\partial t} + \frac{\overline{V}}{\overline{R}} \frac{\partial C}{\partial x} = 0 \tag{4.9}$$

To solve equation 4.8, an implicit finite difference method backward in time is used (Wang and Anderson, 1982):

$$\frac{\partial h}{\partial t} = \frac{h_i^{J+1} - h_i^J}{\Delta t} \qquad (4.10)$$

Implicit formulation will often use a weighted average of the approximation at J and J+1. The weighted parameter is presented by θ, and it lies between 0.0 and 1. The time step J+1 is weighted by θ and time step J is weighted by (1-θ) in the following equation (Eq 4.11). The value for parameter θ is selected by modeler. if θ=1 the space derivatives are approximated at J+1 and the scheme is fully implicit and if θ=0.5 the scheme is called Crank-Nicholson (Bedient et al. 1999). The weighted-central in space is used to discretize the space increment in equation 4.8 as follow:

$$\frac{\partial^2 h}{\partial x^2} = \theta \frac{h_{i+1}^{J+1} - 2h_i^{J+1} + h_{i-1}^{J+1}}{\Delta x^2} + (1-\theta)\frac{h_{i+1}^{J} - 2h_i^{J} + h_{i-1}^{J}}{\Delta x^2} \qquad (4.11)$$

After substituting equations 4.10 and 4.11 into equation 4.8 and some algebraic manipulation, the final discretized flow equation is:

$$h_i^{J+1} = \frac{1}{\frac{1}{2}\frac{\Delta x^2}{\Delta t}\frac{S_s}{\bar{\bar{K}}} + \theta}\left[\theta \bar{h}_i^{J+1} + \frac{1}{2}\frac{\Delta x^2}{\Delta t}\frac{S_s}{\bar{\bar{K}}} h_i^J + (1-\theta)\left(\bar{h}_i^J - h_i^J\right)\right] \qquad (4.12)$$

The arithmetic mean of the head is:

$$\bar{h}_i^J = \frac{h_{i+1}^J + h_i^J}{2} \qquad (4.13)$$

The harmonic mean of hydraulic conductivity is as follow:

$$\overline{K} = \frac{2K_i^j K_{i-1}^j}{K_i^j + K_{i-1}^j} \qquad (4.14)$$

It is reasonable to use the harmonic mean of hydraulic conductivity $\overline{K}$ instead of K in equation 4.1, because the hydraulic conductivity is a function of concentration, since the concentration is the function of space and time so K is the function of space and time too. Hydraulic conductivity is not a point position in porous media like head (h); it is the average of the total volume of the pore space in that section.

To discretize equation 4.9, the Preissmann box scheme, which is an implicit scheme is used (Abbotte and Basco, 1989). The weighted-backward in time is as follow:

$$\frac{\partial C}{\partial t} = \frac{\psi}{\Delta t}\left(C_{i+1}^{j+1} - C_{i+1}^{j}\right) + \frac{(1-\psi)}{\Delta t}\left(C_i^{j+1} - C_i^{j}\right) \qquad (4.15)$$

and the weighted-backward in space is:

$$\frac{\partial C}{\partial x} = \frac{\theta}{\Delta x}\left(C_{i+1}^{j+1} - C_i^{j+1}\right) + \frac{(1-\theta)}{\Delta x}\left(C_{i+1}^{j} - C_i^{j}\right) \qquad (4.16)$$

After substituting equations 4.15 and 4.16 into Eq.4.9 and some simple mathematical manipulation we get:

$$\Delta t = \frac{\psi\left(C_{i+1}^{j+1} - C_{i+1}^{j}\right) + (1-\psi)\left(C_i^{j+1} - C_i^{j}\right)}{-\frac{\overline{V}}{\overline{R}}\frac{\theta\left(C_{i+1}^{j+1} - C_i^{j+1}\right) + (1-\theta)\left(C_{i+1}^{j} C_i^{j}\right)}{\Delta x}} \qquad (4.17)$$

In which ψ and θ are spatial and temporal weighting factors. The final discretized transport equation is:

$$C_{i+1}^{j+1} = \left\{ \left[\frac{\overline{V}}{\overline{R}} \frac{\Delta t}{\Delta x} \theta + \psi - 1 \right] C_i^{j+1} + \left[\psi - (1-\theta) \frac{\overline{V}}{\overline{R}} \frac{\Delta t}{\Delta x} \right] C_{i+1}^{j} + \left[1 - \psi + (1-\theta) \frac{\overline{V}}{\overline{R}} \frac{\Delta t}{\Delta x} \right] C_i^{j} \right\}$$

$$/ \left(\psi + \frac{\overline{V}}{\overline{R}} \frac{\Delta t}{\Delta x} \theta \right) \qquad (4.18)$$

the average seepage velocity is taken in two time levels at j and j+1:

$$\overline{V} = \theta V_i^{j+1} + 0.5(1-\theta)\left(V_i^j - V_{i-1}^j\right) \qquad (4.19)$$

and the harmonic mean of the retention factor is:

$$\overline{R} = \frac{2R_i^j R_{i-1}^j}{R_i^j + R_{i-1}^j} \qquad (4.20)$$

Seepage velocity Equation (Eq 4.3) is written at each nodal point instead of mid-cell position. Arithmetic mean of fluxes in two adjacent mid-cells to compute Darcy velocity and then seepage velocity is:

$$V_i^j = \frac{K_i^j}{n_i^j \Delta x} \left[\frac{K_{i-1}^j \left(K_i^j + K_{i+1}^j\right)\left(h_{i-1}^j - h_i^j\right) + K_{i+1}^j \left(K_i^j + K_{i-1}^j\right)\left(h_i^j - h_{i+1}^j\right)}{\left(K_i^j + K_{i-1}^j\right)\left(K_i^j + K_{i+1}^j\right)} \right] \qquad (4.21)$$

The reason for using this method is to calculate the seepage velocity (V) at the beginning and end of each cell instead mid-cell, because the variation of the heads (directly related to concentration of the particles) are recorded on an hourly bases in the laboratory experiment from beginning and end of the cells, now h and V are calculated from the same position in the column, which is effected by concentration (C).

4.1.2 Solution Methods

To solve the flow equation, upstream (inlet reservoir) and downstream (outlet reservoir) boundary conditions of the column are needed because the governing equation is a parabolic PDE, whereas for solute transport domain only the upstream (inlet reservoir) boundary condition of the column is needed because it is a hyperbolic PDE. In the flow domain, computation is done in a fixed computational grid but in solute transport domain, a moving downstream boundary condition is assumed. Preissmann box scheme also called Four-Point implicit scheme (Figure 4.2) is used to discretize concentration domain, but solution procedure is semi-implicit. Implicit schemes are unconditionally stable and the Priessmann box scheme is suggested to solve hyperbolic PDE's that have kinematics properties means the particles are moving with the groundwater velocity (Abbotte and Basco, 1989).

To solve the solute transport equation, the seepage velocity (V) is required. It is assumed that the flow equation is already solved and the velocity (V) is calculated and can be used in solving the transport equation. The flow model yields heads from which the seepage velocities are obtained (Kinzelbach, 1986). The flow and solute transport equations are solved iteratively.

To solve the flow and transport equations iteratively, fixed Δx is used for solute transport domain and the equation is solved implicitly for each time step. On the other hand, in fixed grid along a physical model the measured hydraulic head can be compared with numerical results. The initial and boundary conditions are:

Initial Conditions:

$C(x, 0) = 0.0$

$K(x, 0) = K_0$

$h(x, 0) = \text{known}$

Boundary Conditions:

$h(0, t) = H_0$

$h(L, t) = H_l$

$C(0, t) = C_0$

Boundary condition may be used as source of contaminant in groundwater aquifer at a specified concentration (Bedient, 1999). The injection rate of influent solution (C_0) can be calculated by having the initial concentration (C_i). The equation that is used to calculate the injection rate is as follow:

$$C_0 = \frac{C_i Q}{nbA} \qquad (4.22)$$

where:

C_0 = injection rate (g/l/s),

C_i = initial concentration (g/l),

n = porosity (dimensionless),

b = length of the screen in saturated zone (L),

A = area of the perimeter of the wells (L^2).

Solution of advection equation yields a sharp concentration front. In this process, the flow is advection dominated and that dispersion is neglected, which is known as plug flow (Bedient et all, 1994). The retained particles occupied most of the pore spaces.

The column-test experiment showed, due to adding more fines to the system the porous media is no longer homogeneous, because most of the fine particles were captured in first two centimeters and the rest was distributed throughout the next four centimeters of the column, so the porous media became heterogeneous.

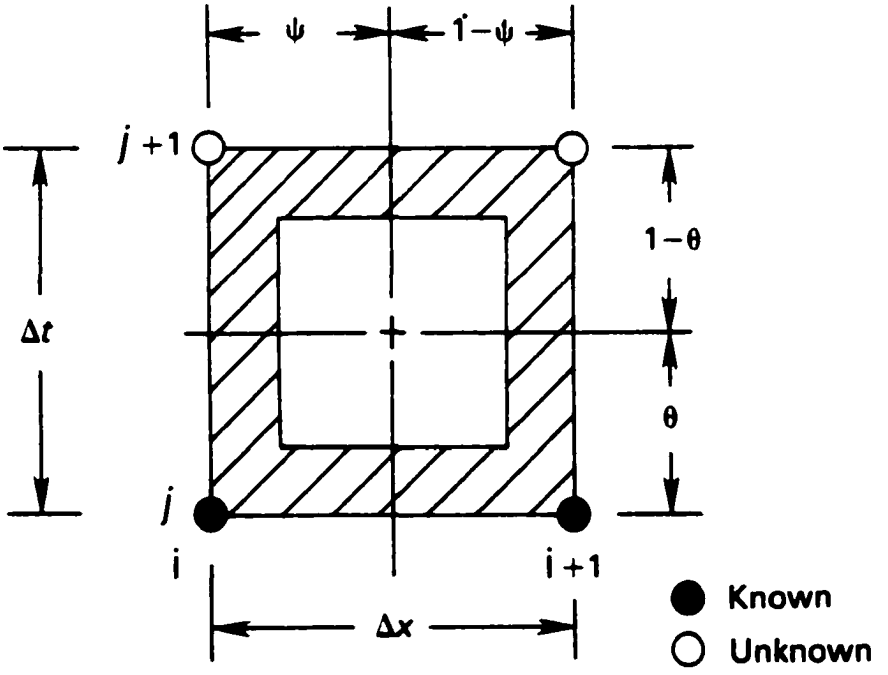

Figure 4.2: Preissmann reference box scheme

4.1.3 Solution Procedure

In first time step (start of injection) flow domain is known from initial conditions, thus the contamination domain can be solved. All variables in equation 4.9 that depend on j^{th} time level are known from initial conditions too. Values of V at time level j+1 are also known based on first assumption, the assumption that the flow and transport equations can be solved individually is called freezing (flow equation is solved first and the result is used in solving the transport equation, this method is used here because the model has to solve two different equations with different boundary conditions). On the other hand, C_i^{j+1} from inlet or left boundary condition ($C_0^{\ 1}$) and distance step (Δx) from flow domain is known. Also C_{i+1}^{j+1} is equal to zero ($C_i^{\ 1}$=0 0) because advancing front has not reached to the node i+1. Therefore, in the first time step the only unknown variable is the time step itself, which after substituting all known values into discretized equation, the equation can be solved by explicit method (this is one of the advantages of this model). Thus in the first step of computation, contamination domain includes only one cell in the grid.

After solving the transport equation for one time step, flow equation must then be solved because flow is affected by concentration of the particles at the first node. The effect of concentration on the flow domain is known by determining potentiometric heads. After solving the flow equation for all nodes to calculate new potentiometric heads, transport equation must be solved for next time step.

The difference between this step and the last one is that in this step two cells contribute in the computational procedure. Two equations must be simultaneously solved for these two cells, because for the second time step $C_i^{\ 2}$ and Δt are unknown. Following

finding these unknowns again one can solve flow equation by the same procedure described above. This sequential solving procedure repeats until the advancing front reaches the end of computational domain or until the time reaches the maximum time limit of the model. Note that at each step of advance phase a cell is added to the contamination domain.

CHAPTER FIVE

RESULTS AND DISCUSSION

5.1 Batch-Test

5.1.1 Calculation of parameter γ in hydraulic conductivity equation

The primary objective of the batch test experiment was to determine the dependence of hydraulic conductivity, porosity, and density on concentration of the particles in suspension. The results from the batch test experiment show that hydraulic conductivity and porosity decrease while the density increases with increasing carbon concentration. In these experiments, various percentages of fines were added to the sand while keeping the volume of the column constant, thus increasing the soil density and reducing the porosity. This has a direct effect on hydraulic conductivity by reducing the cross sectional flow area.

The batch test results are given in Table 5.1 indicating that the values of hydraulic conductivity change some order of magnitude by adding a few percent of fine to the system, consequently changes the homogeneous material to heterogeneous. Figure 5.1 presents saturated hydraulic conductivity (K) versus concentration of the carbon particles in suspension. Hydraulic conductivity decreases more than two orders of magnitude from 0.062 to 0.0002 cm/sec when up to 10% carbon (M/M) is added to the sand. Figure 5.2 shows the plot of natural log of the ratio of measured initial hydraulic conductivity to

hydraulic conductivity ($\ln\frac{K_0}{K}$) versus concentration of the particles in suspension (C). A strong correlation (r^2=0.9216) supports the form of equation 3.3.

The other objective of the batch test experiments was to calculate the parameter γ in equation 3.3. This parameter is the slope of the line in Figure 5.2, yielding a γ value of 0.0118 l/g for sieved Poudre Sand. The concentration of the particles should be in units of g/l when using the constant value of 0.0118 l/g for γ.

Table 5.1: Batch-test results

C (M/M)	C (g/l)	K (cm/sec)	ρ_b (g/cm^3)	n
0	0.0000	0.06200	1.65	0.369
0.009901	45.550	0.03700	1.67	0.363
0.019608	93.345	0.01400	1.69	0.355
0.029126	142.69	0.00500	1.70	0.347
0.038461	194.56	0.00360	1.72	0.340
0.047619	249.57	0.00130	1.74	0.332
0.056604	307.48	0.00110	1.76	0.324
0.06542	365.28	0.00080	1.77	0.317
0.074074	427.71	0.00042	1.79	0.310
0.082569	495.41	0.00023	1.80	0.300
0.090909	562.77	0.00020	1.82	0.294

C = mass fraction-mass of carbon per mass of dry sand plus carbon (M/M)
C = concentration of the particles in suspension (g/l)
K = saturated hydraulic conductivity (L/T)
ρ_b = bulk density of the sand plus fines (g/cm^3)
n = porosity of the sand plus fines (dimensionless).

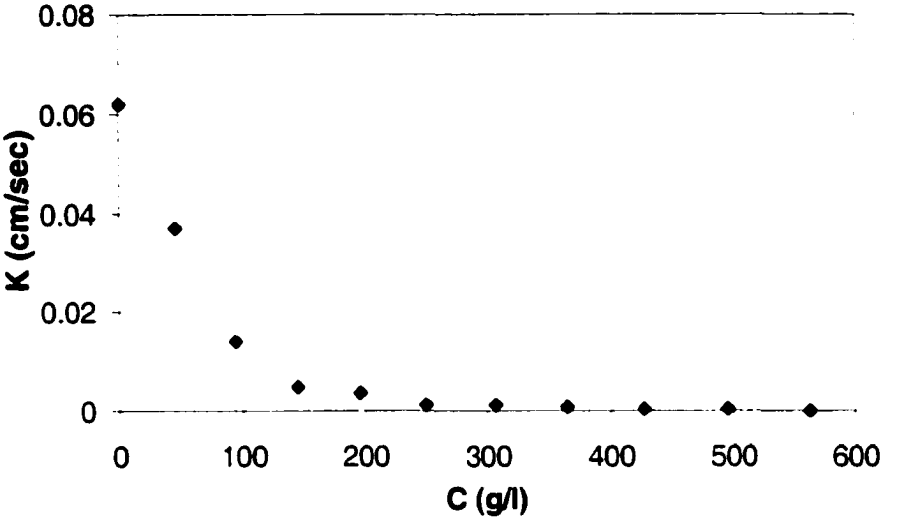

Figure 5.1: Variation of measured hydraulic conductivity (K) with respect to concentration of the particles in suspension (C).

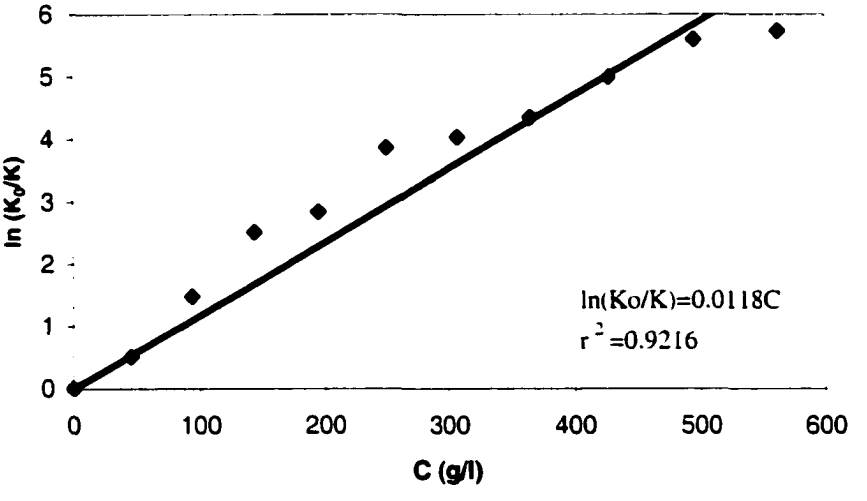

Figure 5.2: Correlation between relative hydraulic conductivity (K_0/K) and concentration of the particles in suspension (C).

5.1.2 Calculation of parameters μ and η in porosity and density equations

The same procedure as in previous section was used to estimate values for parameters μ in porosity equation (Eq 3.6) and η in density equations (Eq 3.7). Soil porosity decreases with increasing concentration of the particles in suspension. The calculated values for porosity (Table 5.1) were plotted versus concentration of the carbon particles in suspension to estimate parameter μ. The value for parameter μ in equation 3.6 was found to be 0.0001 l/g (r^2=0.9964). Figure 5.3 shows that the porosity decreases with increasing concentration of the particles in suspension.

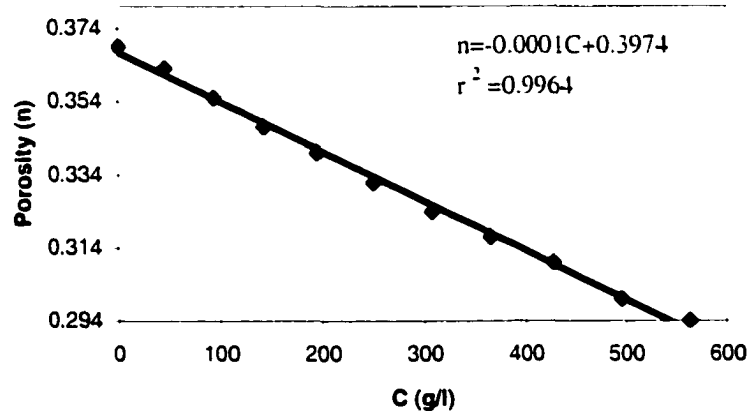

Figure 5.3: Variation of porosity (n) with respect to concentration of the particles in suspension (C)

Soil bulk density was also affected by concentration of the fine particles in suspension. The density was measured by adding percentage (0-10%) of mass of fines to the porous media in a constant volume of a container. The simple density equation (ρ_b=m/v) is used to calculate the bulk density. The bulk density of porous media

increases with respect to concentration of the particles in suspension. Figure 5.4 shows the density values (Table 5.1) plotted with respect to concentration of the particles in suspension to estimate parameter η. The value for parameter η in equation 3.7 was found to be 0.0003 (r^2=0.9889).

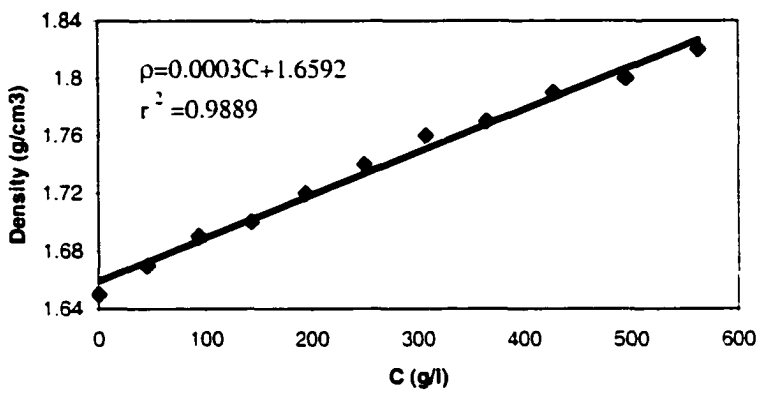

Figure 5.4: Variation of bulk density (ρ_b) with respect to concentration of the particles in suspension (C)

Parameters γ=0.0118 l/g (r^2=0.9216), μ=0.0001 l/g (r^2=0.9964), and η=0.0003 (r^2=0.9889), in hydraulic conductivity (equation 3.3), porosity (equation 3.6), and density (equation 3.7) respectively are used in the numerical model.

5.2 Column-Test

The column test was used to compare the calculated concentration of the particles in suspension with measured concentration (after taking the column apart). Further more the column test results were used to match the concentration profile (C vs. x) to estimate values for parameters α and β in the retention factor equation (Eq 3.9), which were

required by the Simulation Model (Appendix C-C2). After ensuring a steady state of deaired water flow through the horizontal column (Q=100 ml/min), the first set of initial pressure head and inflow/outflow data were collected to compute the initial saturated state of the sand profile.

The suspension of carbon fines was then introduced into the column (t=0). Visual observations showed fine particles moving through the porous media with a sharp and clear interface and the manometers showed rapid changes in pressure heads as the carbon front started to move into the sand. The inflow (carbon and water) continued for 82 hours with no visible carbon fines moving beyond the 2.5 cm of the sand after 12 hours of injection (the last measured data for interface recorded), but precipitation did occur in the tubes, inlet reservoir and screen.

The data used to analyze the clogging process of the sand in the column test includes all data up to 12 hours from beginning of the injection. There is no evidence that any more carbon fines entered the column after 12 hours of injection, but the pressure head dramatically increases in the first manometer, which indicates blocking has occurred.

5.2.1 Measurement of pressure head in manometers

The head distribution showed a very sharp drop in pressure head between the first manometer (manometer #1 at x=0.0 cm) and the second manometer (manometer #2 at x=2 cm) in the sand. The first manometer was connected to a mercury pressure gauge after 12 hours of injection and the head difference between first manometer (at x=0.0 cm) and second manometer (at x=2 cm) was recorded to be about 83 cm. The head difference

kept increasing and approached the limit of the mercury gauge at 986 cm. It was then necessary to shift the first manometer to a water pressure gauge (18.5 hours after beginning of carbon injection).

The carbon particles were retained in the first three centimeters where a sharp solute front was clearly observed during the experiment. The solute front could be observed three hours (t=3) following start of injection of carbon fines at about 1 cm into the sand and at about 2.5 cm after 12 hours. From that point on, it is assumed that no significant carbon moved into the column. The interface was not observed visually to continue into the column for the rest of the experiment. The explanation is that the porous media was almost clogged by this time such that no fines in the influent cell could go through the Poudre Sand anymore, yet the pump was still injecting water into the column with a constant flow rate of 100 ml/min.

It was observed that most of the carbon precipitated in the tubes, reservoir and screen, causing the pressure at the inlet to rise dramatically to 34.5 psi and the head difference between points at x=0 and x=2 cm to rise about 2400 cm. Table D1 (Appendix D) shows the manometer levels in the column test.

5.2.2 Estimation of unknown heads in column test

In order to analyze the clogging process in first six centimeters of the sample in the column test (the area between manometers #1 at x=0.0 cm and #3 at x=6 cm from the beginning of the column test), which contained the carbon fines, only the pressure head data collected from three manometers at distances 0, 2 and 6 centimeters from the inlet of the column were considered out of a total of 17 manometers. To analyze the behavior

and movement of the fine particles in the first 6 cm of the column, the head position at distances 1, 3, 4 and 5 centimeters from the inlet were also required.

Equation 5.1 was developed based on known head values H0 (head in first manometer of the column test at x=0.0 centimeter), H2 (head in second manometer of the column test at x=2 centimeters), and H6 (head in third manometer of the column test at x=6 centimeters). The measured heads from these three manometers were used to calculate unmeasured heads (H1, H3, H4, and H5) at 1, 3, 4, and 5 centimeters. The general form of the equation is:

$$H(x) = (H0 - H6)\exp\left[-\frac{x}{2}\ln\left(\frac{H0 - H6}{H2 - H6}\right)\right] + H6 \qquad (5.1)$$

where:

H(x) = value of head at the point of interest (L),

x = any distance from beginning of the column up to six centimeters (L),

H0 = known head at zero centimeter from beginning of soil, manometer #1 (L),

H2 = known head at two centimeters of soil in the column, manometer #2 (L),

H6 = known head at six centimeters of soil in the column, manometer #3 (L).

The best fit was determined based on the measured values from three manometers at distances 0, 2 and 6 centimeters. Table 5.2 shows the measured heads data that were recorded on an hourly basis at distances 0, 2 and 6 centimeters along with the calculated head values at distances 1, 3, 4, and 5 centimeters of the sample in sand column.

Table 5.2: Head values for the first six centimeter of the sample in the column

heads	H0	H1	H2	H3	H4	H5	H6
x (cm)	0	1	2	3	4	5	6
t= 0 (hrs)	29.3	28.66	28.20	27.86	27.62	27.45	27.00
1	29.4	28.70	28.22	27.87	27.62	27.45	27.02
2	29.5	28.76	28.25	27.89	27.63	27.46	27.05
3	29.6	28.81	28.28	27.90	27.65	27.47	27.08
4	29.7	28.86	28.30	27.91	27.65	27.47	27.10
5	30.3	29.09	28.35	27.88	27.59	27.41	27.12
6	31.0	29.34	28.40	27.86	27.55	27.38	27.15
7	32.0	29.66	28.46	27.84	27.52	27.35	27.18
8	33.5	30.04	28.48	27.77	27.46	27.31	27.20
9	35.5	30.46	28.50	27.73	27.43	27.31	27.24
10	37.8	30.93	28.55	27.72	27.43	27.33	27.28
11	55.6	33.36	28.60	27.57	27.36	27.31	27.30
12	111	39.20	29.00	27.55	27.34	27.31	27.31

H1, H3, H4, H5 = calculated hydraulic heads by fitting (Eq 5.1)
H0, H2, H6 = measured hydraulic heads from manometers 1, 2, 3.
t = time since the carbon injection started
x = distance from beginning of the column to the point of interest (cm)

Figure 5.5 shows the head distribution in each centimeter of the sand column based on measured and calculated values in Table 5.2 after 12 hours of the carbon injection.

The variation of the hydraulic heads in 0, 2, and 6 centimeters of the sample in column test with respect to time is shown in Figure 5.6.

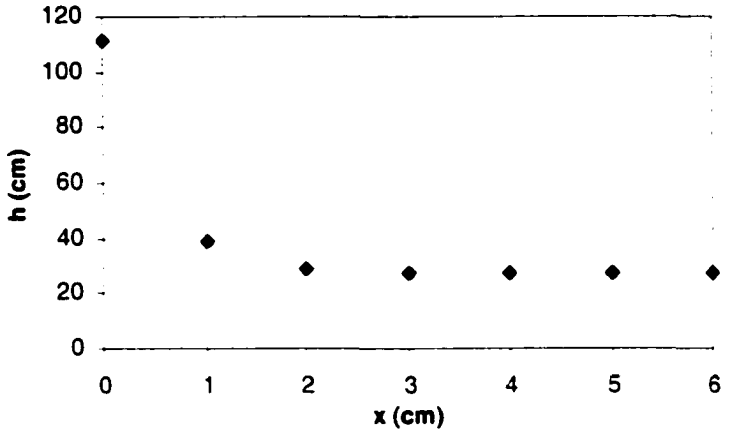

Figure 5.5: Variation of hydraulic heads with respect to distance in the column at t=12 hours

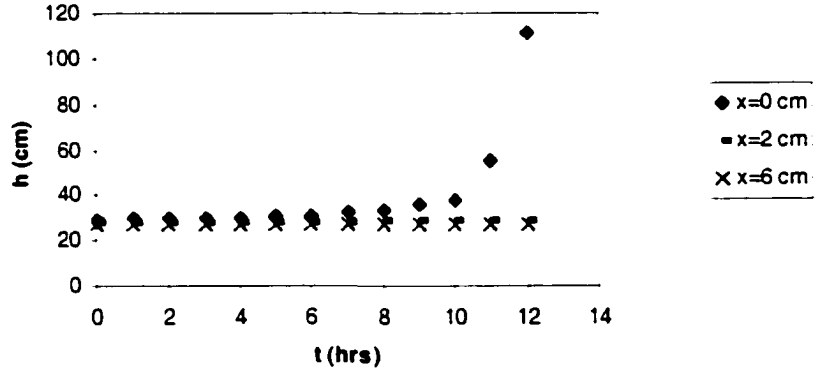

Figure 5.6: Variation of hydraulic heads with respect to time in the column

5.2.3 Calculation of concentration, porosity, and density from pressure heads

In order to calculate concentration of the particles in suspension by equation 3.3, the values for initial hydraulic conductivity (K_0) and hydraulic conductivity (K) were needed. The measured value for K_0 was found to be equal to 0.062 cm/sec (batch test) and the value for hydraulic conductivity was calculated based on the water level difference in the manometers by using Darcy's equation (Eq 3.8). Following calculation of K, the concentration of the particles in suspension, porosity, and density are calculated based on equation 3.3, 3.6, and 3.7. The data for the first, second, and third centimeters of the sample are tabulated in Tables 5.3, 5.4, and 5.5.

Table 5.3: Column test results for the first centimeter of the sample during the experiment

t (hours)	(h0-h1)	K(cm/sec)	ln (K0/K)	C' (M/M)	n	ρ_b (g/cm^3)	C (g/l)
1.00	0.7	0.0293	0.7475	0.0116	0.362	1.670	63.350
2.00	0.74	0.0277	0.8031	0.0124	0.362	1.670	68.060
3.00	0.79	0.0260	0.8685	0.0134	0.361	1.672	73.600
4.00	0.84	0.0244	0.9298	0.0144	0.361	1.673	78.800
5.00	1.21	0.0169	1.2948	0.0201	0.358	1.683	109.73
6.00	1.66	0.0123	1.6110	0.0250	0.355	1.691	136.53
7.00	2.34	0.0087	1.9543	0.0303	0.352	1.699	165.62
8.00	3.46	0.0059	2.3455	0.0364	0.349	1.709	198.77
9.00	5.04	0.0040	2.7216	0.0422	0.346	1.719	230.64
10.00	6.87	0.0030	3.0314	0.0470	0.343	1.727	256.89
11.00	22.24	0.0009	4.2061	0.0652	0.333	1.757	356.45
12.00	71.8	0.0003	5.3781	0.0834	0.323	1.786	455.77

$\Delta h = h_0 - h_1$ head differences between distance 0 and 1 cm of the column
h_0 = measured hydraulic head at x=0.0 cm of the column
h_1 = calculated hydraulic head at x=1 cm of the column (Eq 5.1)
K = calculated saturated hydraulic conductivity (Eq 3.8)
K_0 = measured initial hydraulic conductivity

C	=	calculated concentration of the particles in suspension (Eq 3.3)
C'	=	mass fraction-mass of carbon/mass of carbon plus sand (Eq 3.1)
ρ_b	=	calculated bulk density of the sample (Eq 3.7)
n	=	calculated porosity of the sample (Eq 3.6)
t	=	time in hours

Table 5.4: Column test results for the second centimeter of the sample during the experiment

t (hours)	(h1-h2)	K (cm/sec)	ln (K0/K)	C' (M/M)	n	ρ_b (g/cm^3)	C (g/l)
1.00	0.48	0.0428	0.3702	0.0057	0.366	1.659	31.370
2.00	0.51	0.0403	0.4309	0.0067	0.365	1.660	36.510
3.00	0.53	0.0387	0.4693	0.0073	0.365	1.662	39.770
4.00	0.56	0.0367	0.5244	0.0081	0.364	1.663	44.440
5.00	0.74	0.0277	0.8031	0.0124	0.362	1.670	68.060
6.00	0.94	0.0218	1.0423	0.0161	0.360	1.676	88.330
7.00	1.2	0.0171	1.2865	0.0199	0.358	1.682	109.03
8.00	1.56	0.0131	1.5489	0.0240	0.356	1.689	131.26
9.00	1.96	0.0104	1.7772	0.0275	0.354	1.695	150.60
10.00	2.38	0.0086	1.9713	0.0306	0.352	1.700	167.06
11.00	4.76	0.0043	2.6644	0.0413	0.346	1.717	225.80
12.00	10.2	0.0020	3.4266	0.0531	0.340	1.737	290.39

Δh=h1-h2		head differences between distance 1 and 2 cm of the column
h1	=	calculated hydraulic head at x=1 cm of the column
h2	=	measured hydraulic head at x=2 cm of the column
K	=	calculated hydraulic conductivity by Darcy's law (Eq 3.8)
K_0	=	measured initial hydraulic conductivity
C	=	calculated concentration of the particles in suspension (Eq 3.3)
C'	=	calculated fraction mass (Eq 3.1)
ρ_b	=	calculated bulk density of the sample (Eq 3.7))
n	=	calculated porosity of the sample (Eq 3.6))
t	=	time in hours

Table 5.5: Column test results for the third centimeter of the sample during the experiment

t (hours)	(h2-h3)	K (cm/sec)	ln (K0/K)	C' (M/M)	n	ρ_b (g/cm^3)	C (g/l)
1.00	0.35	0.0587	0.0544	0.0008	0.368	1.651	4.6100
2.00	0.36	0.0571	0.0826	0.0013	0.368	1.652	6.9900
3.00	0.38	0.0541	0.1366	0.0021	0.368	1.653	11.580
4.00	0.39	0.0527	0.1626	0.0025	0.367	1.654	13.780
5.00	0.47	0.0437	0.3492	0.0054	0.366	1.659	29.590
6.00	0.54	0.0380	0.4880	0.0076	0.365	1.662	41.360
7.00	0.62	0.0331	0.6262	0.0097	0.363	1.666	53.060
8.00	0.71	0.0289	0.7617	0.0118	0.362	1.669	64.550
9.00	0.77	0.0267	0.8428	0.0131	0.362	1.671	71.420
10.00	0.83	0.0247	0.9179	0.0142	0.361	1.673	77.780
11.00	1.03	0.0199	1.1338	0.0176	0.359	1.679	96.080
12.00	1.45	0.0141	1.4758	0.0229	0.356	1.687	125.06

$\Delta h=h2-h3$		head differences between distance 2 and 3 cm of the column
h2	=	measured hydraulic head at x=2 cm of the column
h3	=	calculated hydraulic head at x=3 cm of the column
K	=	calculated hydraulic conductivity by Darcy's law (Eq 3.8)
K_0	=	measured initial hydraulic conductivity
C	=	calculated concentration of the particles in suspension (Eq 3.3)
C'	=	calculated fraction mass of carbon (Eq 3.1)
ρ_b	=	calculated bulk density of the sample (Eq 3.7)
n	=	calculated porosity of the sample (Eq 3.6)
t	=	time in hours

The values for hydraulic conductivity in the region past 4 cm were unchanged indicating negligible fines. This is consistent with visual observation of a sharp interface up to 2.5 cm from the beginning of the sample during the experiment. For this reason the concentration profiles were plotted only up to 4 cm of the column. Table 5.6 shows the concentration of the particles in suspension in the 1st, 2nd, and 3rd centimeter of the sample in the column at different times. The concentration in fourth centimeter was assumed to be equal to zero because had minimal effect on hydraulic conductivity.

Table 5.6: Concentration profile data for different times during the experiment based on measured Δh and Eq 3.3

C (g/l) / x (cm)	C1 (t=1 hr)	C4 (t=4 hrs)	C7 (t=7 hrs)	C11 (t=11 hrs)	C12 (t=12 hrs)
0-1	63.35	78.80	165.62	356.45	455.77
1-2	31.37	44.44	109.03	225.8	290.39
2-3	4.61	13.78	53.06	96.08	125.06
3-4	0.0	0.0	0.0	0.0	0.0

5.2.4 Measurement of concentration after taking the column apart

The column was taken apart after 82 hours from the beginning of the carbon injection. The carbon distribution in each centimeters of the column was measured, the values for mass fraction (C) were calculated by dividing the mass of carbon to mass of carbon plus mass of sand, and concentration of the particles in suspension (C) was calculated based on simple equation m=n*C*A. The hydraulic conductivity (K), porosity (n), and density (ρ_b) were calculated using equations 3.3, 3.5, and 3.7.

Table 5.7 shows the data collected after taking the column apart. Figure 5.7 shows the percentage of measured carbon (based on total mass of carbon in the column) in the first six centimeters of the column at the end of the experiment.

Table 5.7: Measured carbon distribution and properties of the sample at the end of the experiment

x (cm)[1]	0-1	1-2	2-3	3-4	4-5	5-6
Carbon (g)[2]	10.556	3.68	0.7486	0.2923	0.0443	0.0174
Carbon %[3]	68.82	24.00	4.88	1.91	0.29	0.1
C (M/M)[4]	0.07312	0.02676	0.00556	0.00218	0.00033	0.00013
C (g/l)[5]	416.324	129.014	25.058	9.716	1.467	0.576
K (cm/s)[6]	0.00045	0.01353	0.04613	0.05530	0.06093	0.06158
ρ (g/cm^3)[7]	1.775	1.689	1.657	1.650	1.650	1.650
n[8]	0.31	0.35	0.36	0.37	0.37	0.37

1-measured distance from beginning of the sample to the point of interest in the soil (cm)
2-measured carbon in the sample after taking the column apart (g)
3-percentage distribution of carbon in the column
4-mass of fine per mass of soil plus mass of fine (g)
5-Calculated from equation m=nCA
6-Calculated from equation 3.3
7-Calculated from equation 3.7
8-Calculated from equation 3.5

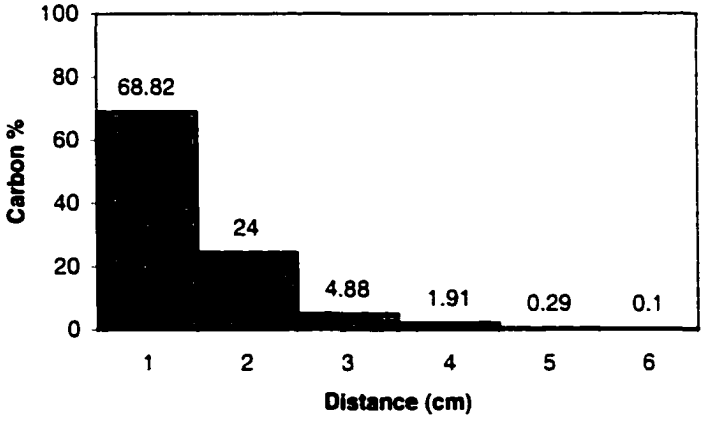

Figure 5.7: Carbon distribution in column test at the end of the experiment

As shown by Figure 5.7, the first centimeter of the sample contains the largest amount of carbon fines. About 69% (10.556 g) of the injected carbon that entered the porous media in the column was retained in this section. The mass fraction of the carbon with respect to the mass of the sand plus carbon ($C^{'}$), in first centimeter of the sample is equal to 0.073 (M/M), which is comparable to 8% carbon mixed with the sand in the batch test method.

The amount of carbon measured in the first three centimeters was 14.98 grams (97.65%) and the rest of the carbon (2.35%) is scattered throughout the next three centimeters of the column. The inlet screen was plugged with 4.33 grams of carbon fines. The proposed explanation is that the carbon was going through the sand at the beginning, but after the pores were occupied by carbon, no fines could infiltrate further, and it slowly backed up and filled the inlet chamber. Ultimately, the first two centimeters became almost impermeable layers. The amount of carbon (4.33 grams) found in the screen is not included in the calculations.

5.2.5 Comparison between measured and calculated concentration

The calculated concentration of the particles in suspension in three centimeters of the sample tabulated in (Tables 5.3, 5.4, and 5.5) is compared with the measured concentration in (Table 5.7) for different distances. The purpose of the comparison is to find out the closest calculated concentration with measured concentration and estimate the specific time which clogging has occurred.

Figure 5.8 shows the variation of concentration in three centimeters of the column at different times. This shows that the measured concentration in the first centimeter was

well approximated with concentration from measured Δh during the column test study at time 11 and 12 hours. In the second and third centimeter the concentration based on measured Δh over approximated the measured concentrations after taking the column apart. This comparison shows that the calculated concentration is closer to measured concentration at about 12 hours, which adds another point to believe that the clogging has occurred about 12 hours after the injection started.

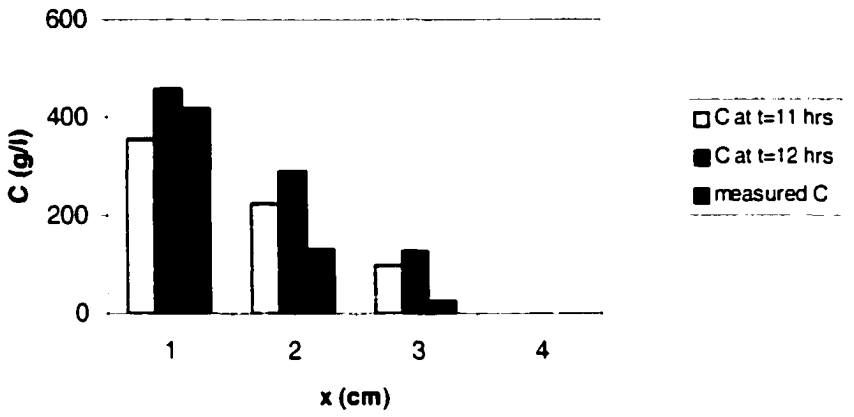

Figure 5.8: Comparison between column test concentrations at different times with measured concentration at the end of the experiment

However, the total mass was approximately the same at about twelve hours. The total measured mass of carbon in the first three centimeter of the sample after taking the column apart (Table 5.7) is compared with the total calculated mass of carbon under the curve (Figure 5.9). The mass calculation of carbon was done by having the area under the curve (the curve was passed through the calculated concentration points to calculate the area under the curve more accurately), assuming a calculated average porosity for this

concentration (n=0.3), the length of the column domain (L=3 cm) and the area of the column (A=81.1 cm^2).

Figure 5.9 shows concentration versus distance in the column calculated from measured Δh (Table 5.6) for time of eleven hours. The calculated mass of carbon under the curve is 16.3 g, which is almost the same as the mass of carbon measured in the first three centimeters of the sample in the column test after taking the column apart which was equal to 14.98 g (Table 5.7), assuming some loss of carbon during the disassembling of the column and measurement of the fines. Therefore, these values show that the initial concentration (C_0=0.25 g/l) with the flow rate of Q=100 ml/min was going into the column continuously for about twelve hours from the beginning of the carbon injection.

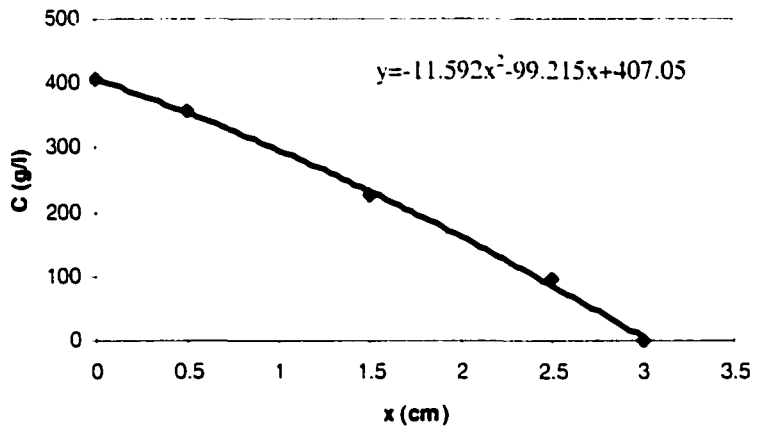

Figure 5.9: Concentration profile in column test based on measured Δh to calculate the mass of carbon under the curve at t=11 hours

As shown in Figure 5.10, the comparison of the calculated hydraulic conductivity from the column test during the experiment after 12 hours of injection with the measured hydraulic conductivity after taking the column apart (Table 5.7) shows an excellent

agreement for the first centimeter but for the second and third centimeter the measured data are almost an order of magnitude higher than the calculated data. At time equal to eleven hours, the agreement between measured hydraulic conductivity (based on Δh) and the column data are closer in second and third centimeters. However, one order of magnitude error in K is the result of less than 30 mg error in measuring carbon content in the column. This is well within measurement error and even in the worst case, the third centimeter represents an error in carbon content of about 4%. Values for time equal to twelve hours will be used assuming small losses of carbon during final weighing when the column was disassembled.

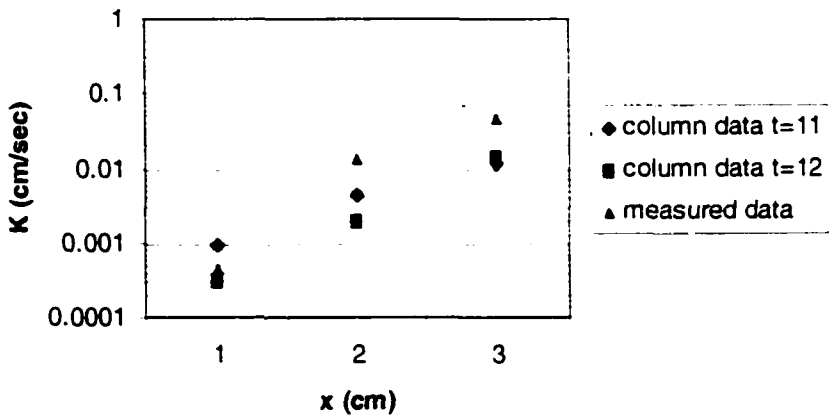

Figure 5.10: Comparison of calculated and measured conductivities in three centimeters of the sample

The calculated values for hydraulic conductivity from measured concentration after taking the column apart (Table 5.7) shows a decrease of K from an initial value of 0.062 to a final value of 0.00045 cm/sec (reduction of 99%) in the first centimeter of the column test. These results are comparable to those from the batch test method (Table

3.1) where over 8% carbon with respect to mass of the sand reduced hydraulic conductivity from 0.062 to 0.00042 cm/sec (reduction of 99%) and also these values match with the value of hydraulic conductivity in Table 5.3, which was calculated during the column experiment up to 12 hours of injection using equation 3.8 which shows the hydraulic conductivity is reduced from initial value 0.062 to the final value 0.00028 cm/sec (reduction of 99%). Figure 5.11 shows the percentages reduction of hydraulic conductivity with respect to concentration of the particles in suspension in all three methods.

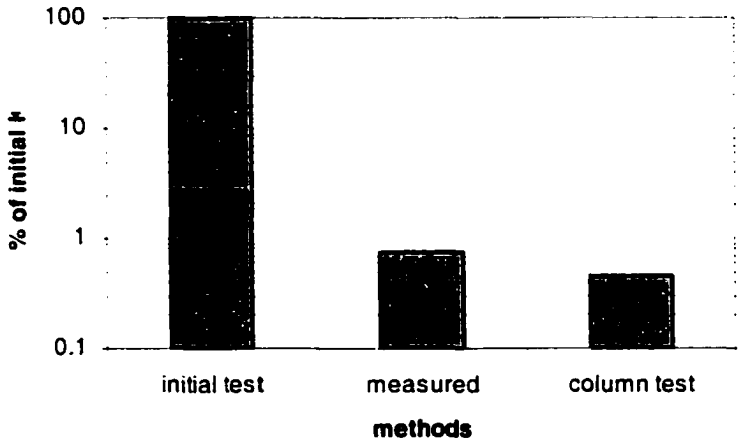

Figure 5.11: Percentage reduction of conductivities in measured, and column test for the first centimeter at t=12 hours

The hydraulic conductivity was reduced by 98%-99% in all three set of experiments. Results show that at about 12 hours of carbon injection, most of the pore spaces were occupied by fine particles and left a small space for water to infiltrate into the soil by pressure. The reduction of conductivity confirms the fact that trapped carbon particles occupying the pore spaces were the source of reduction in conductivity in all

tests and similar amounts of carbon caused similar reduction in conductivity regardless of the test method.

The same correlation also exists for physical and hydraulic properties of the samples (K, n, and ρ) between all three methods by comparing Tables 5.1, 5.3, and 5.7. The results show that the concentration of the particles in suspension effects on the porosity and density of the porous media and the soil texture changed from clean, homogeneous sand to heterogeneous.

The following figures present the comparison between calculated porosity and density data from column test after 12 hours of injection with measured porosity and density data at the end of the experiment (after taking the column apart), showing good agreement. Figure 5.12 shows that the measured and calculated porosity have an excellent agreement for the first centimeter of the sample, but in second and third the measured porosity is higher than calculated porosity.

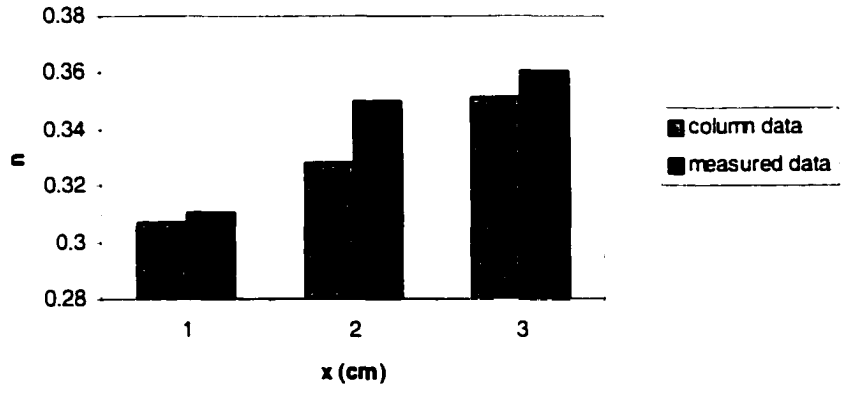

Figure 5.12: Comparison of calculated porosity in column test with measured porosity at the end of the experiment at t=12 hours

Figure 5.13 shows the calculated and measured density in first centimeter of the sample has excellent agreement, but in second and third centimeters the values for column is higher than measured density. Comparison between these two graphs indicates that the retained particles in pore spaces reduce the porosity and increase the density of the porous media with almost the same rate.

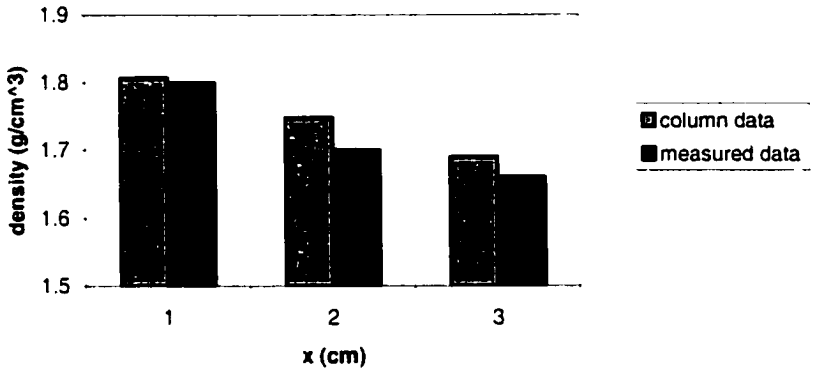

Figure 5.13: Comparison of calculated density in column test with measured density at the end of the experiment at t=12 hours

Results for hydraulic conductivity, porosity, and density are consistent. Difference between second and third centimeters between values calculated from Δh and measured values determined when the column was taken apart can be explained by loss of a small amount of carbon in the weighing process.

5.3 Computer Simulation

5.3.1 Retention Factor (R)

One of the objectives of this study is to propose the retention factor equation and estimate the values for the parameters α and β in the equation. The proposed equation (Eq 3.9) is:

$$\frac{V}{V_{rp}} = R = 1 + \alpha[\exp(\beta C)] \qquad (5.2)$$

where:

V_{rp} = velocity of the retained particles (L/T),

V = seepage velocity (L/T),

R = retention factor greater than one (dimensionless),

C = concentration of the fine particles in suspension (g/l),

α = empirical parameter (dimensionless),

β = empirical parameter (l/g).

In order to estimate the value for parameters α and β in equation 5.2 the values for different R and C are needed. Following the estimation of $R's$ and $C's$, the regression analysis can be done on equation 5.2 to calculate the constant values for α and β and use them as input data in the Simulation Model (Appendix C-C2). The values for C are already known from the column test (Tables 5.3, 5.4, and 5.5), and the values for R for column test are estimated as follow:

The derived equation B20 (Appendix B) is used to estimate values for R in column test experiment is in the form of:

$$R = 1 + \frac{\rho_b}{n}(\chi) \tag{5.3}$$

where:

ρ_b = bulk density of the porous media (g/cm^3),

n = porosity of the porous media (dimensionless),

χ = retention function, assumed as exponential function of concentration (ml/g).

The bulk density and porosity of porous media in equation 5.3 are functions of concentration, so the density equations (Eq 3.7) and porosity equation (Eq 3.6) are substituted into equation 5.3 to get:

$$R = 1 + \frac{\rho_0 + \eta C}{n_0 - \mu C}(\chi) \tag{5.4}$$

where:

R = retention factor (dimensionless),

χ = retention function (ml/g),

ρ_0 = initial bulk density of the porous media (g/cm^3),

n_0 = initial porosity of the porous media (dimensionless),

η = constant parameter in density equation (l/cm^3),

μ = constant parameter in porosity equation (l/g).

In equation 5.4, all the parameters are known (ρ_0=1.65 g/cm^3, n_0=0.369, η=0.0003 l/cm^3, μ=0.0001 l/g, and C from column test) except R and χ. The only way to estimate values for R with respect to known concentration (C) from the column test is by changing the values for χ manually to match the known values of concentration (C) from the column test with the model concentration. For this purpose, a computer program called the Calibration Model (Appendix C-C1) was used.

The values for $R's$ are estimated from the model by having known values for $C's$ from the column test. The calibration model is capable of calculating the model concentration and matching known column test concentrations by manually giving different values to χ in equation 5.4 as an input data. Table 5.8 shows the data calculated for the parameter R for three centimeters of the column by using Calibration Model through changing manually the value for χ. Now values for $R's$ are the actual values of retention factor (R) in experimental column test for different time steps with respect to concentration of the particles in suspension in the column (C).

Table 5.8: Curve matching between model concentration and column test data to determine R in three centimeters of the column

model C g/l	column C g/l	K cm/sec	n	density g/cm^3	R	ln R	Ki ml/g
4.7683	4.6114	0.05861	0.36852	1.651	224.57	5.4142	41
6.9099	6.9987	0.05715	0.36831	1.652	260.35	5.5620	47
11.288	11.580	0.05427	0.36787	1.653	211.16	5.352	38
13.749	13.782	0.05271	0.36763	1.654	237.99	5.4722	43
29.255	29.594	0.0439	0.36607	1.659	230.11	5.4385	41
31.174	31.378	0.04292	0.36588	1.659	225.06	5.4163	50
36.423	36.516	0.04034	0.36536	1.661	261.16	5.5651	58
39.791	39.776	0.03877	0.36502	1.662	212.24	5.3577	47
41.570	41.360	0.03796	0.36484	1.662	220.23	5.3946	47
44.391	44.442	0.03672	0.36456	1.663	239.47	5.4784	53
53.182	53.067	0.0331	0.36368	1.666	222.35	5.4042	48
63.252	63.352	0.02939	0.36267	1.669	205.08	5.3234	45
67.890	68.061	0.02783	0.36221	1.670	205.57	5.3257	45
73.612	73.602	0.02601	0.36164	1.672	224.09	5.4120	49
78.694	78.803	0.0245	0.36113	1.674	229.12	5.4342	50
109.63	109.73	0.017	0.35804	1.683	222.38	5.4044	48
136.42	136.53	0.01239	0.35536	1.691	289.57	5.6684	62
165.62	165.62	0.00878	0.35244	1.700	358.10	5.8808	76
198.75	198.77	0.00594	0.34912	1.710	447.21	6.1030	94
230.28	230.30	0.00409	0.34597	1.719	580.75	6.3643	121
256.88	256.89	0.00299	0.34331	1.727	758.68	6.6315	157
356.42	356.45	0.00092	0.33336	1.757	653.09	6.4817	131
455.85	455.77	0.00029	0.32341	1.787	997.49	6.9052	195

column C = calculated concentration using Darcy's law and equation 3.3
model C = was matched with column C by changing the value for χ
R = was calculated based on retention factor (Eq 5.4).

Figure 5.14 shows one of the matching processes for one time step, the concentration profiles results calculated from Δh at about twelve hours and the match output data from calibration model for three centimeters of the sample. The purpose of matching the concentration values from column test and calibration model is to get the

values for retention factor (R) with respect to concentration of the particles in suspension in the column (C) at the same time.

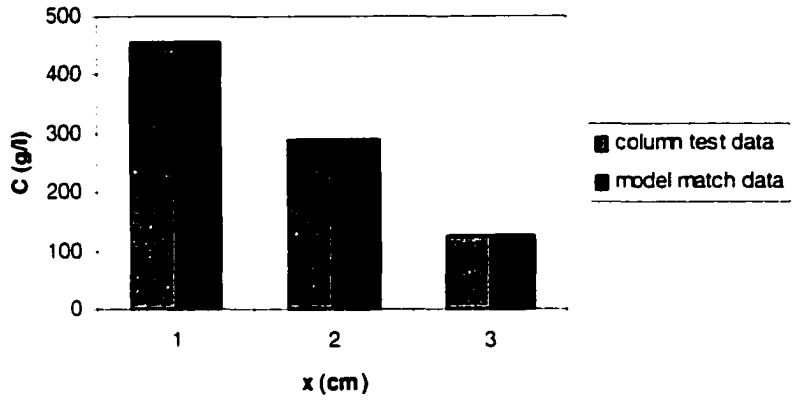

Figure 5.14: Matched concentration profile from calibration model output and column test data at t=12 hours

This process results in values of R for each time step and consequently, a matched with each C from column test. Now the values for $R's$ and $C's$ are available and can be used in regression analysis of retention factor equation (Eq 5.2) to estimate constant values for α and β which are needed as input data to run the Simulation Model (Appendix C-C2).

To calculate the constant parameters α and β in equation 5.2, the resulting values for the retention factor (R) and concentration of the particles in column test (C) were plotted on a semi-log paper (Figure 5.15). Parameters α and β in equation 5.2 were estimated by regression analysis. The constant value for these parameters are α=196.6 (dimensionless) and β=0.0037 (l/g). These constant can be used as input data in the simulation model. It is worth while to indicate that values for α and β are average.

Figure 5.15 shows the natural log of retention factor (R) verses concentration of the particles in suspension (C), which is based on equation 5.2 for the first three centimeters of the sample (Table 5.8).

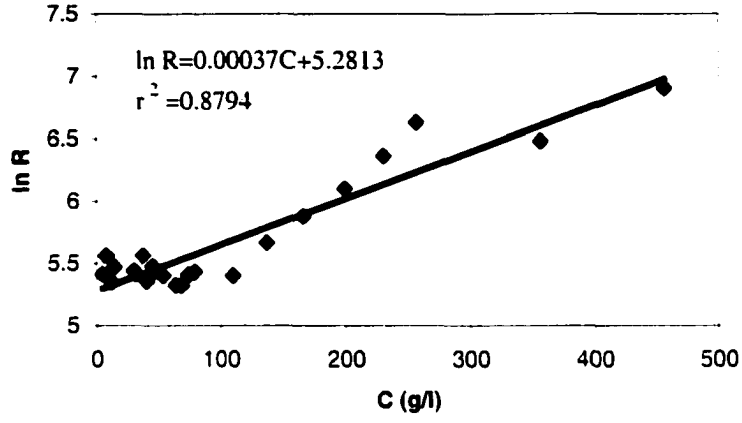

Figure 5.15: Estimated values for parameters α and β in retention factor equation for three centimeters of the sample at t=12 hours

Figure 5.16 shows the relationship between retention function (χ) and concentration of the particles in suspension (C). It is obvious that χ is not a linear function of R and/or C, as would be expected. The non linearity shows that the particles are getting attached to the already retained particles on porous media, also confirms that clogging process is not linear and happens faster particularly when the concentration is high.

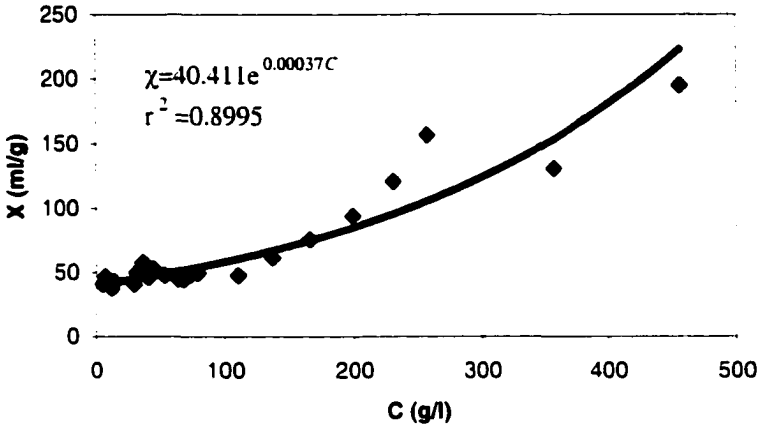

Figure 5.16: Nonlinear isotherm relationship between χ and C at t=12 hours

Data analysis shows that parameter χ is a function of concentration and increases exponentially as shown in Figure 5.16. The form of the developed equation (Appendix B-B21) for χ (C) is:

$$\chi(C) = Me^{NC} \qquad (5.5)$$

where:

χ (C) = retention function (ml/g),

C = concentration of the particles in suspension (g/l),

M = constant parameter (ml/g),

N = constant parameter (l/g).

The values for parameters M=40.411 (ml/g) and N=0.0037 (l/g) in equation 5.5 were calculated by regression in Figure 5.16.

5.3.2 Evaluation

The Simulation Model (Appendix C-C2) was executed using input data given in Table 5.9. The experimental results were used to gauge the applicability of the model by comparing the model results versus laboratory experiment.

Table 5.9: Parameter used as input data in Simulation Model

Parameters	Values	Description
L	4 cm	Length of experimental domain
Δx	1 cm	increment of L (should be correct fraction of length)
R_0	1	constant value in retention factor equation
K_0	0.062 cm/s	initial hydraulic conductivity
n_0	0.369	initial porosity
ρ_0	1.65 g/cm^3	initial bulk density
μ	0.0001 l/g	constant parameter in porosity equation (Eq 3.6)
γ	0.0118 l/g	constant parameter in hydraulic conductivity (Eq 3.3)
α	196.6	constant parameter in retention factor equation (Eq 5.2)
β	0.0037 l/g	constant parameter in retention factor equation (Eq 5.2)
η	0.0003 l/cm^3	constant parameter in bulk density equation (Eq 3.7)
Ψ	0.5	Preissmann factor
θ	0.5	Crank-Nicholson factor
ε	0.001	accuracy factor
S_s	1E-6 l/L	specific storage
C_0	0.011 g/l/s	injection rate of the particles in suspension (Eq 4.22)
C_i	0.25 g/l	initial injection
t_{max}	43200 sec	maximum time to run the model
Hi	known	initial head (cm)
C(x,0)	0.0	clean soil

The applicability of the model was tested with known values as input data (Table 5.9). The comparison between the concentration results from the column tests experiment and model prediction in three centimeters of the sample giving a good correlation. As shown in Figure 5.17, the disagreement is more pronounced at the low concentration values in third centimeter, which the model is over predicting. Considering the complexity of the processes in experiment, model and the inherent simplifying assumptions, the agreement between modeled and column values look promising.

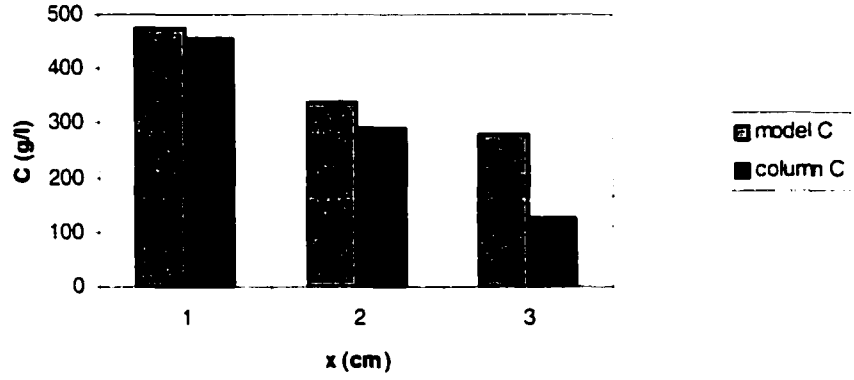

Figure 5.17: Comparison between model and column concentration for three centimeters of the sample at t=12 hours

Table 5.10 presents the changes of hydraulic conductivity in porous media as a function of concentration of the particles in suspension. The tabulated data are the calculated values in column test (i.e., Table 5.3) and the computer simulation values (i.e., Table D2) for the first centimeter of the sample in column test.

Table 5.10: Conductivity results from column test and model simulation for the first centimeter of the column

t (hours)	column C (g/l)	column K (cm/sec)	model C (g/l)	model K cm/sec
0	0	0.06200	0	0.06200
1	63.352	0.02935	39.500	0.03890
2	68.062	0.02777	79.100	0.02438
3	73.603	0.02601	118.80	0.01526
4	78.803	0.02446	158.30	0.00957
5	109.73	0.01698	197.90	0.00600
6	136.53	0.01238	237.60	0.00376
7	165.62	0.00878	277.10	0.00236
8	198.77	0.00594	316.80	0.00148
9	230.64	0.00407	356.40	0.00092
10	256.89	0.00299	396.00	0.00058
11	356.45	0.00092	435.50	0.00036
12	455.77	0.00028	475.10	0.00023

Laboratory and model prediction of the conductivities versus time are shown in Figure 5.18. As shown, the hydraulic conductivity decreases with time, implying the progression of the clogging process (r^2=0.89).

Figure 5.18 shows, the hydraulic conductivity output from the model compared reasonably well with those from the column test. The underestimation by the model in Figure 5.18 is due to the underestimation of ln R between about 50 and 150 g/l of concentration of carbon shown in Figure 5.15, which corresponds to concentration at time up to two hours. It is worth while to indicate that values for α and β are average and the correlation coefficient in Figure 5.15 is r^2=0.88 which coincide with correlation coefficient between column and model hydraulic conductivity (Table 5.10) which is equal to r^2=0.89.

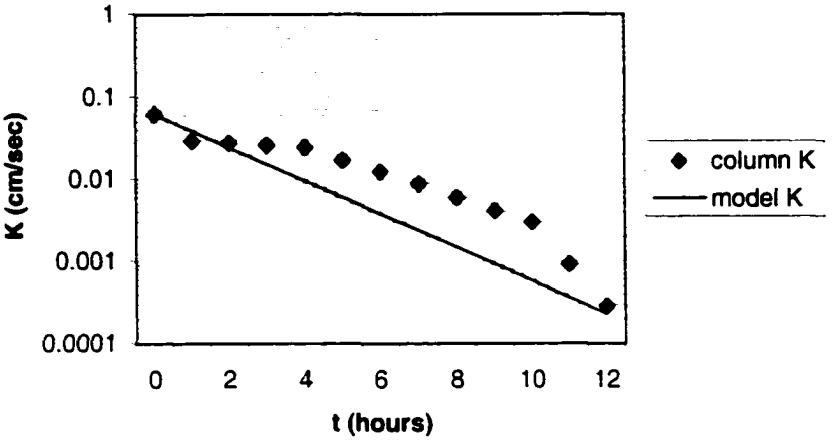

Figure 5.18: Reduction of hydraulic conductivity with respect to time by column test and model simulation for the first centimeter of the sample

CHAPTER SIX

SUMMARY AND CONCLUSIONS

6.1 Summary

Carbon fines, a type of suspended particles that is widely used in water treatment plants throughout the world, cause plugging of aquifer material in artificial recharge wells. The treated water may contain some carbon fines when injected into the underground reservoir through the injection wells, which cause a reduction in recharge capacity, potentially leading to the complete cessation of the well's use. The purpose of this study was to analyze the reduction in hydraulic conductivity of aquifer material due to suspended particles during artificial recharge well.

To meet the objectives of this study, the following processes were undertaken:

- Develop a relationship between hydraulic conductivity and concentration of the particles in suspension, K=K(C), using a constant head permeameter (batch test).
- Derive flow and transport equations with hydraulic conductivity, porosity, density, and a retention factor as functions of concentration.
- Develop a one-dimensional finite difference model to solve the flow and transport equations, using hydraulic conductivity, porosity, density and retention factor relationships mentioned above, and

- Evaluate the results by comparing the computer model output with a data from laboratory column test.

In this study, a set of detailed laboratory column experiments (packed with Poudre Sand) were conducted, coupled with one-dimensional modeling of the flow and transport processes. The experimental studies were intended to establish the necessary functional relationships between hydraulic conductivity and the concentration of the particles in suspension. The adequacy of the computer simulation model was tested against measurements from a laboratory column study.

The first set of the experiments (a constant head permeameter test referred to as the batch test) related the concentration of carbon fines to permeability for a range of concentrations. The following equation was determined from these experiments:

$$K = K_0 e^{-\gamma C} \tag{6.1}$$

where:

K = saturated hydraulic conductivity (L/T),

K_0 = initial saturated hydraulic conductivity (L/T),

C = concentration of the particles in suspension (M/V_l),

γ = empirical constant (V_l/M).

Similar equations were derived for porosity and density as a function of carbon fine concentrations.

The second set of experiments (referred to as the column test) was one-dimensional steady flow experiments in which a constant rate of carbon particles in suspension was injected into an instrumented column of Poudre Sand. As the injected carbon fines clogged the soil in the column, the hydraulic heads measured along the column with piezometers were found to increase. The measured hydraulic heads were used to calculate hydraulic conductivity over time and space. The corresponding concentrations were calculated using equation 6.1.

The column experiment showed that the saturated hydraulic conductivity of the sand was reduced by over 98%, which is comparable with eight percent (based on mass of sand) of trapped carbon particles in the porous media (batch test). The carbon particles were detected up to 6 cm from the column inlet with 69% (based on total mass of the carbon injected) in the first centimeter. The results from the column test were verified by matching concentrations calculated from measured hydraulic heads at time equal to 12 hours with concentrations measured after dissection of the column at the end of the experiment. A time of 12 hours was chosen for comparison with measured values because the total mass injected at 12 hours was similar to the total mass in the column when the column was taken apart and the mass of fines measured.

The results from this experiment suggest that carbon fines move into and remain trapped in the aquifer material causing a near cessation of the flow. At the end of the experiment (t=82 hours), the last set of manometer data were recorded prior to disassembling the column. At this point without adjusting the pump to keep the flow rate constant (Q=100ml/min) the heads start falling to the same place the experiment had started and the outflow was measured it was 7.5 ml/min. The comparison between the

clean sand outflow (Q=100 ml/min) at the beginning of the column test experiment with plugged sand outflow (Q=7.5 ml/min) at the end of the experiment before taking the column apart shows a reduction of 92.5% intake capacity of the porous media.

A one-dimensional, finite-difference flow and transport model that calculates the concentration of the carbon fines and the resulting hydraulic conductivity over time and space was used to model the column results. The groundwater flow equation is solved for head distribution and the solute transport equation is simultaneously solved for concentration of the particles in suspension. The computer model uses a Preissmann box scheme and Crank-Nicholson methods to simulate the experimental runs.

One of the input variables needed for the computer model is a retention factor, defined, as

$$R = 1 + \alpha[\exp(\beta C)] \qquad (6.2)$$

where:

R = retention factor greater than one (dimensionless),

C = concentration of the fine particles in suspension (g/l),

α = empirical parameter (dimensionless),

β = empirical parameter (l/g).

Results from the column test were used to determine the form of the retention factor equation and estimate the values for the parameters α and β in the equation. The values for concentration were determined in the column test at time equal to 12 hours. The values for R were estimated from the following equation:

$$R = 1 + \frac{\rho_0 + \eta C}{n_0 - \mu C}(\chi) \qquad (6.3)$$

where:

R = retention factor (dimensionless),

χ = retention function (ml/g),

ρ_0 = initial bulk density of the porous media (g/cm^3),

n_0 = initial porosity of the porous media (dimensionless),

η = constant parameter in density equation (l/cm^3),

μ = constant parameter in porosity equation (l/g).

In equation 6.3, all the parameters are known (ρ_0=1.65 g/cm^3, n_0=0.369, η=0.0003 l/cm^3, μ=0.0001 l/g, and C from column test) except R and χ. The only way to estimate values for R with respect to known concentration (C) from the column test is by changing the values for χ manually to match the known values of concentration (C) from the column test with the model concentration. For this purpose, a computer program called the Calibration Model (Appendix C-C1) was formulated and used, the results are tabulated in Table 5.8.

The values for α and β were determined from that data by regression and found to be α=196.6 (dimensionless) and β=0.0037 l/g with a correlation coefficient of r^2=0.88 (Figure 6.1).

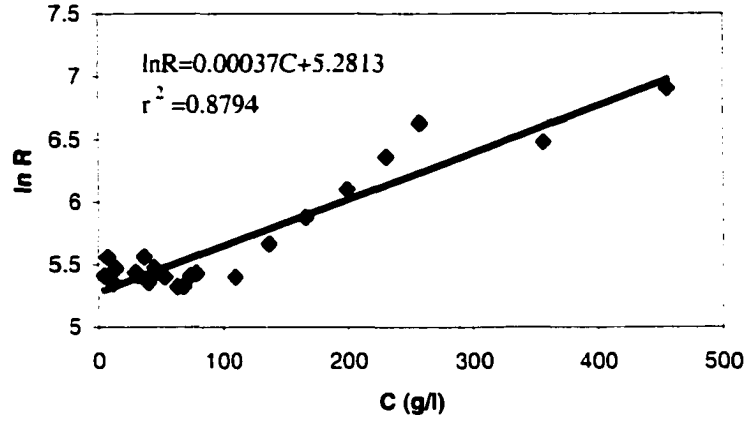

Figure 6.1: Estimated values for parameters α and β in retention factor equation for three centimeters of the sample at t=12 hours

These values for parameters α and β were put back into the Simulation Model (Appendix C-C2), which was run for a simulation period of 12 hours. The hydraulic conductivity output from the model compared well with the concentrations at t=12 hours from the column study (Table 5.10). Figure 6.2 shows, the hydraulic conductivity output from the model compared reasonably well with those from the column test. The overestimation by the model in Figure 6.2 is due to the underestimation of ln R between about 50 and 150 g/l of concentration of carbon shown in Figure 6.1, which corresponds to concentration at earlier time. It is worth to indicate that values for α and β are average and the correlation coefficient in Figure 6.1 is $r^2=0.88$ which coincide with correlation coefficient between column and model hydraulic conductivity (Table 5.10) which is equal to $r^2=0.89$.

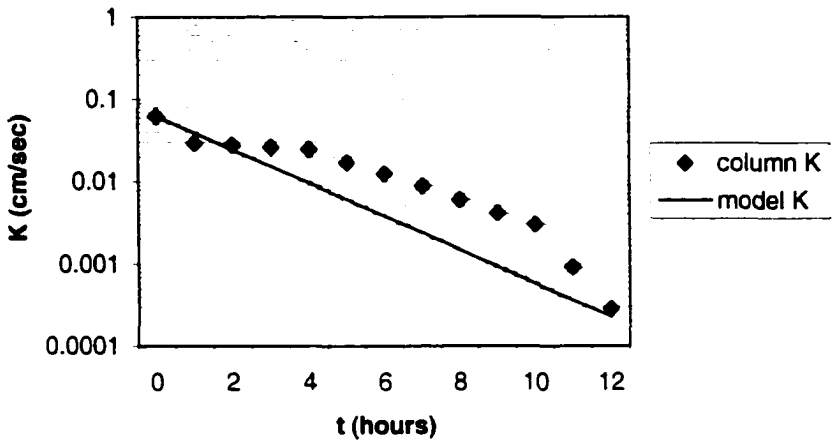

Figure 6.2: Comparison of hydraulic conductivity from column test and model simulation

The experiments in this dissertation should be repeated with other soil types and other carbon fine concentrations to evaluate the universality of the coefficients found in this research. However, the results show that an exponential equation is an appropriate representation for the retention factor R. This nonlinear form of the equation implies that the carbon fines attach more easily to fines than to the soil particles in the column, precipitating rapid clogging of the column and reduction in hydraulic conductivity.

6.2 Conclusion

The purpose of this dissertation was to study the effect of carbon fines on hydraulic conductivity in aquifer materials. Results show that the carbon fines reduce hydraulic conductivity of the soil adjacent to the injection point by two orders of magnitude within 12 hours. The clogging process is very nonlinear and the retention increases exponentially as the concentration of the fine particles increases. Most of the

pore spaces were occupied by fine particles leading to significant reduction in flow cross-sectional area.

The reduction of conductivity confirms the fact that trapped carbon particles occupying the pore spaces were the source of reduction in conductivity in all tests and similar amounts of carbon caused similar degree of reduction in conductivity regardless of the test method. The results show that the concentration of the particles in suspension affects the porosity and density of the porous media and the soil texture changed from clean, homogeneous sand to heterogeneous. The heterogeneity of the porous media due to retained particles make the solution of the flow and transport equations much more complicated, for this reason the computer model is an essential tool in this type of research. The results from this study can be categorized as follow:

- The laboratory experiments show that clogging in porous media by suspended particles is a significant problem.
- The mathematical approach in solving the clogging problem along with the proposed empirical equations proved to be adequate and can be used in future research.
- This research shows that the heterogeneity of the porous media due to retained particles make the solution of the flow and transport equations more complicated.
- The numerical model complimented by the experimental methods used in this research provides a valuable tool to investigate the problem of clogging in recharge wells.

REFERENCES

Abbott, M.B and D.R Basco. 1989. Computational Fluid Dynamics. Longman Singapore Publishers (Pte), Singapore.

Adin, A. and R. Rajagopalan. 1989. Breakthrough curves in granular media filtration. *Journal of Environmental Engineering. 115(4): 785-798.*

Bear, J. 1979. Hydraulics of Groundwater. McGraw Hill, New York, New York.

Bear, J. and A. Verruijt. 1987. Modeling Groundwater Flow and Pollution. Reidel Publishing Company, Dordrecht.

Bear, J. 1972. Dynamics of Fluids in Porous Media. American Elsevier Publishing Co., Inc. New York, New York.

Bedient, P, H. Rafai. and C. Newell. 1999. Ground Water Contamination. Prentice Hall PTR, Upper Saddle River, NJ 07458.

Bouwer, H. 1996. Issues in artificial recharge. IAWQ Water Science Technology vol (33) No 10-11, PP 381-390.

Byers, E. and D.B. Stephens. 1983. Statistical and stochastic analyses of hydraulic conductivity and particle-size in a fluvial sand. *Soil Sci Soc. Am J. 47, pp. 1072-1081.*

Charbeneau, R. 2000. Groundwater hydraulics and pollutant transport. Prentice-Hall, Inc. Upper Saddle River, New Jersey 07458.

Calgon Carbon Corporation. 1987. Type TOG Granular activated carbon. Bulletin 27-154.

Calgon Carbon Corporation. 1990. Pulverized activated carbons. Bulletin 23-100d

Clark, R.M. and B.W. Lykins. 1989. Granular activated carbon. Lewis Publishers. Chelsea, Michigan.

Canter, L, R. Knox and D.Fairchild. 1988. Groundwater Quality Protection. Lewis Publishers, Inc.Chelsea, Michigan.

Corapcioglu, M.Yavuz and A. Haridas. 1984. Transport and fate of microorganisms in porous media: A theoretical investigation. *Journal of Hydrology, 72, pp. 149-169.*

Dullien, F.A.L. 1992. Porous Media-Fluid Transport and Pore Structure. Academic Press, Inc. San Diego, California.

Dillon, P; M. Hickinbotham and P. Pavelic. 1994. Review of international experience in injecting water into aquifers for storage and reuse. Adelaide, Australia.

Duchateau, P and D. Zachmann. 1989. Applied Partial Differential Equation, Harper and Row publisher Inc, New York, New York.

Environmental Protection Agency. 1991. Granular activated carbon treatment. Report EPA-540/2-91/024.

Einstein, H.A. 1968. Deposition of suspended particles in a gravel bed. *Journal of the hydraulic division of ASCE, HY5 Sep, 1968 pp 1197-1204.*

Frycklund, C. 1998. Long- term sustainability in artificial groundwater recharge. Artificial Recharge of Groundwater. Proceeding of the third international symposium on artificial recharge of groundwater-TISAR 98.

Fetter, C.W. 1988. Applied Hydrogeology. Merrill Publishing Company. Columbus Ohio.

Freeze, R.A and J. Cherry. 1979. Groundwater. Prentice-Hall, Inc. Englewood Cliffs, New Jersey.

Hutchinson, A. and R. Randall. 1994. Estimation of injection well clogging with the modified fouling indexes (MFI). Artificial Recharge of Ground Water, II, second international symposium on artificial recharge of groundwater. ASCE. New York, New York.

Hassler, W.J. 1974. Purification with activated carbon. Chemical Publication Company, Inc. New York, New York.

Herzig, J, D. Leclerc. And P. Le Goff. 1970. Application to deep filtration. *Industrial and Engineering Chemistry. 62(5): 9-35.*

Hijnen, W, J.Bunnik, J.Schippers, R.Straatman and H.Folmer 1998. Determining the clogging potential of water used for artificial recharge in deep sandy aquifer. Artificial Recharge of Groundwater. Proceeding of the third international symposium on artificial recharge of groundwater-TISAR 98.

Ives, K.J. 1979. Deep bed filtration: Theory and practice. University College, London, England.

Kinzelbach, W 1986. Groundwater modeling. Development in water science. Elsevier Science Publication Company. 52 Vanderbilt Ave, New York, NY 10017, USA.

Kortleve, M.W. 1998. Berkheide well recharge system: Design, implementation and initial experience of operation. Artificial Recharge of Groundwater. Proceeding of the third international symposium on artificial recharge of groundwater-TISAR 98.

Kovacs, G. and L. Ujfaludi. 1983. Movement of fine grains in the vicinity of well screen. *Hydrological Sciences Journal. 28 (2) 6:247-260.*

Laroussi, C, T. Touzi and L. DeBacker. 1981. Hydraulic conductivity of saturated porous media in relation to their geometric characteristics. Soil Science, Vol. 132, No 6, pp 387-393.

McWhorter, D. and D. Sunada. 1977. Ground-Water Hydrology and Hydraulics. Water Resources Publications. Littleton, Colorado USA.

Millington, R. and J. Quirk. 1961. Permeability of porous solids. *Farady Soc. 57, pp. 1200- 1206.*

Mishra, S., J. Parker and N. Singhal. 1989. Estimation of soil hydraulic properties and their uncertainty from particle size distribution data. *Journal of Hydrology, 108, pp. 1-18.*

Namvargolian, R. 1992. Microbial and biologically reacting solute transport in subsurface environment. Ph.D. Dissertation. Civil Engineering Department Colorado State University, Fort Collins, Colorado.

Neung-won, H., B. Jayendra and R. Carbonel.1985. Longitudinal and lateral dispersion in packed bed: Effect of column length and particle size distribution. *AICHE Journal 31(2): 277-287.*

Olsthoorn, T.N. 1982. The Clogging of Recharge Wells, Main Subjects. KIWA Communications 72, August. Netherland.

Puckett, W, J. Dane and B. Hajek. 1985. Physical and mineralogical data to determine soil hydraulic properties. *Soil Sci Soc. Am J., Vol. 49, pp. 831-835.*

Perez-Paricio, A and J. Carrera. 1998. A conceptual and numerical model to characterize clogging. Artificial Recharge of Groundwater. Proceeding of the third international symposium on artificial recharge of groundwater-TISAR 98.

Pavelic,et al. 1998. Well clogging effects determined from mass balances and hydraulic response at a stormwater ASR site. Artificial Recharge of Groundwater.

Proceeding of the third international symposium on artificial recharge of groundwater-TISAR 98.

Perez-Paricio, A and J. Carrera. 1998. Preliminary study for deep injection experiments at the Cornella site, Barcelona. Artificial Recharge of Groundwater. Proceeding of the third international symposium on artificial recharge of groundwater-TISAR 98.

Rajagopalan, R. and C. Tien. 1979. The theory of deep bed filtration, Filtration and Separation. R.J. Wakeman, Elsevier.

Rajagopalan, R. and R. Chu. 1981. Dynamics of adsorption of colloidal particles in packed beds. Journal of Colloid and Interface Science. 86(2): 299-317.

Rebhun, M. and J. Schwarz. 1968. Clogging and contamination process in recharge wells. *Water Resources Research. 4(6): 1207-1217.*

Rinck-Pfeiffer, S, R.Ragusa and T.Vandevelde, 1998. Column experiments to evaluate clogging and biogeochemical reactions in the vicinity of an effluent injection well. Artificial Recharge of Groundwater. Proceeding of the third international symposium on artificial recharge of groundwater-TISAR 98.

Sakthivadivel, R and H. Einstein. 1970. Clogging of porous column of spheres by sediment. *Journal of the hydraulic division ASCE HY2* Feb 1970 pp 461-472.

Shepherd, R.G. 1989. Correlation of permeability and grain size. Groundwater vol 27 No 5, pp 633-638.

Schippers, J, J. Verdouw and G. Zweere. 1995. Predicting the clogging rate of artificial recharge wells. *Journal of water SRT-Aqua Volume (44), No.1, pp 18-28.*

Simon, D. and F. Senturk, 1992. Sedimentation Transport Technology. Water Resources Publications, Littleton, Colorado, USA.

Straatman, R, Y. Brekvoort and S.Verheijden. 1998. Well recharge pilot in the south-east Netherlands. Artificial Recharge of Groundwater. Proceeding of the third international symposium on artificial recharge of groundwater-TISAR 98.

Takashi A. 1985. Artificial recharge of groundwater. Butterworth Publishers. Massachusetts, USA.

Uma, K., B. Egobka and K. Onuoha. 1989. New statistical grain-size method for evaluating the hydraulic conductivity of sandy aquifers. Elsevier Science Publication B.V. Pp. 343-366.

Visser.J. 1972. Advances in colloid and interface science, vol 3, Pp 331.

Warner, J, T. Gates, R. Namvargolian, H. Vagharfard, P. Miller, and G. Comes. 1992. Sediment and microbial fouling of laboratory and field facilities for groundwater recharge. Colorado State University, Fort Collins, Colorado.

World Meteorological Organization, 1997. Comprehensive assessment of the freshwater resources of the world. www.wmo.ch, Switzerland.

Wang, H. and M. Anderson. 1982. Introduction to Groundwater Modeling. W.H.Freeman and company, New York, New York.

Yao, K., M. Habibin, and C. O'Melia. 1971. Water and wastewater filtration: concepts and applications. *Environ. Sci. Technol., 5(11): 1105-1112.*

Zappi, M. N. Francingues and D. Adrian. 1989. An evaluation of operational factors contributing to reduced recharge capacity of the north boundary treatment system Rocky Mountain Arsenal. Environmental Laboratory, U.S. Army Engineers Waterways Experiment Station. Vicksburg, Mississippi.

APPENDIX A

DERIVATION OF FLOW EQUATION

Flow Equation in Confined Aquifer

The analysis of transient groundwater flow in a confined aquifer requires the introduction of the concept of compressibility, a material property that describes the change in volume by stress. The reduction in volume occurs by rearrangement of the grains and compressibility of water in the pores. It is assumed that the individual grains are incompressible. For flow of water in porous media, it is necessary to define two compressibility terms as follow (Freeze and Cherry, 1979):

Compressibility of the aquifer (α_b)

The total stress that acts downward on the geological material at depth is due to the weight of overlying material and water. This stress is borne in part by granular of aquifer material and fluid pressure (p) of the water in the pores.

$$\sigma_T = \sigma_e + p \qquad \text{(A1)}$$

where:

σ_T	=	total stress (F/L^2)
σ_e	$=\sigma_{es}+\sigma_{ec}$	effective stress (inter granular stress), it is this stress that is actually applied to the grain of aquifer material (F/L^2)
σ_{es}	=	effective stress caused by sand of aquifer material (F/L^2)
σ_{ec}	=	effective stress caused by carbon on the aquifer material (F/L^2)
p	=	pressure of water (F/L^2).

The compression of the porous media is caused by changes in effective stress, not by changes in the total stress. The change in stress is shown as follow:

$$d\sigma_T = d\sigma_e + dp \qquad \text{(A2)}$$

The weight of material and water overlying each point in the system often remain constant through time. In such cases $d\sigma_T = 0$ and

$$d\sigma_e = -dp \qquad \text{(A3)}$$

In this case, if the fluid pressure increases, the effective stress decreases by an equal amount and if the fluid pressure decreases, the effective stress increases by an equal amount. If the stress increases in granular material it will reduce the thickness and pore volume of the confined aquifer.

Pumping water from the well decrease hydraulic head and increases effective stress, resulted in aquifer compaction. Conversely, pumping water into an aquifer (recharging water) increases hydraulic head, decreases effective stress, and causes aquifer expansion (Freeze and Cherry, 1979).

The volume of water released from a unit volume of confined aquifer when water pressure head is reduced by one unit is called Specific Storage (S_s). Both aquifer compaction and decreased water density contribute to the volume released. The general

mass balance is applied on the volume element, which contains sand while fine particles (carbon) are added to the system:

The mass of water in the saturated element of the aquifer is:

$$M = \rho n_s n_c \Delta x \Delta y \Delta z \qquad \text{(A4)}$$

where:

M = mass of the water (M),

ρ = density of water (M/L^3),

n_s = porosity of sand (dimensionless),

n_c = porosity of carbon (dimensionless).

the change of mass is as follow:

$$dM = \left[\rho n_c d(n_s \Delta z) + \rho n_s d(n_c \Delta z) + n_s n_c \Delta z d\rho\right] \Delta x \Delta y \qquad \text{(A5)}$$

$$dM = \left[dM_1 + dM_2 + dM_3\right] \Delta x \Delta y \qquad \text{(A6)}$$

Follows from the chain rule for differentiation of a product and the assumption that the aquifer deforms in vertical direction. Lateral deformation is negligible. The compressibility of the aquifer discussed here is based on the vertical stress.

The quantity of $dM_1 = \rho n_c d(n_s \Delta z)$ and $dM_2 = \rho n_s d(n_c \Delta z)$ are the contribution per unit area due to a change in pore volume at constant density, and $dM_3 = n_s n_c \Delta z d\rho$ is the contribution due to change in water density at constant pore volume.

The change in pore volume, due to vertical compression, per unit pore volume per unit change in intergranular (effective) stress is the bulk vertical compressibility (α_b) and is defined as:

$$\alpha_b = \alpha_p + \alpha'_p \tag{A7}$$

1- compressibility of the aquifer due to sand:

$$\alpha_p = -\frac{1}{n_s \Delta z}\frac{d(n_s \Delta z)}{d\sigma_{es}} = \frac{1}{n_s \Delta z}\frac{d(n_s \Delta z)}{dp} \tag{A8}$$

2- compressibility of the aquifer due to carbon:

$$\alpha'_p = -\frac{1}{n_c \Delta z}\frac{d(n_c \Delta z)}{d\sigma_{ec}} = \frac{1}{n_c \Delta z}\frac{d(n_c \Delta z)}{dp} \tag{A9}$$

after some mathematical manipulation we get:

$$dM_1 = \alpha_p \rho n_c n_s \Delta z dp \tag{A10}$$

$$dM_2 = \alpha'_p \rho n_c n_s \Delta z dp \tag{A11}$$

$$dM_1 + dM_2 = (\alpha_p + \alpha'_p)\rho n_c n_s \Delta z dp \tag{A12}$$

Compressibility of water (β_w):

Stress is imparted to a fluid through the fluid pressure (p). An increase in pressure (dp) leads to a decrease in the volume (V_w) of a given mass of water. The compressibility of water (β_w) can be express as:

$$\beta_w = -\frac{1}{V_w}\frac{dV_w}{dp} \qquad \text{(A13)}$$

equation A13 expresses the relationship between a change of volume and a change of pressure on a constant mass of water. Since the mass is constant, the definition of density yields:

$$d\rho = -\rho\frac{dV_w}{V_w} = \rho\beta_w dp \qquad \text{(A14)}$$

the change of mass per unit area due to water compressibility becomes:

$$dM_3 = n_s n_c \Delta z d\rho \qquad \text{(A15)}$$

$$dM_3 = n_s n_c \Delta z \rho\beta_w dp \qquad \text{(A16)}$$

substituting equations A10, A11, and A16 into equation A6 to get:

$$dM = \rho n_s n_c \Delta z(\alpha_p + \alpha_p + \beta_w)dp\Delta x\Delta y \qquad \text{(A17)}$$

the total change in mass per unit volume of aquifer is:

$$\frac{dM}{\Delta x\Delta y\Delta z} = \rho n_s n_c(\alpha_p + \alpha_p + \beta_w)dp \qquad \text{(A18)}$$

in practice, changes in groundwater storage observed in units of volume rather than mass, so equation A18 can be written as follow:

$$\frac{d\overline{V_w}}{\Delta x\Delta y\Delta z} = n_s n_c(\alpha_p + \alpha_p + \beta_w)dp \qquad \text{(A19)}$$

in which $d\overline{V_w}$ is the change in water volume in the element due to both water and aquifer compressibility. The change in pressure head at a point in the aquifer is as follow:

$$h_p = \frac{p}{\rho g} + z \tag{A20}$$

the changes in pressure is as follow:

$$dp = \rho g dh_p \tag{A21}$$

by replacing of dp in equation A19, and divide by dh_p gives the specific storage, the concept, which is used, almost exclusively in confined aquifer analysis.

$$S_s = \frac{1}{\Delta x \Delta y \Delta z} \frac{d\overline{V_w}}{dh_p} = n_s n_c \rho g (\alpha_p + \alpha'_p + \beta_w) \tag{A22}$$

the final specific storage equation becomes:

$$S_s = n_s n_c \rho g (\alpha_p + \alpha'_p + \beta_w) \tag{A23}$$

where:

S_s = specific storage (1/L),

n_s = porosity of the sand (dimensionless),

n_c = porosity of the carbon (dimensionless),

ρ = bulk density of porous media (M/L^3),

g = gravity force (L/T^2),

α_p = compressibility of the aquifer by porous media (LT^2/M),

α'_p = compressibility of the aquifer by carbon (LT^2/M),

β_w = compressibility of water (LT^2/M).

The specific storage is regarded as a constant; a property of the aquifer material, its contained water, and the overburden stress. Even when fine particles are added and retained on the aquifer material, which causes the change in porosity and effective stress, but the change in specific storage is so minor that can be assumed as constant.

To calculate the constant value for specific storage (S_s) in this case, the following data were collected. The compressibility value for water is $\beta_w = 4.8 \times 10^{-10}$ cm^2/dyne, for sand is $\alpha_p = 4.4 \times 10^{-9} cm^2 / dyne$ (McWhorter and Sunada, 1977), and for clay is $10^{-7} - 10^{-8} cm^2 / dyne$ (Freeze and Cherry, 1979). The compressibility value for carbon is assumed $\alpha_p = 10^{-8} cm^2 / dyne$, porosity of the sand n_s=0.369 and porosity of the carbon n_c=0.68 and the value for ρg=980 dynes/cm^3. Equation A23 is used to calculate the specific storage of porous media in this study. The result is $S_s = 3.7 \times 10^{-6}$ 1/cm.

Derivation of Flow Equation in Confined Aquifer

The groundwater equation in confined aquifer is developed by combining the Darcy equation with the principal of mass balance. Mass balance involves consideration of inflow, outflow, and change in groundwater storage. The mass discharge across any plane of the control volume is the product of the water density and the volume discharge (McWhorter and Sunada, 1977).

The difference between the outflow and inflow mass discharges across the two planes normal to x-axis is:

$$\text{Outflow rate-Inflow rate}=(\rho Q)_{\Delta x}-(\rho Q)_{0x} \qquad (A24)$$

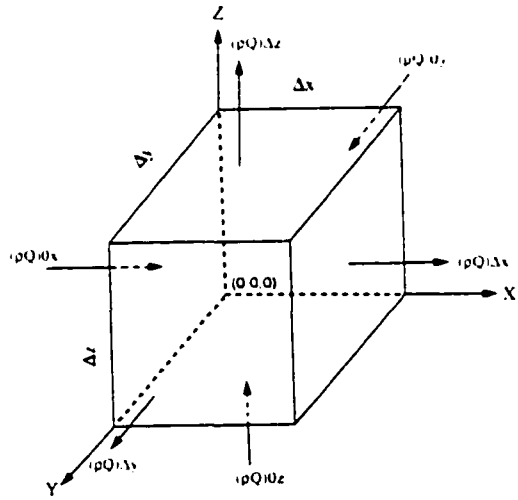

Figure. A1: Control volume for mass balance calculation in flow through porous media

The same expression can be written for y and z directions. The discharge across the plane at $x=\Delta x$ can be related to $x=0x$ by using the Taylor series expansion:

$$(\rho Q)_{\Delta x} = (\rho Q)_{0x} + \frac{\partial}{\partial x}(\rho Q)\Delta x + 0(\Delta x^2....) \qquad (A25)$$

the last term on right hand side called higher order term and can be negligible, because of small Δx. Now equation A25 can be substituted into equation A24 to get:

$$\text{Outflow rate-Inflow rate}=\frac{\partial}{\partial x}(\rho Q)\Delta x \qquad (A26)$$

The volume discharging Q is the product of the Darcy velocity and the area normal to the flow:

$$Q_x = q_x \Delta y \Delta z \qquad (A27)$$

the same equation can be written for Q_y and Q_z. The total outflow rate minus the total inflow rate is:

$$\text{Outflow rate-Inflow rate}=\left[\frac{\partial}{\partial x}(\rho q_x) + \frac{\partial}{\partial y}(\rho q_y) + \frac{\partial}{\partial z}(\rho q_z)\right]\Delta x \Delta y \Delta z \qquad (A28)$$

The net rate of mass outflow in equation A28 must be equal to the time-rate of change of mass (M) within the control volume. Therefore:

$$\left[\frac{\partial}{\partial x}(\rho q_x) + \frac{\partial}{\partial y}(\rho q_y) + \frac{\partial}{\partial z}(\rho q_z)\right]\Delta x \Delta y \Delta z = -\frac{\partial M}{\partial t} \qquad (A29)$$

The terms on left hand side of equation A29 are expanded by chain rule. In x-direction the term becomes:

$$\frac{\partial(\rho q_x)}{\partial x} = \rho \frac{\partial q_x}{\partial x} + q_x \frac{\partial \rho}{\partial x} \qquad (A30)$$

The terms of the form $\rho\frac{\partial q_x}{\partial x}$ are much greater than terms of the form $q_x\frac{\partial \rho}{\partial x}$ allow us to eliminate ρ from equation A29. Now if equation A30 is substituted into equation A29, the mass balance equation in x, y and z coordinates is:

$$\rho\left[\frac{\partial q_x}{\partial x}+\frac{\partial q_y}{\partial y}+\frac{\partial q_z}{\partial z}\right]\Delta x\Delta y\Delta z=-\frac{\partial M}{\partial t} \qquad \text{(A31)}$$

now Darcy equation for flow in heterogeneous and anisotropic aquifer is introduced into equation A31 and divide by $\rho\Delta x\Delta y\Delta z$ to get:

$$\frac{\partial}{\partial x}(K_x\frac{\partial h}{\partial x})+\frac{\partial}{\partial y}(K_y\frac{\partial h}{\partial y})+\frac{\partial}{\partial z}(K_z\frac{\partial h}{\partial z})=\frac{1}{\rho\Delta x\Delta y\Delta z}\frac{\partial M}{\partial t} \qquad \text{(A32)}$$

the change of water mass per unit volume was calculated by equation A18. Therefore, the mass balance can be written as:

$$\frac{\partial}{\partial x}(K_x\frac{\partial h}{\partial x})+\frac{\partial}{\partial y}(K_y\frac{\partial h}{\partial y})+\frac{\partial}{\partial z}(K_z\frac{\partial h}{\partial z})=n_s n_c(\alpha_p+\alpha_p+\beta_w)\frac{\partial p}{\partial t} \qquad \text{(A33)}$$

Finally, since $dp=\rho g dh$, as shown in equation A21 can be written as:

$$\frac{\partial}{\partial x}(K_x\frac{\partial h}{\partial x})+\frac{\partial}{\partial y}(K_y\frac{\partial h}{\partial y})+\frac{\partial}{\partial z}(K_z\frac{\partial h}{\partial z})=n_s n_c\rho g(\alpha_p+\alpha_p+\beta_w)\frac{\partial h}{\partial t} \qquad \text{(A34)}$$

the specific storage (equation A23) becomes:

$$S_s=n_s n_c\rho g(\alpha_p+\alpha_p+\beta_w) \qquad \text{(A35)}$$

now equation A35 can be substituted in to equation A34 to get:

$$\frac{\partial}{\partial x}(K_x\frac{\partial h}{\partial x})+\frac{\partial}{\partial y}(K_y\frac{\partial h}{\partial y})+\frac{\partial}{\partial z}(K_z\frac{\partial h}{\partial z})=S_s\frac{\partial h}{\partial t} \qquad \text{(A36)}$$

equation A36 is a linear partial differential equation, solution that represents time and space distribution of piezometric head in non-homogeneous, anisotropic, and confined

aquifer.

The one-dimensional transient flow equation in heterogeneous and anisotropic confined aquifer is:

$$\frac{\partial}{\partial x}(K_x \frac{\partial h}{\partial x}) = S_s \frac{\partial h}{\partial t} \qquad \text{(A37)}$$

where:

h =h (x, t) piezometric head (L),

K_x = hydraulic conductivity in x-direction (L/T),

S_s = specific storage (1/L).

APPENDIX B

DERIVATION OF SOLUTE TRANSPORT EQUATION

Transport Equation in Confined Aquifer

The common method to develop a differential equation for solute transport in porous media is to write a mass balance equation in fixed element volume in the flow domain. Figure B1 shows a control volume element that is used to derive the solute transport equation.

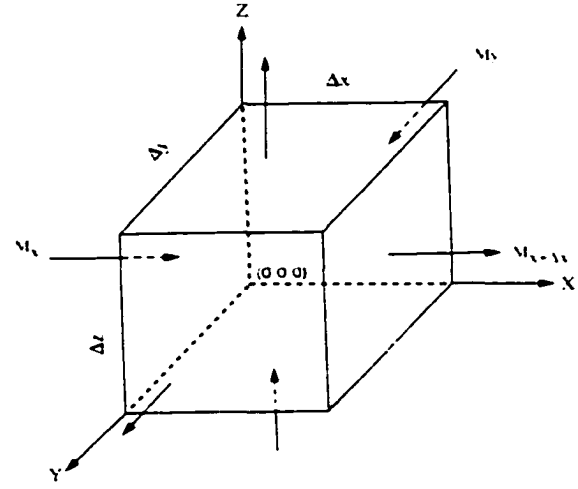

Figure. B1: Control volume for mass balance calculation in transport phenomena

Rate of mass out of the element	– rate of mass into the element	= - time rate change of mass	(B1)

To derive the solute transport equation, the following assumptions are made:

1- porous media is heterogeneous,

2- no dispersion,

3- saturated media,

4- no chemical reaction or radioactive decay,

5- Darcy's law applies,

6- flow is in one-direction.

Mass Transport in x-direction

The physical process that controls the flux into and out of the elemental volume is advection. The advective (convective) flux represents the mass flux of solute transported by the average fluid motion of groundwater.

$$\overline{M}_{x+\Delta x} - \overline{M}_{x} = -\frac{\partial}{\partial t}(M_{cv}) \qquad \text{(B2)}$$

$\overline{M}_{x+\Delta x}$ = rate of mass out of the element (M/T),

$\overline{M}_{x}$ = rate of mass into the element (M/T),

M_{cv} = mass in control volume (M).

To solve the above equation, Taylor series expansion is used:

$$\overline{M}(x+\Delta x) = \overline{M}(x) + \frac{\partial \overline{M}}{\partial x}\Delta x + \frac{\partial^2 \overline{M}}{\partial x^2}\Delta x^2 + \ldots\ldots \qquad \text{(B3)}$$

The second term and beyond are called higher order terms, they are assumed to be equal to zero because of small Δx, equation B3 is approximated by:

$$\overline{M}_{x+\Delta x} = \overline{M}_{x} + \frac{\partial \overline{M}_{x}}{\partial x}\Delta x \qquad \text{(B4)}$$

Now equation B4 can be substitute into equation B2 to get

$$\overline{M}_{x} + \frac{\partial \overline{M}_{x}}{\partial x}\Delta x - \overline{M}_{x} = -\frac{\partial M_{cv}}{\partial t} \qquad \text{(B5)}$$

$$\frac{\partial \overline{M}_x}{\partial x}\Delta x = -\frac{\partial M_{cv}}{\partial t} \qquad \text{(B6)}$$

Advection is the component of solute movement attributed to transport by the flowing groundwater. The rate of transport is equal to the average linear groundwater velocity (seepage velocity):

$$V_x = \frac{q_x}{n} = \frac{I}{n}\left(-K_x \frac{\partial h}{\partial x}\right) \qquad \text{(B7)}$$

Mass rate of solute is transported in the solution by advection in x-direction only is as follow:

$$\overline{M}_x = C\, q_x (area) = Cn V_x (\Delta y \Delta z) \qquad \text{(B8)}$$

$$\frac{\partial \overline{M}_x}{\partial x}\Delta x = \frac{\partial}{\partial x}(C V_x n)\Delta x \Delta y \Delta z \qquad \text{(B9)}$$

$$\frac{\partial}{\partial x}(CnV) = V\frac{\partial}{\partial x}(Cn) + Cn\frac{\partial V}{\partial x} \qquad \text{(B10)}$$

$$\frac{\partial}{\partial x}(Cn) = C\frac{\partial n}{\partial x} + n\frac{\partial C}{\partial x} \qquad \text{(B11)}$$

The first term in equation B11 means change of mass due to pore volume change, it is so small in compare to second term and assumed to be negligible. The second term means change of mass due to concentration change. With this assumption the porosity (n) can be factored, equation B9 becomes:

$$\frac{\partial \overline{M}_x}{\partial x}\Delta x = \frac{\partial}{\partial x}(C V_x) n \Delta x \Delta y \Delta z \qquad \text{(B12)}$$

where:

C (x,t) = concentration of the particles in suspension (M/L^3),

$\overline{M}_x$ = mass rate of solute transported in x-direction (M/T),

V_x = average instantaneous velocity in x-direction (L/T),

CV = instantaneous mass flux of the solute (M/L^2T),

$n\Delta x\Delta y\Delta z$ = volume of solution in the control volume (L^3).

Mass in Control Volume (M_{cv})

Time rate change of mass in control volume depends on the following mass changes:

S = mass of retained particles per unit bulk dry mass of porous media and particles (dimensionless)

Cn ($\Delta x\Delta y\Delta z$) = mass of solute in solution (M), and

$S\rho_b(\Delta x\Delta y\Delta z)$ = mass of retained particles in control volume (M)

$M_{cv} = Cn\Delta x\Delta y\Delta z + S\rho_b\Delta x\Delta y\Delta z$

Change of mass in control volume is as follow:

$$-\frac{\partial M_{cv}}{\partial t} = -\frac{\partial}{\partial t}(Cn\Delta x\Delta y\Delta z + S\rho_b\Delta x\Delta y\Delta z) \qquad \text{(B13)}$$

$$-\frac{\partial M_{cv}}{\partial t} = -\frac{\partial}{\partial t}[(Cn + S\rho_b)]\Delta x\Delta y\Delta z \qquad \text{(B14)}$$

Now, the right hand side of equation B14 can be expanded in two parts, the first part becomes:

$$\frac{\partial(Cn)}{\partial t} = n\frac{\partial C}{\partial t} + C\frac{\partial n}{\partial t} \qquad \text{(B15)}$$

The first term on right-hand side of equation B15 implies the change of mass due to concentration change.

The second term on the right hand side of equation B15 is the change of mass due to pore volume change, which is assumed negligible.

The second part on right hand side of equation B14 is as follow:

$$\frac{\partial(S\rho_b)}{\partial t} = \rho_b \frac{\partial S}{\partial t} + S\frac{\partial \rho_b}{\partial t} \qquad \text{(B16)}$$

The second term on right hand side of equation B16 is so small and assumed to be negligible.

The first term on right hand-side of equation B16 implies the change of mass due to retained particles change and is derived as follow:

$\partial S/\partial t$ represent the rate at which the particles are retained on sand (M/MT).

$\rho_n \frac{\partial S}{\partial t}$ changes of concentration in fluid caused by retained particles (M/TL^3).

The amount of particles that are retained on the aquifer material is a function of concentration of the particles in suspension S=f(C), using chain rule the term can be written as:

$$\rho_b \frac{\partial S}{\partial t} = \rho_b \frac{\partial S}{\partial C}\frac{\partial C}{\partial t} \qquad \text{(B17)}$$

Now equations B11 and B17 can be substituted into equation B14:

$$-\frac{\partial M_{cv}}{\partial t} = -\left[n\frac{\partial C}{\partial t} + \rho_b \frac{\partial S}{\partial C}\frac{\partial C}{\partial t}\right]\Delta x\Delta y\Delta z \qquad \text{(B18)}$$

Equations B12 and B18 can be substituted into equation B6, after dividing both sides by total control volume ($\Delta x\Delta y\Delta z$), porosity (n), and factoring concentration (C) equation B6 becomes:

$$\frac{\partial}{\partial x}(CV_x) = -\frac{\partial}{\partial t}\left[C(1+\frac{\rho_b}{n}\frac{\partial S}{\partial C})\right] \qquad \text{(B19)}$$

The term $\frac{\partial S}{\partial C} = \chi(C)$, is a parameter, which is a function of concentration with a unit of (L^3/M). The retention factor equation is as follow:

$$R = 1 + \frac{\rho_b}{n}(\chi) \qquad \text{(B20)}$$

where:

R = retention factor equation (dimensionless),

ρ_b = bulk density of the porous media (L^3/M),

n = porosity of the porous media (dimensionless),

χ = retention function (M/L^3).

The graphical relations of χ versus C and their equivalent mathematical expressions are known as isotherms. Figure B2 shows a nonlinear isotherm relationship exist between χ and concentration of the particles in suspension (C).

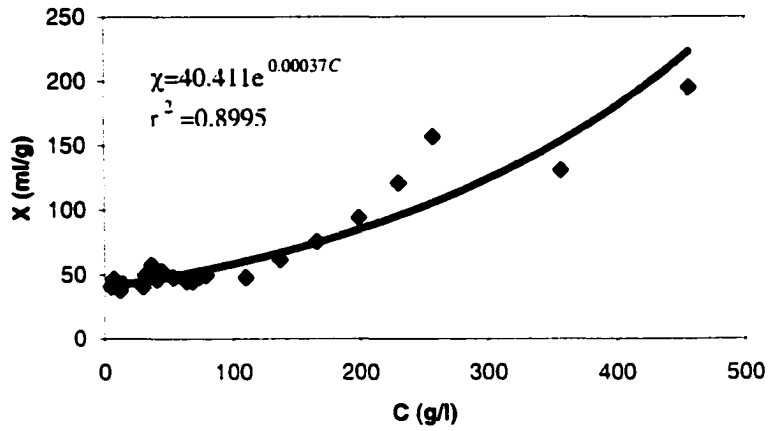

Figure B2: Nonlinear isotherm relationship between χ and C at t=12 hours

The retention function form of the equation is as follow:

$$\chi(C) = \frac{dS}{dC} = Me^{NC} \tag{B21}$$

S = mass of retained particles per unit bulk dry mass of porous media and particles (dimensionless),

C = concentration of the particles in suspension (g/l),

N = constant parameter (l/g),

M = constant parameter (l/g).

To solve equation B21, the following procedure is done:

$$S = \int Me^{NC} dC \tag{B22}$$

$$S(C) = \frac{M}{N} e^{NC} + A^{*} \tag{B23}$$

To calculate constant A^{*}, the initial concentration (C=0.0) is used. In this case

S (0.0)=M/N+A*=0.0, which gives the value for A*=-M/N. Now this value is substituted into equation B23 to get:

$$S(C) = \frac{M}{N}(e^{\lambda C} - 1) \qquad \text{(B24)}$$

Equation B24 shows that S is a nonlinear function of C then, V_{rp} is also a function of C, $V_{rp}=V_{rp}(C)$. This fact means that different concentration move at different speed. Also the concentration distribution in space changes shape from one time period to another. That is, spatial concentration distribution or waves may either sharpen or spread as they move, solely due to the effects of non linearity (Charbeneau, 2000). Now equation B21 can be substituted in to equation B20, after some rearrangement and mathematical manipulation the final retention factor equation becomes:

$$\frac{V}{V_{rp}} = R = 1 + \alpha e^{\beta C} \qquad \text{(B25)}$$

where:

V_{rp} = velocity of the retained particles (L/T),

V = seepage velocity (L/T),

R = retention factor (dimensionless),

C = concentration of the particles in suspension (g/l),

α = constant parameter (dimensionless),

β = constant parameter (l/g).

The final one-dimensional solute transport equation in heterogeneous, saturated porous media with no chemical reaction, radioactive decay, and no dispersion is as follow:

$$\frac{\partial}{\partial t}(RC)+\frac{\partial}{\partial x}(CV_x)=0.0 \qquad \text{(B26)}$$

where:

R = retention factor (dimensionless),

C = concentration of the particles in suspension (M/V_l),

V_x = seepage velocity in x-direction (L/T).

APPENDIX C

ONE-DIMENSIONAL COMPUTER PROGRAM LISTING

C1-Calibration Model

```
C     PROGRAM CSUARM
C*****************************************************************
C     THIS IS A ONE-DIMENSIONAL COMPUTER PROGRAM THAT SIMULATE   *
C     THE UNSTEADY FLOW AND TRANSPORT EQUATIONS IN POROUS MEDIA. *
C     THE RESULT IS CONCENTRATION PROFILE WITH RESPECT TO  SPACE *
C     AND TIME.  OUTPUTS ARE PRESENTED IN FILE FORM.             *
C     THE FINITE DIFFERENCE METHOD IS USED TO SOLVE THE GOVERNING*
C     EQUATIONS.  PREISSMANN BOX SCHEME IS SELECTED TO DISCRETIZE*
C     THE TRANSPORT EQUATION.  AN IMPLICIT FINITE DIFFERENCE     *
C     SCHEME CALLED CRANK-NICHOLSON IS USED TO SOLVE THE FLOW
C     EQUATION TO CALCULATE THE VELOCITY VALUAS.                 *
C     PREPARED BY HASSAN VAGHARFARD, GROUNDWATER PROGRAM         *
C     CIVIL ENGINEERING DEPARTMENT, COLORADO STATE UNIVERSITY    *
C     FORT COLLINS, COLORADO.                                    *
C-----------------------------------------------------------------*
C       PARAMETER SPECIFICATION
C-----------------------------------------------------------------
C  XL=LENGTH OF FLOW DOMAIN
C  DX=DISTANCE INCRENENT
C  C0=UP-STREAM BOUNDARY INJECTION CONCENTRATION
C  K0=INITIAL HYDRAULIC CONDUCTIVITY
C  R0=CONSTANT PARAMETER IN RETENTION FACTOR EQUATION
C  Ss=SPECIFIC STORAGE OF POROUS MEDIA
C  N0=INITIAL POROSITY
C  RO0=INITIAL BULK DENSITY OF POROUS MEDIA
C  ALPHA, BETA=REGRESSION COEFFICIENTS BETWEEN RETENTION FACTOR
C              AND CONCENTRATION
C  GAMA=EXPONENT OF POWER FUNCTION BETWEEN HYDRAULIC CONDUCTIVITY
C       AND CONCENTRATION
C  MU=CONSTANT PARAMETER IN POROSITY EQUATION
C  ETA=CONSTANT PARAMETER IN BULK DENSITY EQUATION
C  TETA=TEMPORAL WEIGHTING FACTOR IN PREISSMANN AND CRANK-NICHOLSON
C       SCHEMES
C  SI=SPATIAL WEIGHTING FACTOR IN PREISSMANN BOX SCHEME
C  TOL=ALLOWABLE ERROR
C  XNODE=NUMBER OF NODES
C  DT=TIME STEP
C  K=ARRAY OF NODAL HYDRAULIC CONDUCTIVITY
C  VOLD=ARRAY OF PREVIOUS NODAL VELOCITIES
C  VNEW=ARRAY OF CURRENT NODAL VELOCITIES
C  COLD=ARRAY OF PREVIOUS NODAL CONCENTRATION
C  COLD=ARRAY OF CURRENT NODAL CONCENTRATION
C  RF=ARRAY OF NODAL RETENTION FACTOR
C  RO=ARRAY OF NODAL BULK DENSITY
C  HOLD=ARRAY OF PREVIOUS NODAL POTENTIOMETRIC HEAD
C  HNEW=ARRAY OF CURRENT NODAL POTENTIOMETRIC HEAD
C  SW=SWITCH OR FLAG OF ADVANCE TIP
C  CODE=FLAG OF CONTINUATION
C-----------------------------------------------------------------
C MEMORY ALLOCATION AND DATA TYPE SPECIFICATION
C-----------------------------------------------------------------
```

```
      CHARACTER IN*50,OUT*50
      REAL XL,DX,R0,K0,N0,RO0,MU,GAMA,ETA,SI,TETA,
     1TOL,Ss,C0,DEADLINE,HOLD(10),COLD(10),VOLD(10),HNEW(10),CNEW(10),
     2VNEW(10),K(10),N(10),RF(10),RO(10),TIME,DT,OBS(10),RMS,KI(10)
      INTEGER JJ,SW,CODE,XNODE
      AUTOMATIC XNODE,DX,R0,K0,N0,RO0,MU,GAMA,ETA,SI,TETA,TOL
     1,Ss,C0,DEADLINE,JJ,SW,CODE,XL,TIME,DT,KI
C-----------------------------------------------------------------
C MAIN ROUTINE
C-----------------------------------------------------------------
C     DEFINITION OF INPUT AND OUTPUT FILE NAMES
      CALL IOMANAGER(IN,OUT)
C     READING INPUT DATA FROM INPUT FILE
      CALL INPUTDATA(IN,XL,DX,R0,K0,N0,RO0,MU,GAMA,ETA,SI,
     1TETA,TOL,Ss,C0,DEADLINE,XNODE,HOLD,COLD,OBS,KI)
C     INITIALIZING VARIABLES
      CALL INITIALIZATION(TIME,DT,JJ,SW,CODE,XNODE,HOLD,HNEW,COLD,CNEW,
     1VOLD,VNEW,K,N,RF,RO,K0,N0,R0,RO0,C0,RMS)
      DO I=1,XNODE
      PRINT*,HOLD(I),COLD(I),OBS(I)
      END DO
C     COMPUTE VELOCITY VECTOR WITH INITIAL CONDITIONS
      CALL VELOCITY(XNODE,HOLD,VOLD,N,K,DX)
C     CHANGING NEW AND OLD VALUE OF VELOCITY VECTOR
      CALL CHANGE(XNODE,VOLD,VNEW)
C     SIMULATION OF FLOW AND SOLUTE TRANSPORT PROCESS
      DO WHILE(CODE.EQ.1)
C     SOLVING SOLUTE TRANSPORT EQUATION FOR DT AND C
      CALL CONCENTRATION(XNODE,SW,JJ,DX,DT,SI,TETA,COLD,CNEW,
     1VOLD,VNEW,RF)
C     COMPUTE NEW PHYSICAL PROPERTIES OF POROUS MEDIA
        CALL PROPERTIES(SW,XNODE,GAMA,MU,ETA,CNEW,N,K,RF,RO,
     1  N0,K0,R0,RO0,KI)
C     SOLVING FLOW EQ. FOR H
        CALL HEAD(XNODE,DX,DT,Ss,TETA,TOL,HNEW,HOLD,K)
C     COMPUTE VELOCITY VECTOR WITH NEW CONDITIONS
        CALL VELOCITY(XNODE,HNEW,VNEW,N,K,DX)
C     REPLACING NEW VALUES BY OLD ONES
        CALL CHANGE(XNODE,CNEW,COLD)
        CALL CHANGE(XNODE,HNEW,HOLD)
        CALL CHANGE(XNODE,VNEW,VOLD)
C     DETERMINATION OF CONTINUATION OF SIMULATION
        CALL CONTINUATION(SW,JJ,XNODE,TIME,DT,CNEW(1),C0,DEADLINE,CODE)
      END DO
C     DETERMINATION OF MODEL ERROR
      CALL RMSERROR(XNODE,CNEW,OBS,RMS)
C     MAKING AN OUTPUT FILE OF RESULTS
      CALL OUPUTDATA(OUT,XNODE,TIME,RMS,CNEW,OBS,K,N,RF,RO)
      DO I=1,XNODE
      PRINT*,CNEW(I)
      END DO
      PRINT*,'RMS=',RMS
      STOP
      END
C-----------------------------------------------------------------
```

```
C END OF MAIN ROUTINE
C-----------------------------------------------------------------
C SUBROUTINES:
C-----------------------------------------------------------------
      SUBROUTINE CHANGE(XNODE,A,B)
C-----------------------------------------------------------------
C THIS SUBROUTINE REPLACES OLD VALUES OF AN ARRAY WITH NEW VALUES IN
C     ANOTHER ARRAY
C-----------------------------------------------------------------
C     COMMON //XNODE,DX,R0,K0,N0,RO0,MU,GAMA,ALPHA,BETA,ETA,SI,
C    1TETA,TOL,Ss,C0,DEADLINE,JJ,SW,CODE,XL,TIME,DT
      INTEGER XNODE
      DIMENSION A(10),B(10)
      DO I=1,XNODE
        B(I)=A(I)
      END DO
      RETURN
      END
C
      SUBROUTINE CONCENTRATION(XNODE,SW,JJ,DX,DT,SI,TETA,COLD,CNEW,
     1VOLD,VNEW,RF)
C-----------------------------------------------------------------
C IN THIS SUBROUTINE THE SOLUTE TRANSPORT EQUATION IS SOLVED WITH A
C SEMI-IMPLICIT SCHEME. THE SCHEME BEING USED, IS CALLED THE
C PREISSMANN BOX SCHEME.  FOR EACH ADVANING CELL (TIP CELL),
C INITIALLY DT IS COMPUTED, THEN NEW CONCENTRATION FOR OTHER CELLS
C AT THIS DT IS CALCULATED.
C-----------------------------------------------------------------
C     COMMON //XNODE,DX,R0,K0,N0,RO0,MU,GAMA,ALPHA,BETA,ETA,SI,TETA,
C    1TOL,Ss,C0,DEADLINE,JJ,SW,CODE,XL,TIME,DT
      INTEGER XNODE,SW,JJ
      REAL DX,DT,SI,TETA,COLD(10),CNEW(10),VOLD(10),VNEW(10),RF(10)
      DO I=2,XNODE
C DETERMINATION OF MEAN BY LAX MEAN AND ARITHMATIC MEAN METHOD
        CMEAN=TETA*CNEW(I-1)+(1.0-TETA)*0.5*(COLD(I)+COLD(I-1))
        RMEAN=0.5*(RF(I)+RF(I-1))
        VMEAN=TETA*VNEW(I-1)+(1.0-TETA)*0.5*(VOLD(I)+VOLD(I-1))
C CONTROL OF ADVANCE TIP
        IF(I.EQ.JJ.AND.SW.EQ.1) THEN
C DETERMINATION OF DT REQUIRED TO ADVANCE ONE DX DOWNSTREAM
C AT TIP CELL C=0
          DT=(SI*(-COLD(I))+(1.0-SI)*(CNEW(I-1)-COLD(I-1)))/
     1    (-VMEAN/RMEAN/DX*(TETA*(CNEW(I)-CNEW(I-1))+(1.0-TETA)*
     2    (COLD(I)-COLD(I-1))))
          EXIT
        ELSE
C DETERMINATION OF C AT NEW TIME LEVEL UNTIL TIP CELL
          CNEW(I)=((VMEAN*DT*TETA/RMEAN/DX-1.0+SI)*CNEW(I-1)+(SI-VMEAN*
     1    DT*(1.0-TETA)/RMEAN/DX)*COLD(I)+(1.0-SI+VMEAN*DT*(1.0-TETA)/
     2    RMEAN/DX)*COLD(I-1))/(SI+VMEAN*DT*TETA/RMEAN/DX)
          IF(CNEW(I).LT.0) CNEW(I)=0.0
        END IF
      END DO
      RETURN
      END
```

```
C
      SUBROUTINE CONTINUATION(SW,JJ,XNODE,TIME,DT,CNEW1,C0,DEADLINE,
     1CODE)
C-----------------------------------------------------------------
C THIS SUBROUTINE STUDIES CONTINUATION OF SIMULATION
C-----------------------------------------------------------------
C     COMMON //XNODE,DX,R0,K0,N0,RO0,MU,GAMA,ALPHA,BETA,ETA,SI,
C    1TETA,TOL,Ss,C0,DEADLINE,JJ,SW,CODE,XL,TIME,DT
      INTEGER SW,JJ,CODE,XNODE
      REAL TIME, DT,CNEW1,C0,DEADLINE
      TIME=DT+TIME
      JJ=JJ+1
C CONTROL OF LOCATION OF TIP CELL
      IF(JJ.LE.XNODE) THEN
C CONTINUE OPERATION WITH AN ADVANCING TIP CELL
        CODE=1
      ELSE
C CONTROL OF TIME INJECTION
        IF(TIME.GT.DEADLINE) THEN
C DO NOT CONTINUE AND EXIT (END OF INJECTION)
          CODE=0
          RETURN
        END IF
C CONTINUE OPERATION WITHOUT AN ADVANCING TIP CELL
        SW=0
        JJ=JJ-1
        CODE=1
      END IF
C CONTINUE INJECTION WITH A CONSTANT RATE
      CNEW1=CNEW1+C0*DT
      RETURN
      END
C
      SUBROUTINE HEAD(XNODE,DX,DT,Ss,TETA,TOL,HNEW,HOLD,K)
C-----------------------------------------------------------------
C WITH CRANK-NICHOLSON METHOD, FLOW EQUATION IS BEING SOLVED. THE
C APPLIED SCHEME IS AN IMPLICIT ONE THAT IS UNCONDITIONALLY STABLE.
C-----------------------------------------------------------------
C     COMMON //XNODE,DX,R0,K0,N0,RO0,MU,GAMA,ALPHA,BETA,ETA,SI,
C    1TETA,TOL,Ss,C0,DEADLINE,JJ,SW,CODE,XL,TIME,DT
      INTEGER XNODE
      REAL DX,DT,Ss,TETA,TOL, HNEW(10),HOLD(10),K(10)
C CONTROL OF REQUIRED PRECISION AND ACCURACY
      DO WHILE(AMAX.GT.TOL)
        AMAX=0.0
C DETERMINATION OF NEW HEAD DISTRIBUTION ALONG THE COMPUTATIONAL DOMAIN
C WITH NEW PHYSICAL AND HYDRAULIC CONDITION
        DO I=2,XNODE
          OLDVAL=HNEW(I)
          H1=(HOLD(I+1)+HOLD(I-1))/2.0
          H2=(HNEW(I+1)+HNEW(I-1))/2.0
          F1=(DX**2)*Ss/2.0/K(I)/DT
          F2=1.0/(F1+TETA)
          HNEW(I)=((F1*HOLD(I)+(1.0-TETA)*(H1-HOLD(I))+(TETA*H2)))*F2
          Epsilon=ABS(HNEW(I)-OLDVAL)
```

```
          IF(Epsilon.GT.AMAX) AMAX=Epsilon
        END DO
C CONTROL OF EXPLICITY AND IMPLICITY OF SCHEME
        IF(TETA.LT.0.1) EXIT
      END DO
      RETURN
      END
C
      SUBROUTINE INITIALIZATION(TIME,DT,JJ,SW,CODE,XNODE,HOLD,HNEW,
     1COLD,CNEW,VOLD,VNEW,K,N,RF,RO,K0,N0,R0,RO0,C0,RMS)
C-----------------------------------------------------------------
C INITIALIZING ALL ARRAYS AND PARAMETERS IS DONE BY THIS SUBROUTINE
C-----------------------------------------------------------------
C     COMMON //XNODE,DX,R0,K0,N0,RO0,MU,GAMA,ALPHA,BETA,ETA,SI,
C    1TETA,TOL,Ss,C0,DEADLINE,JJ,SW,CODE,XL,TIME,DT
      INTEGER JJ,SW,CODE,XNODE
      REALTIME,DT,HOLD(10),HNEW(10),COLD(10),CNEW(10),VOLD(10),
     1VNEW(10),K(10),N(10),RF(10),RO(10),K0,N0,R0,RO0,C0,RMS
      HOLD(0)=HOLD(1)
      HNEW(0)=HOLD(0)
      COLD(0)=COLD(1)
      CNEW(0)=COLD(0)
      K(0)=K0
      N(0)=N0
      DO I=1,XNODE + 1
        HNEW(I)=HOLD(I)
        CNEW(I)=COLD(I)
        VOLD(I)=0.0
        VNEW(I)=0.0
        N(I)=N0
        RF(I)=R0
        K(I)=K0
        RO(I)=RO0
      END DO
      CNEW(1)=CNEW(1)+C0
      TIME=0.0
      DT=0.0
      JJ=2
      SW=1
      CODE=1
 2    RMS=0.0
      RETURN
      END
C
      SUBROUTINE INPUTDATA(IN,XL,DX,R0,K0,N0,RO0,MU,GAMA,ETA,
     1SI,TETA,TOL,Ss,C0,DEADLINE,XNODE,HOLD,COLD,OBS,KI)
C-----------------------------------------------------------------
C INPUT DATA ARE BEING READ BY THIS SUBROUTINE FROM AN INPUT FILE
C DEFINED IN SUBROUTINE IOMANAGER BELOW.
C-----------------------------------------------------------------
C     COMMON //XNODE,DX,R0,K0,N0,RO0,MU,GAMA,ALPHA,BETA,ETA,SI,
C    1TETA,TOL,Ss,C0,DEADLINE,JJ,SW,CODE,XL,TIME,DT
      CHARACTER IN*50
      INTEGER XNODE
      REAL XL,DX,R0,K0,N0,RO0,MU,GAMA,ETA,SI,TETA,
```

```
     1TOL,Ss,C0,DEADLINE,HOLD(10),COLD(10),OBS(10),KI(10)
      OPEN(1,FILE=IN,STATUS='OLD')
      READ (1,*) XL,DX,R0,K0,N0,RO0,MU,GAMA,ETA,SI,TETA,TOL,
     1Ss,C0,DEADLINE
C DETERMINATION OF NUMBER OF NODAL POINTS
      XNODE=INT(XL/DX)
      IF(XNODE.NE.XL/DX) THEN XNODE=XNODE+1
C READING INITIAL HEAD AND CONCENTRATION DISTRIBUTION
      DO I=1,XNODE+1
        READ (1,*) HOLD(I),COLD(I),OBS(I),KI(I)
      END DO
      CLOSE(1)
      RETURN
      END
C
      SUBROUTINE IOMANAGER (IN,OUT)
C-------------------------------------------------------
C INPUT AND OUTPUT FILES ARE DEFINED IN THIS SUBROUTINE
C-------------------------------------------------------
      CHARACTER IN*50,OUT*50
      PRINT *,'Please enter input file name'
      READ *,IN
      PRINT *,'Please enter output file name'
      READ *, OUT
      RETURN
      END
C
      SUBROUTINE OUPUTDATA(OUT,XNODE,TIME,RMS,CNEW,OBS,K,N,RF,RO)
C-----------------------------------------------------------------
C AN OUTPUT FILE DEFINED IN IOMANAGER (ABOVE) IS MADE AND OUTPUT
C RESULTS ARE WRITTEN INTO IT.
C-----------------------------------------------------------------
C     COMMON //XNODE,DX,R0,K0,N0,RO0,MU,GAMA,ALPHA,BETA,ETA,SI,
C    1TETA,TOL,Ss,C0,DEADLINE,JJ,SW,CODE,XL,TIME,DT
      CHARACTER OUT*50
      INTEGER XNODE
      REAL TIME,CNEW(10),K(10),N(10),RF(10),RO(10),OBS(10)
      OPEN(1,FILE=OUT,STATUS='UNKNOWN')
      WRITE (1,*)
      WRITE (1,100) TIME
      WRITE (1,101) RMS
      WRITE (1,*)
      WRITE (1,102)
      WRITE (1,103)
      DO I=1,XNODE
      WRITE (1,104) I,CNEW(I),OBS(I),K(I),N(I),RF(I),RO(I)
      END DO
      CLOSE(1)
100   FORMAT(5X,'TIME=',F12.1)
101   FORMAT(5X,'RMS=',F12.3)
102   FORMAT('  X        CAL.C        OBS.C        K        N
     1RF       RO')
103   FORMAT(' CM          G/L          G/L     CM/S
     2     G/CM^3')
104   FORMAT(1X,I2,2(1X,F12.5),2(1X,F8.5),1X,F12.3,1X,F8.3)
```

```
      RETURN
      END
C
      SUBROUTINE PROPERTIES(SW,XNODE,GAMA,MU,ETA,CNEW,N,K,RF,
     1RO,N0,K0,R0,RO0,KI)
C-----------------------------------------------------------------
C VARIATION OF PHYSICAL PROPERTIES OF POROUS MEDIA ARE DETERMINED
C BY THIS SUBROUTINE
C-----------------------------------------------------------------
C     COMMON //XNODE,DX,R0,K0,N0,RO0,MU,GAMA,ALPHA,BETA,ETA,SI,
C    1TETA,TOL,Ss,C0,DEADLINE,JJ,SW,CODE,XL,TIME,DT
      INTEGER XNODE,SW
      REAL GAMA,MU,ETA,CNEW(10),N(10),K(10),RF(10),
     1RO(10),N0,K0,R0,RO0,KI(10)
      IF(SW.EQ.0) THEN
C DETERMINATION OF PHYSICAL CHARACTERISTICS OF POROUS MEDIA AS SOME
C PREDEFINED FUNCTIONS OF CONCENTRATION
        DO I=1,XNODE
          N(I)=N0-MU*CNEW(I)
          RO(I)=RO0+ETA*CNEW(I)
          RF(I)=R0+KI(I)*RO(I)/N(I)
          K(I)=K0*EXP(-GAMA*CNEW(I))
        END DO
      END IF
      RETURN
      END
C
      SUBROUTINE VELOCITY(XNODE,H,V,N,K,DX)
C-----------------------------------------------------------------
C VELOCITY VECTOR IS CALCULATED BY THIS SUBROUTINE, BY USING DARCY
C EQUATION AND THEN AVERAGE LINEAR VELOCITY VECTOR IS COMPUTED.
C-----------------------------------------------------------------
C     COMMON //XNODE,DX,R0,K0,N0,RO0,MU,GAMA,ALPHA,BETA,ETA,SI,
C    1TETA,TOL,Ss,C0,DEADLINE,JJ,SW,CODE,XL,TIME,DT
      REAL H(10),V(10),N(10),K(10)
      INTEGER XNODE
      DO I=1,XNODE
        V(I)=K(I)*(K(I-1)*(K(I)+K(I+1))*(H(I-1)-H(I))+K(I+1)*(K(I)+
     1  K(I-1))*(H(I)-H(I+1)))/N(I)/DX/(K(I)+K(I-1))/(K(I)+K(I+1))
      END DO
      RETURN
      END
C
      SUBROUTINE RMSERROR(XNODE,CNEW,OBS,RMS)
C-----------------------------------------------------------------
C ROOT MEAN SQUARE OF ERROR (DEVIATION OF CALCULATED CONCENTRATION
C FROM OBSERVED DATA IS DETERMINED BY THIS FUNCTION
C-----------------------------------------------------------------
C     COMMON //XNODE,DX,R0,K0,N0,RO0,MU,GAMA,ALPHA,BETA,ETA,SI,
C    1TETA,TOL,Ss,C0,DEADLINE,JJ,SW,CODE,XL,TIME,DT
      INTEGER XNODE
      REAL RMS,CNEW(10),OBS(10)
      DO I=1,XNODE
      RMS=(CNEW(I)-OBS(I))**2+RMS
      END DO
```

```
      RMS=SQRT(RMS/(XNODE))
      RETURN
      END
C-----------------------------------------------------------------------
C END OF SUBROUTINES
C-----------------------------------------------------------------------
```

C2-Simulation Model

```
C   PROGRAM CSUARM
*****************************************************************
*     THIS IS A ONE-DIMENSIONAL COMPUTER PROGRAM THAT SIMULATES  *
*     THE UNSTEADY FLOW AND TRANSPORT EQUATION IN POROUS MEDIA   *
*     WITH INITIAL INFLOW CONCENTRATION (Co) OF FINES.  THE      *
*     RESULT IS CONCENTRATION PROFILE WITH RESPECT TO SPACE AND  *
*     TIME.  OUTPUTS ARE PRESENTED IN FILE FORM.                 *
*     THE FINITE DIFFERENCE METHOD IS USED TO SOLVE THE GOVERNING*
*     EQUATION.  PREISSMANN BOX SCHEME IS SELECTED TO DISCRETIZE *
*     THE TRANSPORT EQUATION.  AN IMPLICIT FINITE DIFFERENCE     *
*     SCHEME CALLAD CRANK-NICHOLSON IS USED TO SOLVE FLOW        *
*     EQUATION TO CALCULATE THE VELOCITY VALUE.                  *
*     PREPARED BY HASSAN.VAGHARFARD GROUNDWATER PROGRAM,         *
*     CIVIL ENGINEERING DEPARTMENT, COLORADO STATE UNIVERSITY    *
*     FORT COLLINS, COLORADO.                                    *
*----------------------------------------------------------------*
C       PARAMETER SPECIFICATION
C----------------------------------------------------------------
C  XL=LENGTH OF FLOW DOMAIN
C  DX=DISTANCE INCREMENT
C  C0=UP-STREAM BOUNDARY INJECTION CONCENTRATION
C  K0=INITIAL HYDRAULIC CONDUCTIVITY
C  R0=CONSTANT VALUE IN RETENTION FACTOR EQUATION
C  Ss=SPECIFIC STORAGE OF POROUS MEDIA
C  N0=INITIAL POROSITY
C  RO0=INITIAL BULK DENSITY OF POROUS MEDIA
C  ALPHA, BETA=REGRESSION COEFFICIENTS BETWEEN RETENTION FACTOR
C              AND CONCENTRATION
C  GAMA=EXPONENT OF POWER FUNCTION BETWEEN HYDRAULIC CONDUCTIVITY
C       AND CONCENTRATION
C  MU=CONSTANT PARAMETER IN POROSITY EQUATION
C  ETA=CONSTANT PARAMETER IN BULK DENSITY EQUATION
C  TETA=TEMPORAL WEIGHTING FACTOR IN PREISSMANN AND CRANK-NICHOLSON
C       SCHEMES
C  SI=SPATIAL WEIGHTING FACTOR IN PREISSMANN BOX SCHEME
C  TOL=ALLOWABLE ERROR
C  XNODE=NUMBER OF NODES
C  DT=TIME STEP
C  TMAX=DEADLINE
C  K=ARRAY OF NODAL HYDRAULIC CONDUCTIVITY
C  VOLD=ARRAY OF PREVIOUS NODAL VELOCITIES
C  VNEW=ARRAY OF CURRENT NODAL VELOCITIES
C  COLD=ARRAY OF PREVIOUS NODAL CONCENTRATION
C  CNEW=ARRAY OF CURRENT NODAL CONCENTRATION
C  RF=ARRAY OF NODAL RETENTION FACTOR
C  RO=ARRAY OF NODAL BULK DENSITY
C  HOLD=ARRAY OF PREVIOUS NODAL POTENTIOMETRIC HEAD
C  HNEW=ARRAY OF CURRENT NODAL POTENTIOMETRIC HEAD
C  SW=SWITCH OR FLAG OF ADVANCE TIP
C  CODE=FLAG OF CONTINUATION
C----------------------------------------------------------------
```

```
C MEMORY ALLOCATION AND DATA TYPE SPECIFICATION
C-----------------------------------------------------------------
      CHARACTER IN*50,OUT*50
      REAL XL,DX,R0,K0,N0,RO0,MU,GAMA,ALPHA,BETA,ETA,SI,TETA,TOL,Ss,C0,
     1DEADLINE,HOLD(10),COLD(10),VOLD(10),HNEW(10),CNEW(10),VNEW(10),
     2K(10),N(10),RF(10),RO(10),TIME,DT
      INTEGER JJ,SW,CODE,XNODE
      AUTOMATIC XNODE,DX,R0,K0,N0,RO0,MU,GAMA,ALPHA,BETA,ETA,SI,
     1TETA,TOL,Ss,C0,DEADLINE,JJ,SW,CODE,XL,TIME,DT
C-----------------------------------------------------------------
C MAIN ROUTINE
C-----------------------------------------------------------------
C     DEFINITION OF INPUT AND OUTPUT FILE NAMES
      CALL IOMANAGER(IN,OUT)
C     READING INPUT DATA FROM INPUT FILE
      CALL INPUTDATA(IN,XL,DX,R0,K0,N0,RO0,MU,GAMA,ALPHA,BETA,ETA,SI,
     1TETA,TOL,Ss,C0,DEADLINE,XNODE,HOLD,COLD)
C     INITIALIZING VARIABLES
      CALL INITIALIZATION(TIME,DT,JJ,SW,CODE,XNODE,HOLD,HNEW,COLD,CNEW,
     1VOLD,VNEW,K,N,RF,RO,K0,N0,R0,RO0,C0)
C     COMPUTING VELOCITY VECTOR WITH INITIAL CONDITIONS
      CALL VELOCITY(XNODE,HOLD,VOLD,N,K,DX)
C     CHANGING NEW AND OLD VALUE OF VELOCITY VECTOR
      CALL CHANGE(XNODE,VOLD,VNEW)
C     SIMULATION OF FLOW AND SOLUTE TRANSPORT PROCESSES
      DO WHILE(CODE.EQ.1)
C     SOLVING SALUTE TRANSPORT EQ. FOR DT AND C.
      CALL CONCENTRATION(XNODE,SW,JJ,DX,DT,SI,TETA,COLD,CNEW,
     1VOLD,VNEW,RF)
C     COMPUTING NEW PHYSICAL PROPERTIES OF POROUS MEDIA
      CALL PROPERTIES(SW,XNODE,ALPHA,BETA,GAMA,MU,ETA,CNEW,N,K,
     1RF,RO,N0,K0,R0,RO0)
C     SOLVING FLOW EQ. FOR H
        CALL HEAD(XNODE,DX,DT,Ss,TETA,TOL,HNEW,HOLD,K)
C     COMPUTING VELOCITY VECTOR WITH NEW CONDITIONS
        CALL VELOCITY(XNODE,HNEW,VNEW,N,K,DX)
C     REPLACING NEW VALUES BY OLD ONES
        CALL CHANGE(XNODE,CNEW,COLD)
        CALL CHANGE(XNODE,HNEW,HOLD)
        CALL CHANGE(XNODE,VNEW,VOLD)
C     DETERMINATION OF CONTINUATION OF SIMULATION
        CALL CONTINUATION(SW,JJ,XNODE,TIME,DT,CNEW(1),C0,DEADLINE,CODE)
      END DO
C     MAKING AN OUTPUT FILE OF RESULTS
      CALL OUPUTDATA(OUT,XNODE,TIME,CNEW,K,N,RF,RO)
      STOP
      END
C-----------------------------------------------------------------
C END OF MAIN ROUTINE
C-----------------------------------------------------------------
      SUBROUTINE CHANGE(XNODE,A,B)
C-----------------------------------------------------------------
C THIS SUBROUTINE REPLACES OLD VALUES OF AN ARRAY WITH NEW VALUES IN
C ANOTHER ARRAY
C-----------------------------------------------------------------
```

```
      INTEGER XNODE
      DIMENSION A(10),B(10)
      DO I=1,XNODE
      B(I)=A(I)
      END DO
      RETURN
      END
C
      SUBROUTINE CONCENTRATION(XNODE,SW,JJ,DX,DT,SI,TETA,
     1COLD,CNEW,VOLD,VNEW,RF)
C-----------------------------------------------------------------
C IN THIS SUBROUTINE THE SOLUTE TRANSPORT EQ. IS SOLVED WITH A
C SEMI-IMPLICIT SCHEME. THE SCHEME BEING USED, IS CALLED THE
C PREISSMANN BOX SCHEME.  FOR EACH ADVANING CELL (TIP CELL),
C INITIALLY DT IS COMPUTED, THEN NEW CONCENTRATION FOR OTHER
C CELLS AT THIS DT IS CALCULATED.
C-----------------------------------------------------------------
      INTEGER XNODE,SW,JJ
      REAL DX,DT,SI,TETA,COLD(10),CNEW(10),VOLD(10),VNEW(10),RF(10)
      DO I=2,XNODE
C DETERMINATION OF MEAN BY LAX MEAN AND ARITHMETIC MEAN
        CMEAN=TETA*CNEW(I-1)+(1.0-TETA)*0.5*(COLD(I)+COLD(I-1))
        RMEAN=0.5*(RF(I)+RF(I-1))
        VMEAN=TETA*VNEW(I-1)+(1.0-TETA)*0.5*(VOLD(I)+VOLD(I-1))
C CONTROL OF ADVANCE TIP
        IF(I.EQ.JJ.AND.SW.EQ.1) THEN
C DETERMINATION OF DT REQUIRED TO ADVANCE ONE DX DOWNSTREAM
C AT TIP CELL C=0
          DT=(SI*(-COLD(I))+(1.0-SI)*(CNEW(I-1)-COLD(I-1)))/(-VMEAN/
     1    RMEAN/DX*(TETA*(CNEW(I)-CNEW(I-1))+(1.0-TETA)*(COLD(I)-
     2    COLD(I-1))))
          EXIT
        ELSE
C DETERMINATION OF C AT NEW TIME LEVEL UNTIL TIP CELL
          CNEW(I)=((VMEAN*DT*TETA/RMEAN/DX-1.0+SI)*CNEW(I-1)+(SI-VMEAN*
     1    DT*(1.0-TETA)/RMEAN/DX)*COLD(I)+(1.0-SI+VMEAN*DT*(1.0-TETA)/
     2    RMEAN/DX)*COLD(I-1))/(SI+VMEAN*DT*TETA/RMEAN/DX)
          IF(CNEW(I).LT.0.0) CNEW(I)=0.0
        END IF
      END DO
      RETURN
      END
C
      SUBROUTINE CONTINUATION(SW,JJ,XNODE,TIME,DT,CNEW1,
     1C0,DEADLINE,CODE)
C-----------------------------------------------------------------
C THIS SUBROUTINE STUDIES CONTINUATION OF SIMULATION
C-----------------------------------------------------------------
      INTEGER SW,JJ,CODE,XNODE
      REAL TIME, DT,CNEW1,C0,DEADLINE
      TIME=DT+TIME
      JJ=JJ+1
C CONTROL OF LOCATION OF TIP CELL
      IF(JJ.LE.XNODE) THEN
C CONTINUE OPERATION WITH AN ADVANCING TIP CELL
```

```
        CODE=1
      ELSE
C CONTROL OF TIME INJECTION
        IF(TIME.GT.DEADLINE) THEN
C DO NOT CONTINUE AND EXIT (END OF INJECTION)
          CODE=0
          RETURN
        END IF
C CONTINUE OPERATION WITHOUT AN ADVANCING TIP CELL
        SW=0
        JJ=JJ-1
        CODE=1
      END IF
C CONTINUE INJECTION WITH A CONSTANT RATE
      CNEW1=CNEW1+C0
      RETURN
      END
C
      SUBROUTINE HEAD(XNODE,DX,DT,Ss,TETA,TOL,HNEW,HOLD,K)
C-----------------------------------------------------------------
C WITH CRANK-NICHOLSON METHOD, FLOW EQ. IS BEING SOLVED. THE APPLIED
C SCHEME IS AN IMPLICIT SCHEME THAT IS UNCONDITIONALLY STABLE.
C-----------------------------------------------------------------
      INTEGER XNODE
      REAL DX,DT,Ss,TETA,TOL, HNEW(10),HOLD(10),K(10)
C CONTROL OF REQUIRED PRECISION AND ACCURACY
      DO WHILE(AMAX.GT.TOL)
        AMAX=0.0
C DETERMINATION OF NEW HEAD DISTRIBUTION ALONG THE COMPUTATIONAL DOMAIN
C WITH NEW PHYSICAL AND HYDRAULIC CONDITION
        DO I=2,XNODE
          OLDVAL=HNEW(I)
          H1=(HOLD(I+1)+HOLD(I-1))/2.0
          H2=(HNEW(I+1)+HNEW(I-1))/2.0
          F1=(DX**2)*Ss/2.0/K(I)/DT
          F2=1.0/(F1+TETA)
          HNEW(I)=((F1*HOLD(I)+(1.0-TETA)*(H1-HOLD(I))+(TETA*H2)))*F2
          Epsilon=ABS(HNEW(I)-OLDVAL)
          IF(Epsilon.GT.AMAX) THEN AMAX=Epsilon
        END DO
C CONTROL OF EXPLICITY AND IMPLICITY OF SCHEME
        IF(TETA.LT.0.1) EXIT
      END DO
      RETURN
      END
C
      SUBROUTINE INITIALIZATION(TIME,DT,JJ,SW,CODE,XNODE,HOLD,
     1HNEW,COLD,CNEW,VOLD,VNEW,K,N,RF,RO,K0,N0,R0,RO0,C0)
C-----------------------------------------------------------------
C INITIALIZING ALL ARRAYS AND PARAMETERS IS DONE IN THIS SUBROUTINE
C-----------------------------------------------------------------
      INTEGER JJ,SW,CODE,XNODE
      REAL TIME,DT,HOLD(10),HNEW(10),COLD(10),CNEW(10),VOLD(10),
     1VNEW(10),K(10),N(10),RF(10),RO(10),K0,N0,R0,RO0,C0
      HOLD(0)=HOLD(1)
```

```
      HNEW(0)=HOLD(0)
      COLD(0)=COLD(1)
      CNEW(0)=COLD(0)
      K(0)=K0
      N(0)=N0
      DO I=1,XNODE + 1
        HNEW(I)=HOLD(I)
        CNEW(I)=COLD(I)
        VOLD(I)=0.0
        VNEW(I)=0.0
        N(I)=N0
        RF(I)=R0
        K(I)=K0
        RO(I)=RO0
      END DO
      CNEW(1)=CNEW(1)+C0
      TIME=0.0
      DT=0.0
      JJ=2
      SW=1
      CODE=1
      RETURN
      END
C
      SUBROUTINE INPUTDATA(IN,XL,DX,R0,K0,N0,RO0,MU,GAMA,ALPHA,BETA,
     1ETA,SI,TETA,TOL,Ss,C0,DEADLINE,XNODE,HOLD,COLD)
C-----------------------------------------------------------------
C INPUT DATA ARE BEING READ BY THIS SUBROUTINE FROM AN INPUT FILE
C DEFINED IN SUBROUTINE IOMANAGER BELOW.
C-----------------------------------------------------------------
      CHARACTER IN*50
      INTEGER XNODE
      REAL XL,DX,R0,K0,N0,RO0,MU,GAMA,ALPHA,BETA,ETA,SI,TETA,TOL,Ss,C0,
     1DEADLINE,HOLD(10),COLD(10)
      OPEN(1,FILE=IN,STATUS='OLD')
      READ (1,*) XL,DX,R0,K0,N0,RO0,MU,GAMA,ALPHA,BETA,ETA,SI,TETA,TOL,
     1Ss,C0,DEADLINE
C DETERMINATION OF NUMBER OF NODAL POINTS
      XNODE=INT(XL/DX)
      IF(XNODE.NE.XL/DX) THEN XNODE=XNODE+1
C READING INITIAL HEAD AND CONCENTRATION DISTRIBUTION
      DO I=1,XNODE+1
        READ (1,*) HOLD(I),COLD(I)
      END DO
      CLOSE(1)
      RETURN
      END
C
     SUBROUTINE IOMANAGER (IN,OUT)
C-----------------------------------------------------------------
C INPUT AND OUTPUT FILES ARE DEFINED IN THIS SUBROUTINE
C-----------------------------------------------------------------
      CHARACTER IN*50,OUT*50
      PRINT *,'Please enter input file name'
      READ *,IN
```

```
      PRINT *,'Please enter output file name'
      READ *, OUT
      RETURN
      END
C
     SUBROUTINE OUTPUTDATA(OUT,XNODE,TIME,CNEW,K,N,RF,RO)
C-----------------------------------------------------------------
C AN OUTPUT FILE CALLED "OUT" DEFINED IN IOMANAGER (ABOVE) IS
C MADE AND OUTPUT RESULTS ARE WRITTEN INTO IT.
C-----------------------------------------------------------------
      CHARACTER OUT*50
      INTEGER XNODE
      REAL TIME,CNEW(10),K(10),N(10),RF(10),RO(10)
      OPEN(1,FILE=OUT,STATUS='UNKNOWN')
      WRITE (1,*)
      WRITE (1,100) TIME
      WRITE (1,*)
      WRITE (1,101)
      WRITE (1,102)
      DO I=1,XNODE
      WRITE (1,103) I,CNEW(I),K(I),N(I),RF(I),RO(I)
      END DO
      CLOSE(1)
100   FORMAT(5X,'TIME=',F12.1)
101   FORMAT('  X              C          K          N              RF      RO')
102   FORMAT(' CM           G/L      CM/S                                G/CM3')
103   FORMAT(1X,I2,1X,F12.5,1X,F8.5,1X,F8.5,1X,F8.5,1X,F12.3,1X,F8.3)
      RETURN
      END
C
      SUBROUTINE PROPERTIES(SW,XNODE,ALPHA,BETA,GAMA,MU,ETA,CNEW,
     1N,K,RF,RO,N0,K0,R0,RO0)
C-----------------------------------------------------------------
C VARIATION OF PHYSICAL PROPERTIES OF POROUS MEDIA ARE DETERMINED
C BY THIS SUBROUTINE
C-----------------------------------------------------------------
      INTEGER XNODE,SW
      REAL ALPHA,BETA,GAMA,MU,ETA,CNEW(10),N(10),K(10),RF(10),
     1RO(10),N0,K0,R0,RO0
      IF(SW.EQ.0) THEN
C DETERMINATION OF PHYSICAL CHARACTERISTICS OF POROUS MEDIA AS SOME
C PREDEFINED FUNCTIONS OF CONCENTRATION
        DO I=1,XNODE
          N(I)=N0-MU*CNEW(I)
          RO(I)=RO0+ETA*CNEW(I)
          RF(I)=R0+ALPHA*EXP(CNEW(I)*BETA)
          K(I)=K0*EXP(-GAMA*CNEW(I))
        END DO
      END IF
      RETURN
      END
C
     SUBROUTINE VELOCITY(XNODE,H,V,N,K,DX)
C-----------------------------------------------------------------
C VELOCITY VECTOR IS CALCULATED BY THIS SUBROUTINE, BY USING DARCY
```

```
C EQUATION AND THEN AVERAGE LINEAR VELOCITY VECTOR IS COMPUTED.
C-----------------------------------------------------------------
      REAL H(10),V(10),N(10),K(10)
      INTEGER XNODE
      DO I=1,XNODE
        V(I)=K(I)*(K(I-1)*(K(I)+K(I+1))*(H(I-1)-H(I))+K(I+1)*(K(I)+
     1  K(I-1))*(H(I)-H(I+1)))/N(I)/DX/(K(I)+K(I-1))/(K(I)+K(I+1))
      END DO
      RETURN
      END
C-----------------------------------------------------------------
C END OF SUBROUTINES
C-----------------------------------------------------------------
```

APPENDIX D

DATA BANK

Table D1: Manometer levels in column test (cm)

Data	t (hours)	#1	#2	#3	#4	#5	#6	#7
11/21/99	0*	29.3	28.2	27	26	24.5	24	22.5
	1	29.4	28.22	27.02	25.8	24.4	23.7	22.5
	2	28.5	28.23	27.05	25.6	24.2	23.7	22.3
	3	29.6	28.28	27.08	25.7	24.2	23.4	22.3
	4	29.7	28.3	27.1	26	24.5	24.3	22.6
	5	30.3	28.35	27.12	26.1	24.6	24.4	22.7
	6	31	28.4	27.15	26.1	24.7	24.4	22.6
	7	32	28.46	27.18	26.1	24.7	24.5	22.5
	8	33.5	28.48	27.2	26.2	24.7	24.6	22.6
	9	35.5	28.5	27.24	26.2	24.7	24.6	22.6
	10	37.8	28.55	27.28	26.1	24.7	24.5	22.6
	11	55.6	28.6	27.3	26.3	24.7	24.6	22.6
	12**	111	29	27.31	26.7	24.7	24.4	22.3
	13.5	202	29.1	27.32	26.7	24.8	24.5	22.8
11/22/99	14.5	305	29.2	27.33	26.8	24.9	24.5	22.5
	16.5	689	29.7	27.34	26.4	24.9	24.3	22.2
	17.5	825	30	27.35	26.2	24.9	24.2	22.8
	18.5***	986	30.1	27.36	25.9	24.5	23.4	22.5
	19.5	1121	30	27.2	25.9	24.7	23.4	22.5
	20.5	1262	30	27.4	26	24.7	23.5	22.6
	21.5	1296	30	27.1	26.1	24.6	23.5	22.4
	22.5	1367	30.2	27.2	26.1	24.5	23.6	22.4
	23.5	1381	30.1	27.3	26.1	24.5	23.7	22.5
	24.5	1402	30.1	27.3	26.1	24.6	23.7	22.5
	25.5	1416	30.2	27.3	26.1	24.5	23.8	22.5
	26.5	1437	30.3	27.5	26.2	24.7	23.8	22.5
	27.5	1367	29.1	26.3	25.2	23.8	23.6	21.9
	30	1402	28.9	26.2	25.1	23.7	23.3	21.8
	31.5	1423	29	26.2	25.2	23.7	22.6	21.8
	33.5	1458	29.5	26.5	25.4	24	22.9	21.9
	35.5	1536	29.5	26.6	25.6	24.1	23	22
	37.5	1578	29.9	26.8	25.8	24.3	23.1	22.1

Table D1: Manometer levels in column test (cm)

Data	t (hours)	#1	#2	#3	#4	#5	#6	#7
11/23/99	40.5	1578	29.5	26.4	25.5	23.9	23.2	22
	45.5	1669	29.5	26.8	25.6	24.2	23.3	22.1
	47.5	1712	30	26.9	25.7	24.2	23.2	22.2
	55.5	1789	30.3	27.3	26.2	25.6	23.8	22.6
	57.5	1789	29.3	26.2	25.2	23.8	23	21.6
	59.5	1789	29.8	26.1	25.1	23.6	23	21.6
	61.5	1859	29.2	26.1	25.1	23.6	23	21.6
11/24/99	63.5	1930	29.2	26.2	25.2	23.7	23	21.7
	65.5	1894	29.6	26.3	25.3	23.8	23.2	21.7
	70.5	1930	28.8	25.7	24.7	23.3	22.5	21.2
	72.5	2113	28.8	25.5	24.5	23.1	22.5	21.1
	74.5	2352	29	25.7	24.7	23.2	22.5	21.3
	76.5	2366	29.8	26.4	25.2	23.7	23.1	21.6
	78.7	2703	30	26.5	25.3	23.8	23.1	21.7
	82	2422	29	25.8	24.7	23.3	22.6	21.4

* Beginning of carbon solution injection

** Connecting the first manometer to mercury gauge due to high pressure

*** Connecting the first manometer to water pressure gauge due to high pressure

Table D1: Manometer levels in column test (cm)

Data	t (hours)	#8	#9	#10	#11	#12	#13	#14
11/21/99	0*	21.8	20.3	19.1	17.8	16.8	15.6	14.7
	1	21.6	20.2	19.1	17.9	16.8	15.6	14.7
	2	21.5	20	18.9	17.7	16.7	15.5	14.7
	3	21.6	20.1	19	17.7	16.8	15.5	14.7
	4	21.8	20.2	19.1	17.9	17	15.7	14.7
	5	21.8	20.2	19.1	17.8	16.8	15.6	14.7
	6	21.7	20.2	19	17.8	16.8	15.5	14.8
	7	21.8	20.3	19.2	17.9	16.8	15.5	14.8
	8	21.8	20.2	19.2	17.9	16.8	15.6	14.8
	9	21.8	20.2	19.1	17.9	16.8	15.6	14.7
	10	21.7	20.2	19.1	17.9	16.8	15.6	14.7
	11	21.7	20.3	19.2	17.9	16.8	15.6	14.7
	12**	21.9	20.6	19.4	17.5	16.5	15.7	14.7
	13.5	21.9	20.7	19.6	17.9	16.9	15.8	14.8
11/22/99	14.5	21.7	20.7	19.8	17.9	16.7	15.9	14.9
	16.5	21.5	20.5	19.6	17.6	16.5	15.9	14.9
	17.5	21.4	20.4	19.5	17.6	16.8	15.8	14.8
	18.5***	21.6	20.2	19	17.6	16	15.6	14.7
	19.5	21.7	20.2	19.1	17.8	16.8	15.7	14.8
	20.5	21.7	20.1	19.1	17.8	16.8	15.4	14 7
	21.5	21.7	20.1	19.1	17.7	16.8	15.4	14.7
	22.5	21.7	20.1	19.1	17.8	16.7	15.4	14.7
	23.5	21.7	20	19.1	17.7	16.8	15.4	14.7
	24.5	21.7	20	19.1	17.7	16.7	15.5	14.7
	25.5	21.7	20	19.1	17.7	16.8	15.5	14.6
	26.5	21.7	20	19.1	17.7	16.8	15.5	14.7
	27.5	21.2	19.5	18.7	17.3	16.4	15.3	14.4
	30	21	19.4	18.5	17.2	16.3	15.2	14.4
	31.5	20.9	19.4	18.4	17.1	16.1	14.9	14.2
	33.5	21	19.4	18.5	17.2	16.3	15	14.2
	35.5	21.1	19.5	18.5	17.2	16.3	15	14.4
	37.5	21.3	19.7	18.6	17.3	16.4	15.1	14.4

Table D1: Manometer levels in column test (cm)

Data	t (hours)	#8	#9	#10	#11	#12	#13	#14
11/23/99	40.5	21.3	19.6	18.6	17.2	16.3	15.1	14.4
	45.5	21.3	19.7	18.7	17.2	16.3	15	14.3
	47.5	21.3	19.7	18.6	17.3	16.3	15	14.3
	55.5	21.9	20	18.6	17.5	16.5	15.3	14
	57.5	20.9	19.3	18.1	17	16	14.7	14
	59.5	20.8	19.2	18	16.8	16	14.6	14
	61.5	20.9	19.2	18	16.8	16	14.6	14
11/24/99	63.5	20.9	19.2	18	16.9	16	14.7	14
	65.5	21	19.4	18.2	17	16	14.9	14.1
	70.5	20.4	18.9	17.8	16.6	15.8	14.7	13.8
	72.5	20.2	18.8	17.7	16.6	15.8	14.6	13.8
	74.5	20.4	19	17.8	16.7	16	14.7	13.9
	76.5	20.7	19.3	18	16.9	16	14.7	13.9
	78.7	20.7	19.3	18.1	16.9	16	14.7	14
	82	20.6	19.1	18.1	16.8	15.9	14.7	13.9

* Beginning of carbon solution injection

** Connecting the first manometer to mercury gauge due to high pressure

*** Connecting the first manometer to water pressure gauge due to high pressure

Table D1: Manometer levels in column test (cm)

Data	t (hours)	#15	#16	#17
11/21/99	0*	13.8	12.9	11.7
	1	13.8	12.9	11.7
	2	13.8	12.8	11.7
	3	13.8	12.7	11.7
	4	13.9	12.8	11.7
	5	13.9	12.8	11.7
	6	13.9	12.8	11.7
	7	13.9	12.7	11.7
	8	13.9	12.7	11.7
	9	13.9	12.7	11.7
	10	13.9	12.7	11.7
	11	13.9	12.7	11.7
	12**	13.9	12.4	11.7
	13.5	13.8	12.9	11.7
11/22/99	14.5	13.8	12.9	11.8
	16.5	13.9	12.6	11.9
	17.5	13.8	12.4	11.8
	18.5***	13.7	12.8	11.7
	19.5	13.9	12.8	11.7
	20.5	13.7	12.7	11.6
	21.5	13.7	12.7	11.5
	22.5	13.6	12.7	11.4
	23.5	13.6	12.7	11.4
	24.5	13.6	12.8	11.4
	25.5	13.6	12.7	11.4
	26.5	13.6	12.6	11.3
	27.5	13.5	12.5	11.2
	30	13.4	12.5	11.3
	31.5	13.2	12.2	11.3
	33.5	13.3	12.3	11.4
	35.5	13.4	12.4	11.2
	37.5	13.4	12.3	11.2

Table D1: Manometer levels in column test (cm)

Data	t (hours)	#15	#16	#17
11/23/99	40.5	13.4	12.4	11.2
	45.5	13.3	12.3	11.2
	47.5	13.3	12.3	11.1
	55.5	13.5	12.3	11.2
	57.5	13	12	11
	59.5	12.9	11.9	11
	61.5	12.9	11.9	11
11/24/99	63.5	12.9	12.1	11.1
	65.5	12.9	12.2	11
	70.5	13.2	12	10.5
	72.5	13.2	11.9	11
	74.5	13.1	11.9	11
	76.5	13.1	12	11
	78.7	13	12	11
	82	12.9	12	11

* Beginning of carbon solution injection

** Connecting the first manometer to mercury gauge due to high pressure

*** Connecting the first manometer to water pressure gauge due to high pressure

Table D2: Computer output data

t sec	x cm	model C g/l	K cm/sec	n	R	density g/m^3
3606.3	1	39.5	.03890	.36505	211.079	1.66185
3606.3	2	17.9	.05018	.36721	198.726	1.65538
3606.3	3	1.5	.06088	.36885	107.600	1.65046
3606.3	4	.0	.06200	.36900	1.000	1.65000
7205.9	1	79.1	.02438	.36109	235.535	1.67373
7205.9	2	47.7	.03532	.36423	213.477	1.66431
7205.9	3	21.0	.04840	.36690	110.089	1.65630
7205.9	4	6.2	.05760	.36838	1.000	1.65187
10814.3	1	118.8	.01526	.35712	259.532	1.68564
10814.3	2	74.0	.02589	.36160	230.061	1.67220
10814.3	3	41.3	.03808	.36487	116.993	1.66239
10814.3	4	22.8	.04736	.36672	1.000	1.65685
14405.9	1	158.3	.00957	.35317	282.375	1.69750
14405.9	2	96.9	.01976	.35931	245.747	1.67907
14405.9	3	59.2	.03083	.36308	124.105	1.66776
14405.9	4	38.9	.03917	.36511	1.000	1.66167
18005.3	1	197.9	.00600	.34921	303.343	1.70938
18005.3	2	116.3	.01571	.35737	260.742	1.68490
18005.3	3	75.3	.02551	.36147	130.973	1.67258
18005.3	4	53.6	.03295	.36364	1.000	1.66607
21609.1	1	237.6	.00376	.34524	337.378	1.72128
21609.1	2	145.2	.01118	.35448	287.536	1.69355
21609.1	3	101.8	.01865	.35882	143.173	1.68054
21609.1	4	77.8	.02475	.36122	1.000	1.67335
25203.8	1	277.1	.00236	.34129	371.040	1.73314
25203.8	2	170.9	.00825	.35191	314.192	1.70128
25203.8	3	125.8	.01404	.35642	154.921	1.68775
25203.8	4	99.3	.01921	.35907	1.000	1.67979
28806.5	1	316.8	.00148	.33732	408.062	1.74504
28806.5	2	196.7	.00609	.34933	343.857	1.70901
28806.5	3	150.3	.01052	.35397	167.497	1.69509
28806.5	4	120.5	.01496	.35695	1.000	1.68615
32403.0	1	356.4	.00092	.33336	450.841	1.75692
32403.0	2	223.7	.00443	.34663	378.189	1.71711
32403.0	3	176.1	.00776	.35139	181.236	1.70283
32403.0	4	141.9	.01161	.35481	1.000	1.69258
36005.1	1	396.0	.00058	.32940	494.834	1.76880
36005.1	2	248.9	.00329	.34411	413.985	1.72468
36005.1	3	200.6	.00581	.34894	194.173	1.71018

36005.1	4	160.7	.00931	.35293	1.000	1.69820
39601.8	1	435.5	.00036	.32545	534.278	1.78065
39601.8	2	269.7	.00257	.34203	449.057	1.73091
39601.8	3	222.6	.00448	.34674	206.598	1.71679
39601.8	4	177.5	.00763	.35125	1.000	1.70326
43200.1	1	475.1	.00023	.32149	688.612	1.79253
43200.1	2	338.4	.00114	.33516	554.631	1.75152
43200.1	3	279.8	.00228	.34102	238.415	1.73395
43200.1	4	216.4	.00482	.34736	1.000	1.71492